THE

LONDON, EDINBURGH, AND DUBLIN

PHILOSOPHICAL MAGAZINE

AND

JOURNAL OF SCIENCE.

[SEVENTH SERIES.]

JANUARY 1934.

I. *Energy Balance, Electron Temperature, and Voltage Gradient in the Positive Column in Mixtures of* Na *Vapour with* Ne, He, *and* Ar.

By M. J. DRUYVESTEYN *and* N. WARMOLTZ, *Natuurkundig Laboratorium der N. V. Philips' Gloeilampenfabrieken, Eindhoven, Holland* *.

SUMMARY.

IN a positive column in Na vapour the power input is equal to the sum of the radiation and of the energy given off by the electrons and positive ions to the wall. When a rare gas at a few cm. pressure is admixed to the Na vapour a volume energy is measured, originating from the elastic collisions between the electrons and the rare gas atoms. The behaviour of the electron temperature and the voltage gradient in the positive column in Na vapour with a few mm. of Ne can, for low current density, be explained by means of the formulæ for the positive column.

§ 1. *Introduction.*

IN this article † measurements will be described concerning the energy balance in the positive column in Na vapour with and without the admixture of rare

* Communicated by Dr. B. van der Pol.

† A preliminary report is given in *Phys. Zs.* xxxiii. p. 822 (1932).

gases. When the work was started very little was known of the energy balance in positive columns. Two publications on this subject have appeared since. By a thermometric method Sommermeyer * has measured both the heat produced in the gas volume and the radiation in the positive column in rare gases. He found at a pressure of 1 mm. of Ne the heat produced in the gas volume to be about 20 per cent. of the power input in the positive column. On the other hand Sommermeyer calculated the total energy loss of the electrons in elastic collisions as 2 per cent. The reason for this discrepancy is not clear.

Mohler † measured the energy balance in the positive column in Cs vapour. The power input was measured on a part of the positive column between two sounding electrodes; the radiation emitted by this part was measured with a thermopile, whereas the energy given off by the electrons and the positive ions to the wall (wall-energy) was also measured. Mohler found that at low current density and low pressure the power input is given by the sum of the radiation and of the wall energy; at higher current density, however, the power input is greater than this sum. We will call this sum "the output." In two later papers, which we will discuss later on, Mohler and Boeckner ‡ give some details of the electrical properties of this discharge.

Our measurements were carried out, in almost the same way as those of Mohler, in a positive column in Na vapour. As our tube was not sealed off from the pump we could also measure the energy balance in Na vapour with the admixture of rare gases; so in this respect our results stand between those of Mohler and those of Sommermeyer.

Our results are as follows:—In pure Na vapour the power input is equal to the output (radiation+wall energy); also at current densities, where Mohler finds an unknown surplus of energy; for Na vapour+a rare gas the same result is obtained when the pressure of the rare gas is a few mm.; at higher pressures an extra energy is found, which can be attributed to the energy

* K. Sommermeyer, *Ann. d. Phys.* xiii. p. 315 (1932).

† F. L. Mohler, Bur. of Stand. Journ. of Res. ix. p. 25 (1932).

‡ F. L. Mohler, Bur. of Stand. Journ. of Res. ix. p. 493 (1932); C. Boeckner and F. L. Mohler, *id.* x. p. 357 (1933).

lost by the electrons in elastic collisions with the rare gas atoms, as this energy is calculated to be of the same order of magnitude as the one found experimentally. From these measurements we see that the energy balance in the positive column in Na vapour can for the greater part be understood.

In the following also some of the electrical properties of the positive column in Na vapour are discussed, *e. g.*, the behaviour of the voltage gradient, the electron temperature, and the mean free path of the electrons. The results are compared with those of Mohler, and can mostly be explained by the well-known formulæ of the positive column.

§2. *Method.*

Fig. 1 shows the tube as used in most of the experiments ;

Fig. 1.

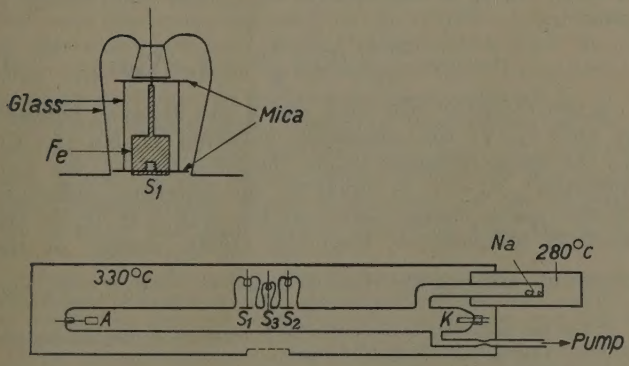

the length of the tube is about 1 metre ; the diameter was in some experiments 18 mm., but usually 36 mm. Nearly all the glass parts are of borax-glass, which is proof against Na vapour. The tube was for the greater part placed in a furnace (*e. g.*, at 330° C.). The Na vapour pressure was regulated by means of a small furnace, brought to 255°, 273°, or 287° C. Theoretically in these cases the pressure of the Na vapour should be resp. $2 \cdot 10^{-3}$,

$4 \cdot 10^{-3}$, and $6 \cdot 10^{-3}$ mm., but in the experiments large deviations from these values may have occurred *.

K is an oxyd-coated cathode, A an anode; in most tubes there was also a cathode at A and an anode at K, so that the current could be commutated; s_1 and s_2 are two flat-sounding electrodes whose surface almost coincides with the wall, s_3 is a thin wire electrode in the tube axis (of W or of Au, diameter 0·175 mm., length about 2 mm.). The power input between s_1 and s_2 was found by measuring the potential difference between s_1 and s_2 when no current was going to these electrodes †. The radiation of the portion between s_1 and s_2 was measured in the direction perpendicular to the tube by means of a calibrated thermopile. The wall energy consists of the kinetic energy given off to the wall by the electrons and the positive ions and their recombination energy. The positive ion-current to s_1 (i_{ws}) was found by extrapolating the measured positive ion current to s_1 to the potential at which the total current to s_1 is zero. If 0_s is the surface of s_1, the wall energy is given by

$$\epsilon_w = i_{ws} \frac{2\pi r l}{0_s} (V_i + \frac{4}{3} V_0 + V_r - V_w) ; \quad . \quad . \quad (1)$$

r is the radius of the tube and l the distance between s_1 and s_2, V_i the ionization potential of Na (5·1 V), V_r the space potential before the wall, and V_w the wall potential; $V_r - V_w$ is equal to the potential difference of the space charge layer on the wall. If V_0 is the electron temperature, then the kinetic energy of the electrons striking the wall is equal to $\frac{4}{3} eV_0$ ‡. V_0 and

* For the following reasons the Na pressure at s_1 can be unequal to the Na pressure in the small furnace :—

1. As the tube is connected to the pump some Na will escape through the capillary. This effect will, however, be small when the capillary is narrow.

2. When the tube is new the glass will absorb some of the Na vapour but after a few days the wall will be saturated.

3. The Na vapour density can be considerably changed by the electrophoresis in the positive column. In the presence of a rare gas in the tube the Na vapour will go to the cathode, but we can eliminate this effect by measuring fast enough. In a positive column in pure Na vapour the pressure at the anode is higher than at the cathode, and we will always have to take this effect into account when the current is high. We hope in due time to give a fuller report on the electrophorese in the positive column.

† W. Elenbaas, *Zs. f. Phys.* lxxviii. p. 604 (1932).

‡ I. Langmuir, Journ. of the Frankl. Inst. cxcvi. p. 751 (1923).

$V_r - V_w$ are measured by means of the wire electrode s_3 because the current to s_1 is very large at the space potential. The value of $V_r - V_w$ was taken to be equal to the potential difference of s_3 at the space potential and at the potential when the current is zero.

It is supposed in formula (1) that the positive ion current to the wall was measured correctly by means of the plate electrode s_1 and that in i_{ws} secondary electrons were absent *. It was also supposed that the energy which the positive ions obtained between their formation and the moment they enter the layer on the wall, could be neglected †. Sometimes the temperature of the electrons V_0 at the middle of the tube and near the wall differed by 10 per cent.

In most cases the wall energy was less than 15 per cent. of the power input (except at high current densities), and a mistake of 10 per cent. in the wall energy corresponds to a mistake of only 1·5 per cent. in the energy balance, which is less than the errors of observation.

In some tubes we measured the power input between two wire electrodes mounted in the middle of the tube; in this case, however, greater irregularities were found than with the plates; in our opinion these irregularities must be attributed to irregular contact potentials ‡.

The radiation consists mainly of the D lines (0·589 μ) and the three infra-red lines 0·82 μ ($2p$–$3d$), 1·14 μ ($2p$–$2s$), and 2·20 μ ($2s$–$3p$). The higher visible lines are weak, they form together about 2 per cent. of the D lines. As the tube was made of u.v. absorbing glass the ultra-

* As the ionization potential of Na is but 5·1 V, we may expect that the number of secondary electrons liberated by a positive ion is low; as the Na tube gives but little ultra-violet radiation we may neglect the photo-electrons from s_1.

† The potential difference which the positive ions pass in the tube before reaching the space charge layer on the wall consists of two parts: 1, a radial potential difference between the centre of the tube and the inner boundary of the space charge layer on the wall; the value of this potential difference was measured in some cases as about 0·5 volt; 2, an axial potential difference, which can be roughly calculated. It is supposed that both factors give together less than 1 volt. As the potentials between the brackets in (1) are generally about 10 volts, we may neglect this effect in most cases.

‡ Another disagreeable effect occurred sometimes with the wire electrode; when the potential of the wire was higher than the space potential the current to the wire diminished with the time, and we could only obtain a good curve by measuring very fast. This effect did occur at high currents when a W-wire was used, but never in the case of an Au-wire being used.

violet lines (especially 3303) were neglected (but these lines are probably weak). The total radiation was measured in the direction perpendicular to the tube by means of a Moll surface thermopile combined with a Zernicke *c*-galvanometer ; the absorption of the glass tube and of the glass window in the furnace were measured. Due to the hot furnace the galvanometer current had to be compensated and the radiation measured by switching on the tube current during half or one minute. With a $CuCl_2$ filter and with an infra-red glass filter the D line and the three infra-red lines could be measured separately.

The thermopile was calibrated in three different ways. The first method consisted in using a Heffner lamp in the way described by Coblentz * ; the Heffner lamp, giving much infra-red radiation, not transmitted by glass, first a thermopile with a fluorite window was calibrated, and, with the aid of the light of a W-lamp with a water-filter, was then compared with the surface thermopile with glass window. The second method, published since by Krefft and Pirani †, was used by us in the following way : the visible radiation of the Na tube of fig. 1 was measured first with a flicker photometer and then once more by means of a thermopile with a (calibrated) $CuCl_2$ filter. As the sensitivity of the eye for the D lines is 0·765, and the mechanical equivalent of light 620 lumen per 1 watt, we can calculate the sensitivity of the thermopile. The third method is very simple : the radiation of a W-ribbon lamp, burning at 2800° K., is practically totally transmitted by quartz. Of a ribbon-lamp in quartz (with a correction of 7 per cent. for reflexion) the total radiation could be measured by means of a thermopile (without a window).

The results of the three methods were that a galvanometer deflexion of 10 cm. was caused by the radiation of a light source at a distance of 1 m., radiating a number of watts equal to 0·624 and 0·64 (Heffner lamp), 0·641 (Na tube), 0·647 (W-ribbon), or $0{\cdot}643 \pm 3$ per cent.

As the sensitivity of the thermopile and of the galvanometer always changes somewhat ($\pm$ 5 per cent.) we calibrated the thermopile before each measurement by means of a standard lamp.

* W. W. Coblentz, Bur. of Stand. Journ. of Res. xi. p. 89 (1915).
† H. Krefft and M. Pirani, *Zs. f. techn. Phys.* xiii. p. 367 (1932).

Sometimes some K lines appeared in the spectrum, but they were always weak; no other lines except the Na lines were visible. In our experiments we never saw a recombination spectrum of Na as described by Krefft *, so in our case (Na pressure less than 0·01 mm.) we may neglect the number of recombinations in the gas volume.

§3. *Radiation Measurements.*

It is well known that at low current density a very large part of the power input of the positive column in Na vapour is radiated in the D lines; when a higher current density is used the infra-red lines become stronger. Table I. gives the percentage of the total radiation

TABLE I.

Percentage of the Infra-red Lines.

Tube.	Current.	Vac.	1 mm. Ar.	1 cm. Ar.
I	0·2 amp.	12·3%	15·7	
	1·5	23·5	24·2	
	3·0	32·5		
II.	0·2	14·8	13·3	9·7
	1·0	21·3	22·0	17·5

attributed to the three infra-red lines measured with two tubes (at 273°). With the first tube we saw that by increasing the current from 0·2 to 3 amp. the percentage of the infra-red lines increased from 12 to 32 per cent., at still higher current density up to 50 per cent. of the total radiation. With the other tube it was found that the percentage of the infra-red radiation was somewhat weakened by the admixture of a rare gas (Ar) of 1 cm. pressure; at increasing temperature (from 273° to 287°) the infra-red lines became in all cases somewhat stronger (about 3 per cent.).

The increase in intensity of the lines originating from higher levels (for Na infra-red lines) with increasing current density is a normal phenomenon † and can be explained by the increase of step-by-step excitation.

* H. Krefft, *Zs. f. Phys.* lxxvii. p. 752 (1932).
† M. Pirani, Congr. Int. d'el. Paris, 1932, 6e Sect. Rapport no. 5.

At high current density the concentration of the excited $2p$ atoms (in Na) is so large * that excitation from higher levels out of $2p$ atoms becomes more probable. It is very remarkable that the infra-red lines change so little when admixing 1 cm. Ar, as the electronic density is considerably altered by such a high Ar pressure (see § 5).

The dependence of the intensity of the radiation of the angle (ϕ) formed by the direction of the emitted radiation and the plane perpendicular to the axis of the positive column was measured with a tube, as shown in fig. 2. The tube was blackened at the outside except for the part b; the lamp was rotated in a furnace about the axis a–a, and the radiation of the part b was measured. The radiation was measured first when

Fig. 2.

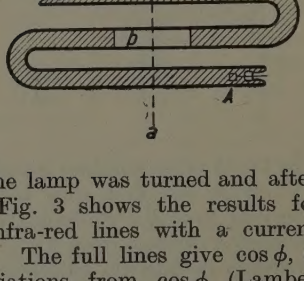

$\phi=0°$; then the lamp was turned and afterwards turned back again. Fig. 3 shows the results for the D line and for the infra-red lines with a current of 0·3 amp. ($2r=15$ mm.). The full lines give $\cos\phi$, and it is seen that the deviations from $\cos\phi$ (Lambert's law) are small †. Although a precise explanation why Lambert's law holds is difficult ‡, the main cause is the great absorption of the Na radiation in the Na vapour. For the D line this effect is well known. The absorption for the infra-red lines must be attributed to the high concentration of excited Na atoms in the discharge. When Lambert's law holds we can find the total radiation by multiplying the radiation in the direction perpendicular to the tube per unit solid angle by $\pi^2=4\pi.0{\cdot}785$.

* M. J. Druyvesteyn, *Physica*, xiii. (1933).
† v. Göler and M. Pirani, *Licht und Lampe*, iv. p. 67 (1931).
‡ W. de Groot, *Physica*, xii. p. 289 (1932).

§ 4. *Energy Balance in* Na *Vapour.*

With a great number of tubes of a diameter of 36 mm. it was found that at 273° and 287° C., with a current between 0·2 and 3 amp. in the positive column in Na vapour, the input was equal to the output (radiation + wall energy). Sometimes a difference between the input and the output was found, but in most cases this difference could be attributed to contact potentials when measuring the input (this was found by commutating the current), or to the tube not being clean and giving off some (molecular) gas. When everything was right

Fig. 3.

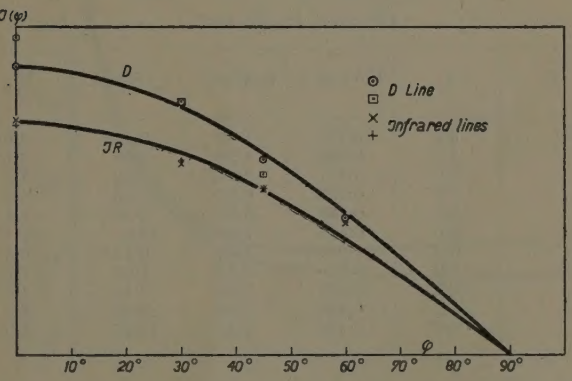

the input was always found to be equal within a few per cent. to the output at the above-mentioned temperatures. With the 36 mm. tube the output at 255° C. was greater than the input, which is very remarkable, and may be ascribed to the fact that in this case we have not to do with a homogeneous positive column, but are too near the beginning of the column, so that fast electrons from the cathode can enter the part of the tube between s_1 and s_2. Table IV. gives some results at 255°, 273°, and 287° C.

For the higher current densities a tube with a diameter of 18 mm. was used. The results at 273° and 287° are given in Table II. (E is the voltage gradient, R the radiation, ϵ_w the wall energy, and $\frac{E_v}{iE}$ the difference

between the input and the output in per cent. of the input.

The difference between the input and the output is called E_v*, and it is seen that at 273° at high current density the value of E_v is about −8 per cent., whereas at 287° the value of E_v is less than 3 per cent. At higher current densities the wall energy increased; at 6 amp. it amounted to 70 per cent. of the power input; in this case a possible mistake in the wall energy (see § 2) of 10 per cent. comes to an error of 7 per cent. in the energy

TABLE II.

Energy Balance in Na Vapour.

($2r=18$, $l=95$ mm.)

T.	i.	E(V/cm.).	R(Watt).	ϵ_w(Watt).	$\frac{E_v}{iE}$.
273°	0·2	0·724	1·26	0·130	−2·6%
	1·0	0·540	4·26	1·04	−3·1
	2·0	0·417	5·41	2·80	−3·5
	3·0	0·388	6·07	5·45	−4·2
	4·0	0·389	6·59	9·30	−7·4
	6·0	0·413	7·45	18·0	−7·8
287°	0·2	1·06	1·86	0·114	+0·8
	1·0	0·60	4·61	1·01	+1·8
	2·0	0·451	5·54	3·15	−1·0
	4·0	0·420	6·58	9·90	−2·8
	6·0	0·446	7·41	18·65	−2·0

balance, and for this reason the errors in the energy balance at 6 amp. may amount to about 8 per cent. However, it is also possible that the negative values of E_v at 273° must be explained in the same way as discussed in the case of the 36 mm. tube at 255°, so that the difference between the input and the output must be real. At 287° the difference between the input and the output was smaller than the errors of measurement. Mohler † found with an 18 mm. tube with 4 amp. (pressure 0·003–0·013 mm.) the input to be 15 per cent. larger than the output. It is clear that such an effect does not occur in Na vapour.

* We will call this difference E_v ($=iEl-R-\epsilon_w$) because with the measurements in gas this difference is equal to the volume energy.

† F. L. Mohler, Bur. of Stand. Journ. of Res. ix. p. 25 (1932).

We will now discuss the electrical properties of this positive column, *e. g.*, the voltage gradient per cm. E, the electron concentration in the axis n_e, the electron temperature V_0, and the mean free path of the electrons λ_-, which can be calculated from the mobility of the electrons, the tube current (i.) being equal to the product of $n_e E$ and the mobility of the electrons. By using the Langevin mobility formula we can solve for λ_- *:

$$\lambda_- = 1{\cdot}91 \cdot 10^{11} \frac{i\sqrt{V_0}}{n_e E r^2}. \quad . \quad . \quad . \quad . \quad . \quad (2)$$

Fig. 4.

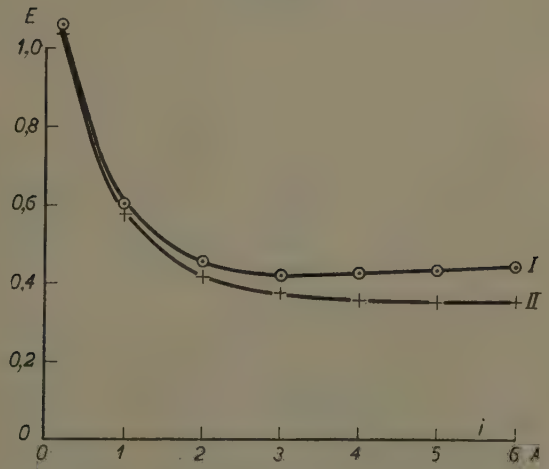

It was found that the electrical properties changed considerably when commutating the current at a high current, but at 0·2 amp. the commutation gave practically no change at all. This must be attributed to the electrophorese ; at high current densities †, the Na pressure at the anode is much higher than at the cathode. Fig. 4 gives the voltage gradient as a function of the current

* For the derivation of this formula see, *e. g.*, M. J. Druyvesteyn, *Zs. f. Phys.* lxxxi. p. 571 (1933). It is not quite certain that in our case Langevin's mobility formula is correct, as the potential difference on one free path is sometimes 1 volt. In that case the energy obtained on one free path is of the same order as the electronic energy.

† I. Langmuir, Journ. of the Frankl. Inst. cxevi. p. 751 (1923).

for the cathode near the pump I, and for the anode near the pump II.

Table III. gives some results at 295° (with the tube of Table II.) ; it is seen from this table that, with the cathode near the pump (in fig. 1 K cathode) the value λ_- decreases with increasing current between 0·2 and 1 amp. while with the anode near the pump (in fig. 1 A cathode) λ_- is almost constant. The dependence of the value of λ_- on the electron concentration in Cs vapour was attributed by Boeckner and Mohler * to the scattering of the electrons by the positive ions ; as they used a tube analogous to our tube, with the cathode near the pump, it must be feared that at least a great deal of the effect in their experiments must be ascribed to the electrophoresis.

Table III.

	I.	E.	$n_e . 10^{-10}$.	λ_-.
Cathode near pump.	0·2	1·067	5·71	1·00
	1·0	0·606	67·5	0·56
	2·0	0·453	182	0·53
Anode near pump.	0·2	1·045	5·31	1·18
	1·0	0·577	46·2	0·99
	2·0	0·418	104	1·06

The 1*n* i_s, V_s characteristic of s_3 (i_s current to s_3, V_s voltage on s_3) showed a very curious behaviour at high current density (see fig. 5). With a current less than 4 amp. the form of the characteristic is normal, but with a higher current the characteristics have an abnormal form near the space potential. We can explain this behaviour in two ways :

1. The space potential can be at D and the curve ACD gives a velocity distribution of the electrons which is not at all Maxwellian ; a group of electrons coming from the cathode (primary electrons) could give this abnormal form as found by Langmuir and Wehrli †. In our case we do not consider this to be the explanation, one of the reasons being that the form of the curve is the same at varying distances of the probe to the cathode.

* C. Boeckner and F. L. Mohler, Bur. of Stand. Journ. of Res. x. p. 357 (1933).

† I. Langmuir, Phys. Rev. xxvi. p. 585 (1925) ; M. Wehrli, *Helv. Phys. Act.* iii. p. 180 (1930), iv. p. 290 (1931).

2. In our opinion the space potential is at B, and the electrons have a Maxwell distribution corresponding to AB. The abnormal characteristic is caused by the probe disturbing the discharge. Especially at high current density an abnormal space charge, existing even when the probe is at space potential, comes round

Fig. 5.

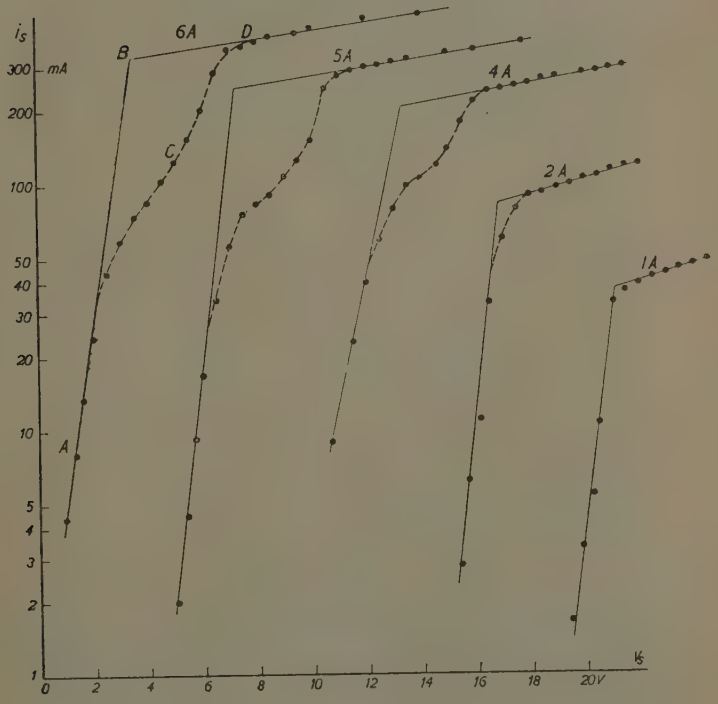

the probe, this space charge arising in this case from the high probe current. On account of this space charge the electron current (ACD) is less than the normal electron current (ABD) near the space potential. An argument for this explanation is the fact that at 6 amp. a small probe near the wall gave a normal characteristic, while the greater probe in the axis of the tube gave the curve of fig. 5.

§5. *Energy Balance in Na Vapour+rare Gases.*

With a number of tubes of a diameter of 36 mm. the energy balance was also measured when rare gases had been admixed to the Na vapour. First the energy balance in pure Na vapour was measured, after which, the gas being admitted, the gas pressure was measured by means of a MacLeod gauge or a manometer ; as the temperature of the tube was always about 330° C., the density of the gas at 1 mm. was equal to the density at room temperature of 0·5 mm.

The energy balance was measured in the same way as without rare gases, the measurements being only

Fig. 6.

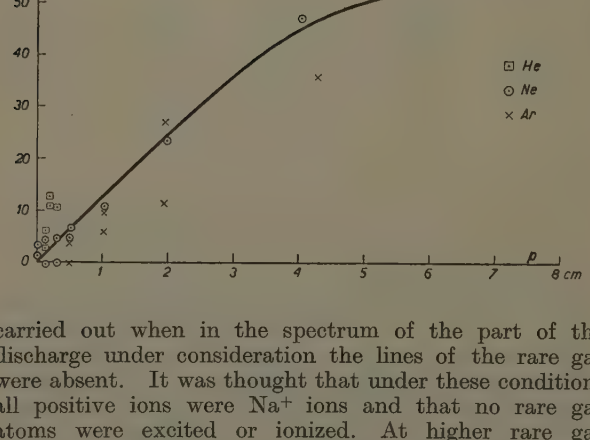

carried out when in the spectrum of the part of the discharge under consideration the lines of the rare gas were absent. It was thought that under these conditions all positive ions were Na^+ ions and that no rare gas atoms were excited or ionized. At higher rare gas pressures the lines of the rare gas appeared after some time, but with 0·2 amp. we could still measure sometimes at a pressure of 8 cm. The appearance of the rare gas lines will be studied in a separate paper.

Fig. 6 and Table IV. give the results of these measurements (in neon).

We see that in pure Na vapour the input is almost equal to the output (the difference is given in per cent.

TABLE IV.

($2r = 36$ mm., $l = 96{\cdot}5$ mm.)

	p. mm.	i. amp.	E. V/cm.	V_0. Volt.	R. Watt.	εw. Watt.	$\frac{E_v}{iE}$ exp.	$\frac{E_v}{iE}$ calc.	$n_\varepsilon . 10^{-10}$.	i_{ws}. mA.	$\lambda_- p$.	$\mu_+ p 10^{-4}$.
255°	0	0·2	0·432	4·00	0·76	0·11	− 5·9%	..	1·01	0·028	4·82	2·0
	0	1·0	0·398	2·48	3·60	0·53	− 7·5	..	4·55	0·180	4·55	4·6
	1·1	0·2	1·021	2·28	1·82	0·14	− 0·8	0·9%	4·45	0·050	0·38	1·5
	1·1	1·0	0·504	1·18	4·32	0·54	0·0	1·2	39·9	0·25	0·31	1·7
	3·0	0·2	1·067	1·63	1·87	0·113	2·2	3·0	8·95	0·045	0·43	2·6
	3·0	1·0	0·461	1·04	3·93	0·46	1·3	5·3	67	0·22	0·52	2·7
	4·8	0·2	1·086	1·44	1·88	0·085	5·0	5·3	12·2	0·036	0·46	2·8
	4·7	1·0	0·457	0·91	3·87	0·41	3·0	10	98	0·21	0·52	3·1
	9·7	0·2	1·100	1·44	1·80	0·074	10·4	13	14·8	0·032	0·75	4·1
	20·8	0·2	1·295	1·95?	1·63	0·064	31·5	30	11·9?	0·030	1·98	7·7
273°	0	0·2	0·748	2·94	1·32	0·087	0·5	..	1·25	0·029	1·93	2·3
	0	1·0	0·555	1·63	4·91	0·43	0·3	..	8·64	0·18	1·40	3·6
	1·1	0·2	1·188	1·83	2·12	0·072	2·9	0·5	3·74	0·030	0·35	1·4
	1·1	1·0	0·481	1·04	4·20	0·46	− 0·1	1·1	39·9	0·23	0·31	1·7
	3·2	0·2	1·205	1·37	2·14	0·085	2·8	2·3	9·54	0·037	0·34	2·6
	3·2	1·0	0·440	0·98	3·80	0·41	0·8	6·2	77	0·19	0·49	2·4

TABLE IV. (*continued*).

	p, mm.	i. amp.	E. V/cm.	V_g. Volt.	R. Watt.	ϵ_w. Watt.	E_g / iE exp.	E_g / iE calc.	$n_e . 10^{-10}$	i_{ws}. mA.	$\lambda_- p$.	$\mu_+ p 10^{-4}$.
	5·0	0·2	1·260	1·24	2·20	0·068	5·1	3·2	10·3	0·031	0·45	3·5
	5·0	1·0	0·438	0·97	3·71	0·37	3·6	11	85	0·18	0·69	3·1
	10·3	0·2	1·220	1·37 ?	1·97	0·052	12·8	11	14·3	0·023	0·74	3·4
	18·5	0·2	1·328	1·04	1·90	0·044	22·8	14	16·8	0·021	0·89	6·4
	38·5	0·2	1·663	0·98	1·73	0·036	44·5	24	18·4	0·017	1·29	10·3
287°	0	0·2	1·082	3·80	1·91	0·090	3·3	..	1·03	0·029	1·83	2·1
	0	1·0	0·668	1·24	5·95	0·41	1·2	..	14·8	0·19	0·60	3·0
	1·07	0·2	1·384	1·62	2·44	0·078	4·3	0·3	3·79	0·033	0·27	1·6
	1·07	1·0	0·517	1·04	4·59	0·43	— 0·6	1·0	39·8	0·21	0·28	1·6
	3·1	0·2	1·370	1·33	2·41	0·071	4·6	1·6	8·24	0·032	0·33	2·6
	3·1	1·0	0·443	0·92	3·87	0·41	— 0·2	5·1	75	0·20	0·47	2·5
	5·0	0·2	1·380	1·11	2·40	0·054	6·7	2·8	11·6	0·025	0·35	2·8
	5·0	1·0	0·440	0·85	3·71	0·34	4·7	10	97	0·18	0·56	3·0
	10·2	0·2	1·301	0·91	2·15	0·052	10·8	5·2	13·6	0·024	0·58	5·6
	19·7	0·2	1·372	0·85	1·96	0·037	23·5	12	18·3	0·019	0·77	6·9
	40·5	0·2	1·720	..	1·71	(0·037)	46·8	..	..	0·017	..	..
	81·5	0·2	2·59	..	1·89	(0·037)	61·0	..	..	..	..	..

E is the voltage gradient in volt per cm. ; R and ϵ_w are the radiation and the wall energy in Watts on the part between s_1 and s_2; $\lambda_- p$ is the mean free path in cm. multiplied by the gas pressure in mm. (for pure Na vapour, p is taken to be 1).

of the input under $\frac{E_v}{iE}$ exp) at 273° and 287°; at 255°, however, the output is greater than the input; these results were discussed in the last section. If we add a few mm. of Ne to the Na vapour the input remains equal to the output but for the errors of measurement. In 1 cm. Ne the output is about 10 per cent. less than the input, and at higher pressures the difference increases till at a pressure of 8 cm. Ne we find this difference to be about 60 per cent. We could not measure at higher pressures (at this temperature) because of the appearance of the Ne lines during the measurements.

The difference between the input and the output can be attributed to the volume energy which the electrons give off to the Ne atoms when making elastic collisions with these atoms. At an elastic collision an electron loses on the average a fraction $=\frac{2m}{M}$ of its energy, m being the mass of the electron, M that of the rare gas atom.

We find for the volume energy

$$E_v = \int \frac{2m}{M} \tfrac{1}{2} m v^2 f(v) \frac{v}{\lambda_-} \, dv$$

$f(v)$ is the Maxwell distribution of the electrons and

$$\frac{E_v}{iE} = 1{\cdot}7 \cdot 10^{-14} \frac{n V_0^{3/2} p r^2}{p E i A}; \quad . \quad . \quad . \quad . \quad (3)$$

A is the atomic weight of the rare gas. The volume energy was calculated by means of this formula, taking $\lambda_- = 0{\cdot}24$. We will discuss this value later on. The calculated values are given in the ninth column of Table IV.; they are of the same order of magnitude as the difference between the input and the output. We could not expect a better agreement when we take into account the errors in the experiments and the value of $\lambda_- p$, which is probably not quite correct. Still it seems that at 0·2 amp. the values are in better agreement than at 1 amp. At 1 amp. the calculated value seems to be always a little too high. We also get this impression from our other measurements, which we cannot give in detail. The conclusion we can draw from these results is that at 0·2 amp. in a positive column in Ne+Na we can

explain the difference between input and output, and it is proved that there is no unknown process in the column, participating for more than a few per cent. in the energy balance. At 1 amp. a difference may exist.

We may ask whether, although the volume energy is pretty well explained by (3), there are no other processes which can explain part of the volume energy too. We have already referred (in § 2) to the energy given off by the positive ions to the gas atoms, and in this case this energy may also be neglected. Another process is the collisions of the second kind. If an excited Na atom makes a collision of the second kind with an electron this atom gets into the normal state and the electron obtains a greater energy; but this process does not give any difference between the input and the output—it may have a great effect on the radiation, but we need not discuss it apart for the energy balance. According to measurements of the Franck school * the collisions of the second kind between excited Na atoms and atoms of a rare gas are very improbable.

Although we may say that we understand the energy balance, this does not apply to the many measured electrical properties of the positive column.

Fig. 7 represents the dependence of the voltage gradient in the positive column on the Ne pressure at three temperatures; we see that at a pressure higher than 0·5 mm. Ne the gradient is almost independent of the gas pressure; in the last section of this paper we will deal with this point.

It is possible to deduce from our measurements some simple properties, as, *e. g.*, the mean free path of the electrons λ_- and the mobility of the positive ions μ_+.

Column 12 of Table IV. gives the values of $\lambda_- p$ (for Na vapour without gas the value of λ_- is given), calculated by means of formula (2) of § 4. We find that $\lambda_- p$ is by no means constant. At 1 and 2 mm. it varies generally in all our measurements from 0·2 to 0·35, and this value is of the same order as that of 0·24 which we should expect from direct measurements of λ_- †. At higher pressures the value of $\lambda_- p$ increases with increasing pressure and faster with higher currents.

* R. Mannkopf, *Zs. f. Phys.* xxxvi. p. 315 (1926); L. v. Hamos, *Zs. f. Phys.* lxxiv. p. 379 (1932).

† R. Kollath, *Phys. Zs.* xxxi. p. 985 (1930).

First we will only speak of the results at 0·2 amp. We could give two explanations of the dependence of λ_p on the pressure :—

1. It is possible that at the higher Ne pressure the value of the electron concentration is measured too small because of the electrons colliding with the gas atoms in the space-charge layer on the wire electrode. We think this explanation is very improbable, the gas pressure

Fig. 7.

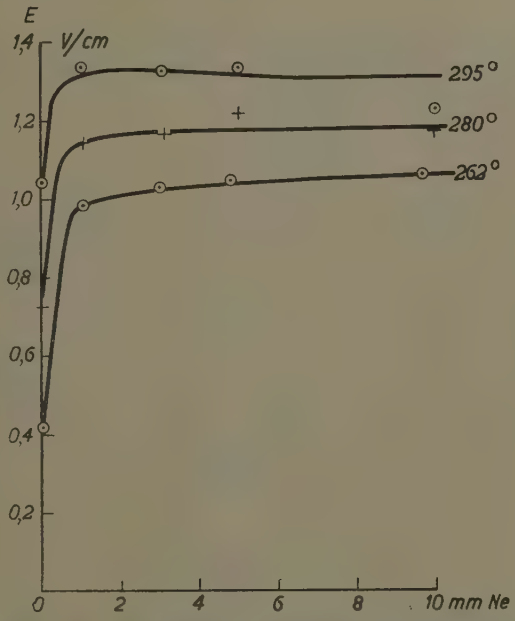

being too low for these collisions ; moreover, if this explanation were true we cannot understand the volume energy, as in (3) the value of n_e at high pressure would be about five times too low.

2. The second explanation, which we consider the correct one, is that formula (2) is wrong for high pressures and that the mobility of the electrons is much larger at these pressures than given by (2). This great mobility could be explained if the electrons had no Maxwell distribution at high pressures, but if there were, besides the

main group, a group of very slow electrons (slow electrons having a great mobility). If this group would have an electron concentration much smaller than the main group with the higher value of the electron temperature measured by us, the volume energy could still be calculated by means of (3). The fact that the calculated values of $\frac{E_v}{iE}$ at 1 amp. are somewhat too high can be explained in the same way.

In the thirteenth column we give the values of the mobility of the positive ions μ_+ multiplied by the pressure (for Na vapour without gas the value of μ_+ is given), which we derived from the Schottky equation

$$i_{ws} = \frac{0_s}{2\pi r} 7{\cdot}83\, \mu_+ \frac{2}{3}\, e\, V_0 n_e. \quad . \quad . \quad . \quad . \quad (4)$$

The values of $\mu_+ p$ also increase with the pressure, and we ascribe this effect also to the higher mobility of the electrons at a high pressure. At 1 mm. we suppose the values of $\lambda_- p$ and $\mu_+ p$ to be almost correct, but at the higher pressures the formulæ (2) and (4) are wrong because of the effect of the group of slow electrons.

Fig. 8 gives the values of $\frac{i_{ws}}{n_e}$, which is proportional to the number of ions formed by one electron in 1 cm. of the positive column. If the electrons have a Maxwell distribution, and if they ionize only normal Na atoms, $\frac{i_{ws}}{n_e}$ could be represented by

$$\frac{i_{ws}}{n_e} = \text{constant} \int f(v) v\, dv\, P(v),$$

where $P(v)$ is the ionization probability. If we take *

$$P(v) = \text{const.}\ \frac{\frac{1}{2}mv^2 - eV_i}{v^2},$$

then

$$\frac{i_{ws}}{n_e} = \text{const.}\ \sqrt{V_0}\left(1 + \frac{4V_0}{3V_i}\right) e^{-\frac{3V_i}{2V_0}} \quad . \quad . \quad . \quad (4)$$

* E. W. Pike, *Phys. Zs.* xxxiii. p. 457 (1932).

We see (fig. 8) that the values of 0·2 amp. lie on another curve than those of 1 amp.; either the electrons of the higher velocities do not have a Maxwell distribution given by the electron temperature, or at the higher current (1 amp.) not only ionization of normal atoms but also ionization of excited atoms occurs, and this seems very probable at the higher current densities. (The theoretical curve from (4) is found to increase more with V_0 than the experimental curve for 0·2 amp., fig. 8.)

Fig. 8.

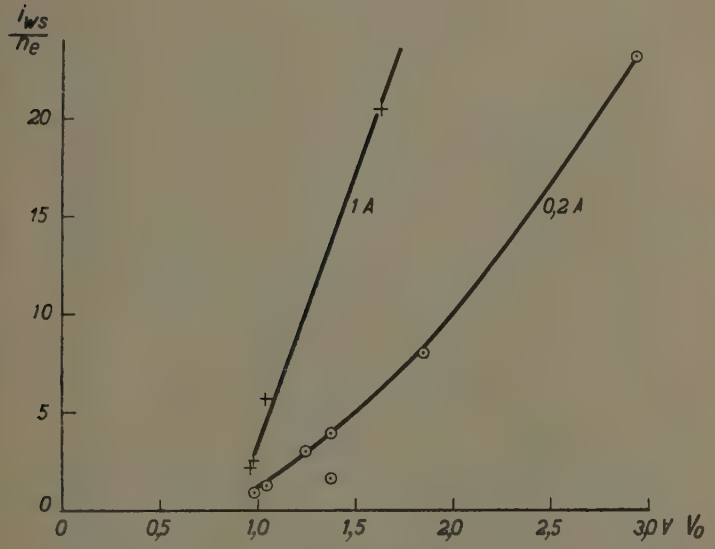

As we have extensively discussed the results with neon we will be briefer on the results in He and Ar, which are shown in Table V.* for 273°.

The volume energy $\frac{E_v}{iE}$ in He is somewhat larger than in Ne. In Ar and Ne they are of the same order of magnitude (fig. 6). As in these gases the Ramsauer effect of the free path of the electrons is large it is

* The values for He and Ar of Table V. were found with another tube than used for the Ne values of Table IV.

Table V.

($2r=36$ mm., $l=100{\cdot}3$ mm.)

	p. mm.	i. amp.	E. V/cm.	V_0. Volt.	R. Watt.	ϵ_w. Watt.	$\frac{E_v}{iE}$ exp.	$\frac{E_v}{iE}$ calc.	$n_e.10^{-10}$.	i_{ws}. mA.	$\lambda_- p$.	$\mu_+ p 10^{-4}$.
He	1·0	0·2	2·46	1·89	4·28	0·26	3·5%	4·2%	5·76	0·095	0·095	2·5
	1·0	1·0	0·93	1·95	7·59	1·52	6·2	12	29·4	0·61	0·27	3·0
	2·0	0·2	2·82	2·28	4·55	0·40	8·3	12	6·8	0·145	0·17	5·4
	2·0	1·0	1·04	..	7·69	1·37	16·2	..	..	0·60	..	..
	3·0	0·2	3·32	3·95	5·20	0·63	8·1	32	6·6	0·16	0·29	5·3
Ar	1·0	0·2	1·25	1·30	2·38	0·044	2·1	0·3	6·6	0·018	0·15	0·60
	1·0	1·0	0·38	0·98	3·70	0·21	0·9	0·8	46·7	0·10	0·29	0·62
	3·1	0·2	1·22	1·04	2·30	0·038	3·0	1·2	12·9	0·016	0·21	1·10
	3·1	1·0	0·33	0·72	3·21	0·13	1·4	3·3	83	0·064	0·51	0·95
	5·0	0·2	1·14	0·85	2·15	0·034	3·6	1·8	15	0·016	0·28	1·73
	5·0	1·0	0·32	0·79	3·11	0·13	3·3	11	142	0·062	0·51	0·78
	10·3	0·2	1·01	0·78	1·85	0·025	5·9	4·6	19	0·012	0·50	2·40
	10·3	1·0	0·33	0·72	2·92	0·11	13·4	18	134	0·053	1·02	1·61
	19·2	0·2	1·00	0·82	1·72	0·024	11·3	9·6	19	0·011	0·97	3·9
	19·2	1·0	0·39	0·78	2·78	0·075	30·6	35	148	0·035	1·58	1·67
	43	0·2	1·21	0·78	1·51	0·024	36·0	19	22	0·011	1·47	7·6

With this tube the data on pure Na and Na vapour with He, Ne, and Ar were measured; the results of He and Ar only are given here. The meaning of the symbols is the same as in Table IV.

difficult to calculate these values. From the measurements of $\lambda_- p$ at 1 mm. we choose the value of $\lambda_- p$ in He to be 0·1, in Ar 0·2, and, by calculating with (3), we find the values of the volume energy, which are given in the ninth column. We see that the calculated and the measured values are of the same order of magnitude, and so we may explain the volume energy in the same way as in the case of Ne. As with Ne the values of $\lambda_- p$ and $\mu_+ p$ increase with the pressure. We find that the values of $\frac{i_{ws}}{n_e}$ for He, Ne, and Ar, measured with the same tube at 0·2 amp., lie on one curve, as was to be expected, since the rare gas only changes the electron temperature, and not the process of ionization.

By comparing the results of He, Ne, and Ar we see that the mobility $\mu_+ p$ of Na^+ ions in these gases at 1 mm. is equal to $2{\cdot}8.10^4$, $1{\cdot}5.10^4$, and $0{\cdot}6.10^4$; at higher pressures these values change due to the abnormal mobility of the electrons, but at 1 mm. pressure we consider these values to be correct. The agreement with the direct measurements of Tyndall and Powell * is rather good, as they find for Na^+ ions in He, Ne, and Ar, $3{\cdot}52.10^4$, $1{\cdot}35.10^4$, and $0{\cdot}49.10^4$. Of course these values are much more precise than our results.

§ 6. *Energy Balance in Noble Gases.*

Some time ago † we made some measurements of the energy balance of the positive column in Ne. Table VI. gives some new results obtained with a tube ($2r = 45$ mm.) filled with He, Ne, and Ar (pressure 0·5 mm.), and measured by the same method as with Na vapour ‡, but the electrical measurements are less exact than with Na. Of course the interpretation is quite different; as in the rare gases the resonance lines lie in the extreme ultra-violet and are not measured, the energy of this radiation forms with the real volume energy the difference between the input

* A. M. Tyndall and C. F. Powell, Proc. Roy. Soc. A, cxxxvi. p. 145 (1932).

† M. J. Druyvesteyn, *Zs. f. Phys.* lxxxi. p. 571 (1933), especially Tables II. and IV.

‡ In the measurements published here the radiation was measured by means of the thermopile. In this case the radiation is independent of the direction; here Euler's law instead of Lambert's law applies (v. Göler and M. Pirani, *Licht und Lampe*, iv. p. 67 (1931) and M. Laporte, *Rev. d'Opt.* xii. p. 21 (1933)).

and the output (E_v). In this case the experimental values of the wall energy ϵ_w can be a little too large on account of the effect of secondary electrons leaving the sounding electrode. The results may be compared with those of Sommermeyer *. It is interesting that in our former experiments with Ne we found that $\lambda_- p$ and $\mu_+ p$ increased with increasing pressure, just the same as is the case in the discharge in Na+a rare gas.

§ 7. *Interpretation of the Results.*

We will now try to interpret our results by means of the equations for the positive column. Our aim is to calculate all the properties of the positive column, as,

TABLE VI.

(l=97·2 mm.)

	i.	E.	V_0.	R.	ϵ_w.	$\frac{E_v}{iE}$.	$\lambda_- p$.	$\mu_+ p . 10^{-4}$.
He .	0·2 amp.	2·24	6·35	0·79	2·58	21%	0·18	2·45
	0·5	2·12	6·85	2·21	6·15	19	0·35	3·86
Ne .	0·2	1·35	5·35	0·41	1·13	40	0·24	1·14
	0·5	1·34	4·80	1·27	2·27	46	0·25	1·21
Ar..	0·2	0·71	3·58	0·31	0·41	47	0·11	0·25
	0·5	0·48	2·67	0·71	1·21	18	0·13	0·43

e. g., the voltage gradient E, electron temperature V_0, intensity distribution in the spectrum when the current i, the gas density, and the radius are given; the atomic properties must of course be known.

The equations † for the positive column are the following :—

$$\frac{\mu_+}{r^2} = A \frac{n}{\sqrt{V_0}} \left(1 + \frac{4V_0}{3V_i}\right) e^{-\frac{3V_i}{2V_0}} + \left[B \frac{n_a}{\sqrt{V_0}} \left(1 + \frac{4V_0}{3(V_i - V_a)}\right) e^{-3\frac{V_i V_a}{2V_0}} \right], \quad . \quad . \quad (5)$$

* K. Sommermeyer, *Ann. d. Phys.* xiii. p. 315 (1932).

† For these formulæ see L. Tonks and I. Langmuir, Phys. Rev. xxxiv. p. 876 (1929); R. Seeliger, *Phys. Zs.* xxxiii. pp. 273, 313 (1932); F. L. Mohler, Bur. of Stand. Journ. of Res. ix. p. 493 (1932); M. J. Druyvesteyn, *Zs. f. Phys.* lxxxi. p. 571 (1933).

$$iE = R + \left[i_w \left(V^i + \frac{4}{3} V_0 + V_r - V_w \right) + C \frac{n_e V_0^{\frac{3}{2}} r^2}{\lambda_-} \right], \quad (6)$$

(energy balance equation),

$$i = D \frac{\lambda_- n_e r^u E}{\sqrt{V_0}}, \quad . \quad . \quad . \quad . \quad . \quad (7)$$

(mobility equation),

$$i_w = F \mu_+ V_0 n_e, \quad . \quad . \quad . \quad . \quad . \quad (8)$$

$$R = f(n_a . n), \quad . \quad . \quad . \quad . \quad . \quad (9)$$

$$R = G n\, n_e r^2 \sqrt{V_0} \left(1 + \frac{3 V_a}{2 V_0} \right) e^{-\frac{3 V_a}{2 V_0}}, \quad . \quad . \quad . \quad (9\,a)$$

$$n_a = g(n_e, V_0, n); \quad . \quad . \quad . \quad . \quad . \quad (10)$$

n is the number of normal atoms per cm.^{3}, n_a the number of excited atoms, and, supposing that only one excited state exists, the radiation R is the resonance radiation. If the atomic properties are known the constants A, B, C, D, F, G, μ_+ and λ_- are also known. It is supposed that the electrons have a Maxwell distribution.

We should like to solve these equations when i and n * are given; we have six equations for the six unknown variables V_0, E, n_e, n_a, i_w, and R †, but the form of the equations makes it difficult to solve them explicitly.

Equation (5) gives the equality between the positive ion current to the wall and the number of ionizations in the positive column, the first term on the right side corresponding with the number of ionizations of normal atoms, the second with that of excited atoms. When the second term may be neglected, as is the case at low current density, (5) immediately gives the electron temperature V_0, but the dependence of V_0 on the current can only be explained by taking into account the second term. With a current of 0·2 amp. we calculated V_0 from (5) without the second term. The value of A ‡ was found

* Strictly speaking n is not given, as it varies with the current through the electrophorese, but this is a second order effect. We suppose that n_a and n_e are much smaller than n.

† $V_r - V_w$ is not an unknown variable; how it can be derived will not be discussed here (see Tonks and Langmuir).

‡ From the value of A we can find the ionization probability (P); defined by the number of ionizations by electrons of an energy V

$$P = C \frac{V - V_i}{V_i}$$

at a Na pressure of 1 mm. C was found to be 3·4; this is a plausible value (E. W. Pike, *Phys. Zs.* xxxiii. p. 457, 1932).

by taking the V_0 value at 1 mm. Ne and 273° (1·83 V): from this value we calculated the other V_0 values (V_0 calc. in Table VII., $\mu_+ p$ was taken to be a constant), which are in pretty good agreement with the experimental values. (These values are the same as in Table IV.)

Formula (6) is the energy balance equation, the input being equal to the sum of the radiation, the wall energy, and the volume energy. In a positive column in Na vapour at not too high a pressure of the rare gas the volume energy may be neglected. With 0·2 amp. the infra-red radiation and the wall energy may in first order

TABLE VII.

	V_0 exp.	E exp.	V_0 calc.	E calc.
255° vac	4·00	0·432	..	0·41
1·1 mm. Ne	2·28	1·021	2·21	0·96
3·0 „ „	1·63	1·067	1·71	1·19
4·8 „ „	1·44	1·086	1·54	1·29
9·7 „ „	1·44	1·100	1·32	1·57
273° vac.....	2·94	0·748	..	0·75
1·1 mm. Ne	1·83	1·188	(1·83)	(1·188)
3·2 „ „	1·37	1·205	1·44	1·81
5·0 „ „	1·24	1·260	1·32	1·59
287° vac.....	2·7–3·8	1·082	..	0·84–1·21
1·07 mm Ne	1·62	1·384	1·68	1·51
3·1 „ „	1·33	1·370	1·34	2·21
5·0 „ „	1·11	1·380	1·23	2·04
10·2 „ „	0·91	1·301	1·10	1·33

be taken into account by taking $0{\cdot}8\, i\mathrm{E}=\mathrm{R}$. If for R we take equation $(9\,a)$ * we can calculate E from the experimental values of n_e and V_0.

Table VII. gives the results of these calculations; to obtain G † the E value of 1 mm. Ne at 273° was taken. As the result is strongly dependent on the value of V_0 a small mistake in this experimental value gives a large deviation. It is seen that considerable deviations occur between the experimental and the calculated values; still the equation explains the low values for Na vapour without a rare gas, and also the increase of E with the

* Formula $(9\,a)$ is obtained by supposing the excitation probability (g) to be a constant. $\mathrm{S}=\int f(v).v.g.dv$.

† From G we can derive the excitation probability (g) to be $2{\cdot}10^{-15}$ cm.²; this value is of the same order of magnitude as the value $5{\cdot}4\,.\,10^{-15}$ cm.², which Mohler found for Cs.

gas temperature, whereas V_0 decreases in this case. However, the fact that E is independent of the gas pressure is not explained by the calculations, as all the calculated values increase with increasing gas pressure. The value of 1 amp. cannot be calculated very well in this way.

Formula (7) is the Langevin mobility equation, and (8) the wall current according to Schottky. The deviations from these formulæ for high gas pressures were discussed in § 5.

Formula (9) is only simple when collisions of the second kind are absent (9 *a*). At higher current densities de Groot * has tried to obtain (9) and (10), and, although his formulæ considerably elucidate the problem of the diffusion of the resonance radiation through the gas, the problem cannot be considered as being solved.

We see that the properties of the positive column in Na vapour with a rare gas can be rather well explained by the equations (5)–(10) at 0·2 amp., although there are some deviations. However, for a detailed explanation of the results at higher current density we do not know accurately enough the concentration of the excited atoms. If the atomic properties were well known, we would be able to calculate *à priori* the values of V_0, n_e, and E at 0·2 amp.

Eindhoven.
June 28th, 1933.

II. *On the Behaviour of Liquid Films in a Vibrating Air Column.* *By* N. W. Robinson, *B.Sc., A.R.C.S.*, *and* R. W. B. Stephens, *B.Sc., A.R.C.S., Imperial College of Science and Technology* †.

[Plates I.–V.]

A previous paper by Mann and Stephens in this Journal ‡ contains the description of a method for producing a series of plane parallel soap films along the length of a glass tube, each film occupying a section of the tube. The present work deals with the attempted

* W. de Groot, *Physica*, xii. p. 289 (1932).
† Communicated by the Authors.
‡ Phil. Mag. ser. 7, xv. p. 143 (1933).

use of these films to denote the positions of nodes and antinodes in a Kundt's tube. The complete arrangement for obtaining this system of films is shown in fig. 1 of the previous paper *. In this instance the bubble-tube was uniform in diameter throughout its length, a condition which facilitated the production of plane films. A loud speaker, driven by a valve oscillator and amplifier, was connected as indicated in figs. 1 and 2 of the present paper. The brass side-tube A served as an outlet for the air displaced by the movement of the films along the tube.

The initial experiments were made upon a stationary system of films, about 1 cm. apart, the bubble-

Fig. 1.

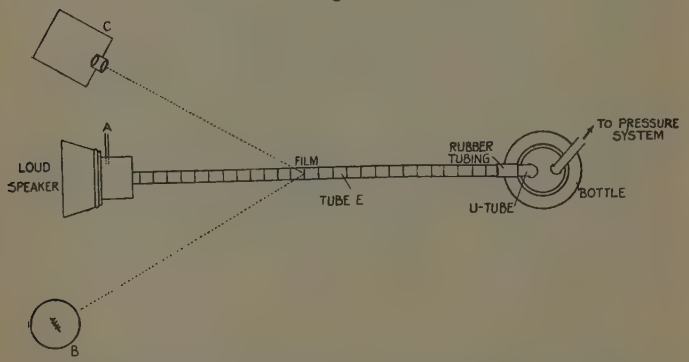

tube E being disconnected from the U-tube and closed by a cork. The films were illuminated by a 500 c.p. metal filament lamp B, so that their reflected light was observed at C. A variation in the intensity of this reflected light was noticed immediately upon switching-on the loud speaker. Further inspection revealed the existence of alternate regions of maximum and minimum vibration at certain frequencies over a wide range (300 to 3000 cycles per second). The phenomenon was rendered visible by the scattering of the light incident on the vibrating films, and is illustrated by Pl. I. fig. 1, in which the arrows denote the positions of antinodes. A " close-up " of a vibrating film is indicated in Pl. I. fig 2.

* *Ibid.* p. 144.

By visual observation it was found that the stationary film system responded most markedly to the following frequencies :—740, 840, 930, 1010, 1060, and 1240 cycles per second. Measurements were made of the positions of maximum vibration, and the results are tabulated below. The frequency (f) is stated in cycles per second, and the natural numbers indicate the order of consecutive positions of the maximum disturbance. The omissions occurring in the table correspond to those places where no definite maximum was observed owing to the unsuitable disposition of the films in that region.

Fig. 2.

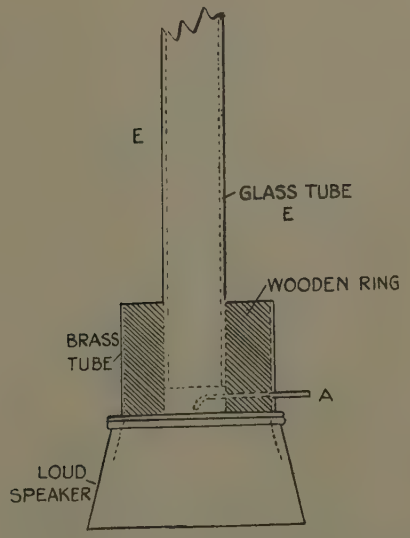

	Positions (in cm.) of the maxima along the tube :									
f.	(1).	(2).	(3).	(4).	(5).	(6).	(7).	(8).	(9).	(10).
740....	7·0	15·5	—	30·0	37·2	45·0	—	—	—	—
840....	8·0	15·0	—	30·2	—	45·0	—	63·5	—	—
930....	7·0	15·0	23·0	30·5	—	46·0	—	—	69·0	75·8
1010....	—	15·5	22·7	—	(34·0)	(42·6)	56·2	—	69·0	75·8
1060....	—	13·0	22·7	—	—	(42·5)	56·5	—	69·0	75·8
1240....	—	13·2	23·0	—	(34·2)	45·2	57·6	—	66·5	75·8

On plotting these distances against their respective numbers (fig. 3) the same linear relation was found to hold for all frequencies, and the mean distance between consecutive maxima was calculated to be 7·6 cm. This result is contrary to what would be expected if the membranes were acting as true acoustic indicators of the positions of the nodes and antinodes of a "normal Kundt's tube." As an explanation it is

Fig. 3.

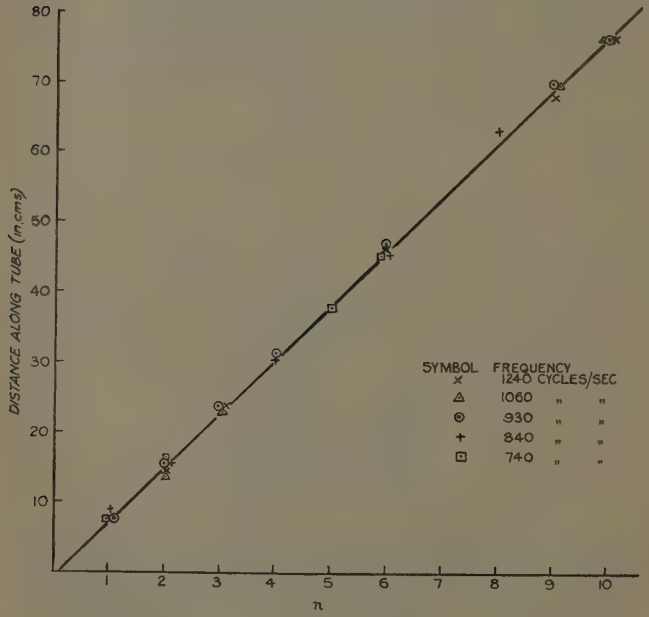

suggested that the mode of vibration of the system is not determined solely by the acoustic vibration of the air, but also by the properties of the films and the interspaces. In this connexion it is not without significance that, below 740 and above 1240 cycles per second, the intensity of vibration diminished uniformly down the tube. Attempts are being made to obtain a permanent system of collodion films to verify the above suggestion.

It was thought that conditions more nearly in keeping with those existing in a Kundt's tube might be obtained by the use of a system of widely separated films moving slowly up the tube. In this procedure each film in turn could pass through a position of a node or antinode when the tube was in resonance. Experiment showed that if the source of sound was sufficiently intense the positions of maximum vibration could be located with some degree of certainty by the pronounced vibration, or even bursting, of the film at these points. Pl. II. fig. 3 shows a series of films approaching the loud speaker; film no. 1 is nearing a place of maximum disturbance, which is indicated by its opacity, due to the violence of its vibration. Film no. 2 appears transparent, though vibrating slightly. Pl. II. fig. 4 exhibits the films a stage later in their progress up the tube, and it is evident that film no. 1 is on the point of bursting. Preliminary experiments enabled the positions of maximum displacements to be approximately located, and then the leading film of a system moving up the tube was kept under observation. When it reached the proximity of one of these noted positions the loud speaker was switched on, and the place of bursting was carefully fixed. The experiment was repeated for the various positions along the tube.

Measurements of three consecutive positions were 66·0, 83·0, and 100·0 cm. respectively.

Hence mean wave-length = 34·0 cm., frequency of vibration = 957 cycles per sec., and the velocity of sound in the tube (at 15° C.) = $3{\cdot}26 \times 10^4$ cm./sec.

The next feature to come under review is the mode of vibration of a typical film. By reference to Pl. III. fig. 5 it is seen that for small vibrations a definite system of radial and circular nodal lines makes itself clearly apparent on the surface of the film. Pl. III. fig. 6 shows a more intense disturbance, which, at a subsequent stage, becomes so violent as to cause the ejection of liquid particles, an effect illustrated in Pl. IV. fig. 7. It may be mentioned that often during the course of these experiments a miniature rainstorm took place in the interspace of a pair of films (about 1 cm. apart) moving together up the tube. The effect was produced by a mutual bombardment with liquid particles ejected when the films passed through a region of maximum disturbance.

The concluding part of this paper is an account of preliminary investigations of the nature of the vibrations of single liquid films. The apparatus used in these experiments is illustrated in fig. 4. A and B are two closely-fitting brass tubes, approximately 8 cm. diameter, and together they form a resonator of variable volume, the tube A being rigidly attached to the loud speaker.

Fig. 4.

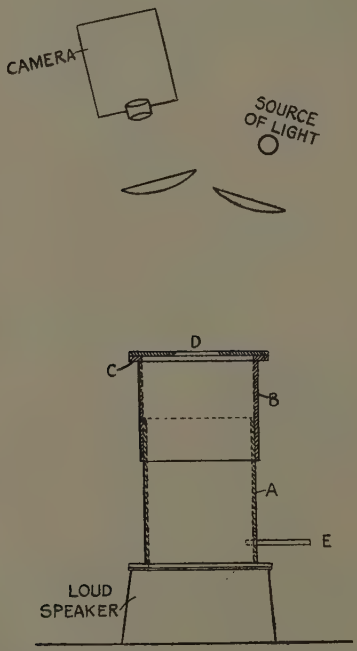

The film under investigation is stretched across a chamfered orifice D (2·5 cm. diameter), which rests in position on the flange C of the tube B. A side tube E enables the pressure in the resonator to be suitably adjusted. The liquid film, consisting of soap or saponin solution, was set into oscillation by the vibrating air column, and at certain frequencies gave standing wave patterns. The latter were photographed, using the optical

system shown in fig. 4. Pl. IV. fig. 8, of a vibrating soap film (frequency of the order of 1200 cycles per sec.), clearly indicates the existence of radial and circular nodal lines. The source of light was a 500 c.p. lamp and the exposure 1/250 second. Pl. V. fig. 9 is a spark photograph, the frequency of vibration being 648 cycles per second. In this case the illumination was provided by the condensed discharge of a Wimshurst electrical machine. It was found that the resonant frequencies of the vibrations of the plane films were independent of those of the vibrating air column, but the intensities were much greater when the resonant frequencies were coincident. Pl. V. fig. 10, shows the type of vibration assumed by a hemispherical soap film, which by visual observation displayed both longitudinal and latitudinal nodal lines. The authors are at present engaged in a fuller investigation of the vibrations of both plane and spherical, liquid and collodion films.

In conclusion, we desire to express our gratitude to Prof. G. I. Finch, M.B.E., for the loan of the ciné camera used in the photography of Pls. I.–V.

III. *The Relative Intensities of Atomic Spectral Lines from a Hydrogen Discharge-Tube.* *By* W. W. Jackson, *B.Sc.*, *M.Sc.* (*Manchester*), *Ph.D.* (*Aberdeen*), *Carnegie Teaching Fellow in Natural Philosophy in the University of Aberdeen* *.

[Plate VI.]

Introduction.

FROM a study of the intensities of the lines in the spectrum of atomic hydrogen we may be able to calculate the relative transition probabilities between the different quantum levels in the hydrogen atom. For example, if we can compare the intensities of H_β and P_α, then we are concerned with transitions from the same level to two different levels, and if these are compared under identical conditions, then the intensities will depend directly on the transition probabilities. Thus we may

* Communicated by Professor J. A. Carroll.

compare the probability of an electron falling from a level of total quantum number 4 to a level of total quantum number 2, with the probability of it falling from a level of total quantum number 4 to a level of total quantum number 3. Slack * has published data giving the values of the transition probabilities computed on the basis of wave-mechanics.

The following is an account of an experimental study of the change in intensity of H_β, H_α, and P_α as the current through the discharge-tube is altered from 200 m.a. to about 800 m.a., in order to investigate the constancy or otherwise of the ratios of these intensities.

Using a polarization spectrophotometer, and comparing the intensities of the lines from a tube in which the current could be varied, with the intensities of the lines from a tube under constant conditions, Nutting and Tugman † found that up to a current of 450 m.a. the intensities of H_α, H_β, and H_γ increased By photographing the spectrum using the wedge method ‡, Merton and Nicholson § give

$$H_\alpha : H_\beta : H_\gamma = 1{\cdot}00 : 0{\cdot}262 : 0{\cdot}185,$$

but the experimental conditions under which these ratios were found are not fully stated. Schlesinger || has worked with the electrodeless discharge and finds that the ratio $H_\alpha : H_\beta$ increases as the pressure increases beyond 0·19 mm. of mercury.

Crew and Hulburt ¶ measured the ratios by a spectrophotometric comparison with a calibrated tungsten lamp, and at a pressure of 0·54 mm. of mercury, with the tube using 400 watts found

$$H_\alpha : H_\beta : H_\gamma = 1{\cdot}00 : 0{\cdot}207 : 0{\cdot}054$$

when viewed from the sides of the tube.

Using currents up to 150 m.a. through the discharge-tube Ornstein and Lindeman ** measured the intensities by a photometric method, and showed that the intensities increased continuously.

* F. G. Slack, Phys. Rev. xxxi. p. 527 (1928).
† Nutting and Tugman, Bull. Bur. St. vii. p. 49 (1911).
‡ Merton and Nicholson, Phil. Trans. ccxvi. p. 462 (1916).
§ Merton and Nicholson, Phil. Trans. ccxvii. p. 260 (1917).
|| Schlesinger, *Zeits. f. Phys.* xxxix. p. 215 (1926).
¶ Crew and Hulburt, Phys. Rev. xxix. p. 843 (1927).
** Ornstein and Lindeman, *Zeits. f. Phys.* lxiii. p. 8 (1930).

With regard to the relative intensities of H_β and P_α, Ornstein and Burger * used a thermoelement connected to a relay galvanometer devised by Moll and Burger †, and found

$$H_\beta : P_\alpha = 2{\cdot}6.$$

In the investigation of which this is an account, the energy in a single line was focussed on to a linear thermoelement, which was connected directly to a sensitive galvanometer. By measuring the sensitivity of the galvanometer and that of the thermoelement, it was found that this involved the measurement of rates of energy flow of the order of 10^{-3} erg per second, falling on the element. Thus all the complications involved in photometry were avoided, but at the same time the experimental difficulties gave rise to no little trouble.

The Apparatus.

It will be convenient to describe the apparatus under the following headings :—

(*a*) Hydrogen supply, discharge-tube, and pumping system.

(*b*) High tension supply.

(*c*) The spectrometer.

(*d*) Thermocouple and galvanometer.

These sections will be dealt with in order.

(a) *Hydrogen Supply, Discharge-Tube, and Pumping System.*

The hydrogen is generated by the electrolysis of a solution of barium hydroxide in water ; this solution was found convenient, and, moreover, it does not attack tap grease to any appreciable extent. The gas then passes through a bulb containing moist glass wool in order to keep the hydrogen mixed with water vapour, as moist hydrogen in the discharge-tube tends to prevent the formation of molecular hydrogen. Thus, by suppressing the molecular spectrum, we can observe the

* Ornstein and Burger, *Zeits f. Phys.* lxii. p. 636 (1930).
† Moll and Burger, *Zeits. f. Phys.* xxxiv. p. 109 (1925).

atomic spectrum. The photograph (Pl. VI.) taken on an Imperial Special Rapid Plate, using a Hilger quartz spectrograph, shows how free the atomic spectrum is from other lines. In practice, by observing the discharge through a direct vision spectroscope, the first four lines of the Balmer series were clearly visible on a black background. After passing through the moist glass wool, the gas comes to a leak (designed and constructed for the purpose from a suggestion of Prof. R. W. Wood), which, because of its simplicity of construction and efficiency in practice, merits description. Referring

Fig. 1.

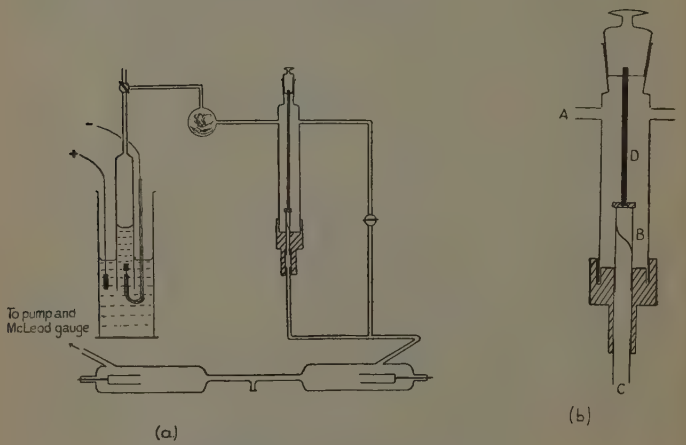

(*a*) Hydrogen leak and discharge-tube.
(*b*) Leak.

to the diagram, fig. 1 (*b*), the gas enters at A, and, after passing through a helical crack in the glass tube B, leaves at C. The shaded portion is made of brass, the rest being glass. The tubes B and C are fixed into the brass with wax, which has a low vapour pressure at ordinary temperatures. The brass cap on B is partly bored and threaded, so that the rod D screws into it for a few threads, D being fixed to the ground glass stopper with wax. The action then is clearly that, on turning the stopper, the upper end of the tube B is slightly

raised, and thus the helical crack can be opened and closed allowing the flow of gas to be regulated. This leak was found to work extremely satisfactorily and enabled a continuous flow of hydrogen to be maintained through the discharge-tube whilst the discharge was running. A balance was obtained between the rate of generation of the gas and the rate of pumping, whilst the pressure in the tube could be altered either by adjusting the leak or altering the rate of pumping. In either case the electrolytic current would have to be altered to maintain the balance under the new conditions.

The pumping system consists of a four-stage steel mercury diffusion pump, made by Leybold, backed by a Hyvac oil pump. The pressure in the tube was measured by using a McLeod gauge constructed to suit the particular range of pressures. The gauge used covered a pressure range up to 1 mm. of mercury, and the pressures used in the experiment were mostly in the region from 0·2 mm. to 0·5 mm. of mercury. Mercury vapour from the pumping system or from the McLeod gauge was prevented from reaching the discharge-tube by the use of vapour traps cooled with liquid air.

The discharge-tube was of glass and had a short side tube with plane quartz window, at right angles to the central part of the tube. The overall length of the tube was 110 cm., the central portion being of length 30 cm. and 1 cm. diameter, whilst the remaining portions were of diameter 5 cm. in order to keep the total resistance small, but yet have a high current density in the observed part of the discharge. The electrodes were hollow aluminium cylinders 12 cm. in length and $1\frac{1}{2}$ cm. in diameter, supported by an aluminium rod encased in a glass tube, which was sealed into the tube. The whole discharge-tube, apart from the quartz window, was surrounded by a water bath through which a continuous flow of water was maintained in order to dissipate the heat generated by the large discharge currents used.

(b) *The High Tension Supply.*

The mains supply is 220 volts D.C., and this was used as the input for a motor generator capable of delivering a power of 5 Kw. at 400 volts A.C. This latter was connected through a variable resistance to an auto-

transformer, the output of which serves as the input for an oil immersion transformer constructed to specification by Zenith (fig. 2). The transformer is wound so that there are output terminals from four sections, and by connecting these in series, series-parallel, or parallel, a power output is obtainable of 1 Kw. at alternating voltages of 10,000 v., 5000 v., 7500 v., or 2500 v. The discharge-tube being symmetrical the A.C. voltage was connected directly across the tube, and the discharge ran smoothly without the use of a rectifying circuit. Discharge currents which could be varied from 100 m.a. up to 1000 m.a. were used.

A Ferranti A.C. voltmeter was used to measure the voltage across the tube, and a Ferranti A.C. milliammeter registered the discharge current. The current passing through this type of instrument heats a thermojunction, which sends a current through a coil, which is deflected

Fig. 2.

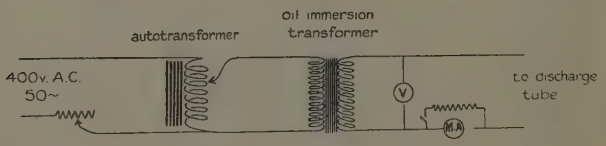

Diagram of high tension supply.

by a magnetic field just as in a moving coil galvanometer. This milliammeter was calibrated using D.C. and was shunted in order to increase its range.

(c) *The Spectrometer.*

This instrument has been designed and constructed during the course of the work, the major portion of the construction having been carried out by the firm of Fraser and McKay. It is of the Wadsworth type *, and can be used as a quartz transmission spectrometer of numerical aperture f. 3·5, or as a reflecting spectrometer of numerical aperture f. 8. It will be described first as a reflecting spectrometer by reference to the diagram (fig. 3). S is a symmetrically opening slit, and the light coming from the slit is reflected by a silvered plane surface to the first concave mirror of diameter 8 cm.

* Phil. Mag. xxxviii. p. 346 (1894).

and focal length 45 cm. From the latter a parallel beam is reflected, and is incident on the silvered front surface of the plane mirror on the turn table, which reflects the light to a 60° Cornu quartz prism, the length of the refracting edge being 5 cm. and the other side of the face containing the refracting edge being 7 cm. in length. The dispersed beam then passes to the second concave mirror, identical with the first, and is again reflected by a small plane silvered surface. The object of introducing the small plane reflectors is so that the beams incident on the concave mirrors can be kept as near as possible to the axis of the mirror concerned, and so reducing aberration to a minimum.

Fig. 3.

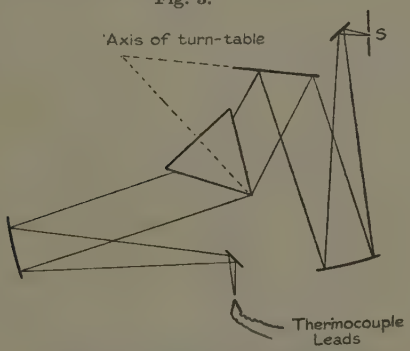

Path of light through spectrometer.

To use the instrument as a quartz transmission spectrometer the small reflecting surfaces are removed, and as a collimator, a telescopic tube with a scale in $\frac{1}{2}$ mm. engraved, is fixed in position. This tube carries a quartz lens of diameter 57 mm. and focal length $17\frac{1}{2}$ cm., and a similar tube acts as a telescope. By using the scales on the tubes, the collimator and telescope can be altered in length by a known amount.

Using the standard notation we have

$$\frac{1}{f} = (\mu - 1)\left(\frac{1}{r_1} - \frac{1}{r_2}\right),$$

$$\therefore \quad -\log f = \log(\mu - 1) + \text{const.}$$

$$\therefore \quad -\frac{df}{f} = \frac{d\mu}{\mu - 1}.$$

$\therefore$ If $\delta\mu$ represents a small change in refractive index of quartz corresponding to a change in wave-length, then the consequent change in focal length of the lens is given by δf where

$$\delta f = -f.\frac{\delta\mu}{\mu - 1}.$$

Thus from the dispersion curve of quartz the collimator and telescope, once set for a visible line, can be set to focus any other line of known wave-length whether visible or invisible.

The whole of the moving parts of the spectrometer are carried on two steel tubes at right angles, and on a cross bar, the supports of which can move along the steel tubes. The cross bar is also slotted so that it can be moved parallel to itself, and carries the whole of the turning mechanism of the table. The table turns on an accurately ground joint in a cylindrical casting, which itself can turn about the same axis, and which can move parallel to this axis. An arm, which can be clamped to the cylinder, extends at right angles to the axis and carries a screw with a graduated head. The hemispherical end of the screw bears against a projection from the table, and thus by clamping the cylinder, and also the arm carrying the screw, it is possible to turn the table through a known angle. The plane mirror on the turn-table can rotate round a central boss, and can be adjusted for tilt as well as possessing a backward and forward movement. Each concave mirror holder has many possible adjustments; they can slide along the steel tubes, they can move radially as well as in a circle about their point of support, and each mirror can rotate about an axis passing through the pole of the mirror and parallel to the axis of the turn-table. Also each mirror has a backward and forward motion, as well as an adjustment for tilt. The prism rests on an auxiliary table, with levelling screws bearing on the surface of the turn-table, and the auxiliary table can rotate, relative to turn-table, about the axis of the latter.

(d) *The Thermocouple and Galvanometer.*

After having been dispersed by the prism, the light is focussed by the telescope lens or mirror, and one

line of the spectrum is focussed on the linear thermo-element, which is a Moll vacuum thermocouple supplied by Kipp and Zonen. The leads from the thermojunction are shielded and rigid, and are connected directly to a sensitive galvanometer. A Paschen galvanometer was first used, and the effects of mechanical disturbances were removed by mounting the instrument on a slab supported on two brick columns with cotton wool in place of mortar. Surrounding the galvanometer was a double shield of laminated iron, but this did not prevent changing electromagnetic fields due to the electric trams, from producing irregular deflexions to such an extent that the galvanometer could not be used during the daytime. Satisfactory results could not be obtained even during the night, due to effects from the electrical machinery of the local printing works which only stop on Saturday nights, and even in these few hours other variations made it impossible to obtain results in which confidence could be placed.

A null method which was tried might be worth describing. A coil of several turns of wire was placed outside the shield of the galvanometer, and a current passing through this coil produced a deflexion which was proportional to the current. Thus, theoretically, the energy incident on the thermocouple could be measured by measuring the current through the coil necessary to keep the galvanometer undeflected. Unfortunately, even this method could not be used under the conditions obtained in the research. It was comparatively easy to produce a deflexion due to the energy in H_α, but the deflexion could not be measured with any degree of satisfaction.

A Kipp and Zonen galvanometer was kindly lent to me by Dr. Tocher *, and although at the sensitivity at which this was used, it possessed drifts, it was found to be more satisfactory than the Paschen from the point of view of measuring the deflexion.

Calibration of Spectrometer.

The turning mechanism of the spectrometer table, as given in the description of the apparatus, utilizes

* I take this opportunity of expressing my sincere thanks to Dr. Tocher for the loan of this instrument.

a screw with a graduated head, and therefore, before the readings on the head could be translated into the angle turned through by the table, a calibration graph was necessary. The pitch of the screw and distance of travel were calculated so that they were suitable for including the whole of the Paschen and Balmer series, and yet be of sufficiently fine adjustment to deal with individual lines.

In order to obtain this graph, a scale and mirror method was used. The illuminated scale was fixed at right angles to the line joining the centre of the scale to the axis of the table, whilst the mirror was mounted on the table. A fine straight scratch was made on the reflecting surface of the glass, and the position and tilt of the mirror were altered until, when viewed by a low power microscope, the scratch showed no sideways displacement on turning the table. When this condition was secured the line coincided with the axis, and therefore the reflecting surface contained the axis of rotation. Then the image of the scale, formed by reflexion at the surface of the glass, was viewed by a telescope with a cross wire in the focal plane of the eyepiece. As the table was turned, by means of the screw, the cross wire coincided with a different division on the scale, and knowing the distance of the scale from the axis and the number of divisions on the graduated head to correspond to a certain number of divisions on the scale, it was a simple matter to calculate the angle through which the table had turned as a result of turning the graduated head a known number of divisions. The head was marked off into 180 divisions along its circumference, and one complete rotation turned the table through an angle of $7'\ 32''$.

Thus, suppose light of any particular wave-length is focussed on to the thermoelement, after passing through the spectrometer along the path of minimum deviation, then, by turning the head through a known number of divisions, the angle through which the table has turned is known. The light now being brought to a focus on the thermoelement will still have suffered minimum deviation, but will have been deviated by the prism through an angle differing from the deviation of the light of the first wave-length by $\pm \frac{\theta}{2}$, where θ is the angle turned through by the table. Therefore, knowing the

dispersion of quartz, the wave-length of the light now being focussed on the element can be calculated. A graph was drawn connecting the angle through which the table must be turned from some standard position, with the wave-length of the light focussed on the thermoelement. Using the spectroscope as a transmission instrument, the lengths of the telescope and collimator must, of course, be altered for light of different wave-lengths.

Method of taking the Results.

The first part of the work has been to clear up some of the confusion regarding the relative intensities of H_α and H_β, the second part to investigate the ratio of H_β to P_α. First of all a Hilger quartz spectroscope was used to photograph the spectrum, and, keeping the flow of gas through the tube steady and the pressure constant, photographs were taken on an Imperial Special Rapid Plate, with the same time of exposure and increasing discharge current. The whole of the technique necessary for determining intensities photographically was not employed, because this photographic part was used only as a preliminary qualitative investigation. On the same plate were taken twelve exposures with the current varying from 197 m.a. up to 424 m.a.

A Dobson-Skinner instrument, by the Cambridge Instrument Co., was used to measure the blackness in different parts of this plate.

With this instrument the blackness of the first four lines H_α, H_β, H_γ, H_δ, was measured in each of the twelve spectra. This showed undoubtedly that the intensities of the lines increased with the current, but, of course, the intensities are not directly proportional to the blackness. The relative blackness in H_α, H_β etc., was not used, but only the increase in blackness of the same line traced through the various spectra, and thus the sensitivity of the plate with regard to wave-length was not involved. Neither was any investigation into the characteristic of the plate with regard to the intensity-blackness relation carried out, because of the essential qualitative nature of this part of the work. The only interpretation given to these photometric results was that without doubt the intensities of the first four lines of the Balmer series increased with increasing discharge current.

In the measurement of the intensities by the direct method of thermoelement and galvanometer the final image of the slit in any one wave-length, say that of H_α, was broader than the thermoelement. Then, as the image of the slit was moved across the element one would expect that the deflexion of the galvanometer would increase from the deflexion corresponding to the energy in the background until it reached a steady value as the image of the slit passed over the element, finally decreasing again as the image passes off the element.

Survey of a Line in the Spectrum.

The image of line was brought to a position such that the thermoelement received only the background energy. Then the shutter was made to intercept the light, the discharge current being kept on continuously. The galvanometer showed a drift, and the following method was used in taking a reading. At a certain time the shutter was opened and the energy allowed to fall on the element for a known interval of time and then the shutter was dropped back into place again. The galvanometer reading was taken at the time of opening the shutter, again just before closing the shutter, and then at the end of a time interval after this equal to the interval between opening and closing the shutter. The mean of the first and last readings gave the effective zero. Thus three readings of the galvanometer were taken to obtain one measurement of the energy at any part of the spectrum. This was repeated at any one part of the spectrum using different time intervals, until the time interval was found to be sufficient to allow the galvanometer to take up its full deflexion and then to come back to its final zero. In other words, a time interval was found which was suitable for the measurement of a deflexion superposed on a drift. Times of $1\frac{1}{2}$ minutes for deflexions greater than 3 cm., and of 1 minute for those less than 3 cm., were used.

First the background was measured and then the line moved slightly by turning the graduated screw, and readings were taken at regularly spaced intervals as the line was moved over the element and down to the background on the other side of the line. Fig. 4 shows the type of curve obtained, and the top shows the expected

flatness when the line is broader than the thermoelement (fig. 4).

In the measurement of the intensities of the lines, the line to be measured was brought so that the thermoelement was in a position corresponding to the middle of the flat portion on top of the curve. The deflexion of the galvanometer was then measured, as has been explained, and the value obtained corrected for background energy. This quantity was then taken to be directly proportional to the intensity of the line under the conditions obtaining at the time. It must be noticed that this curve cannot be interpreted as representing

Fig. 4.

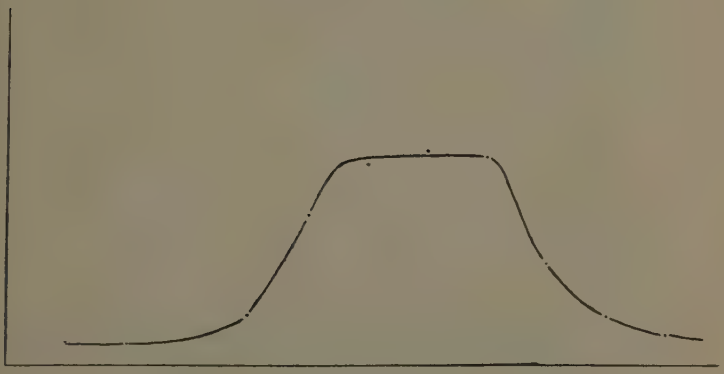

Survey of $H\beta$ peak.

the shape of the line, as can clearly be seen in the case when the image of the line is just as broad as the thermoelement. Then although the intensity distribution in the line will have a flat top, the curve obtained by the thermoelement will have only one point corresponding to this maximum value.

Results.

The following results are the average values of the deflexions actually observed in the experiment; the corrections to be applied are discussed later.

(a) *Results for* H_β.

The results for the intensity of H_β are shown in Table I., and a graphical representation is shown in fig. 5.

TABLE I.

Deflexion produced by H_β at different Discharge Currents at a Pressure of 0·26 cm. of Hg.

Deflexion due to H_β (peak). cm.	Deflexion due to background. cm.	Deflexion due to H_β alone. cm.	Current in m.a.
0·32	0·03	0·29	290
0·41	0·04	0·37	365
0·49	0·05	0·44	436
0·76	0·07	0·69	705

Fig. 5.

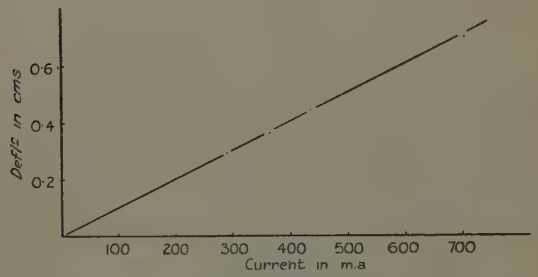

Deflexion due to H_β.

Although no systematic study of the variation of H_β with pressure has so far been made, the variation with the current has been repeated at a pressure of 0·30 cm. of Hg and the variation was found to be linear, the line passing through the origin as does the above line.

(b) *Results for* H_α.

The results in Table II. and fig. 6 show the variation of the deflexion due to H_α as the discharge current is altered. The conditions under which these results

were taken were precisely the same as the condition for H_β.

TABLE II.

Deflexion produced by H_α at different Discharge Currents at a Pressure of 0·26 cm. of Hg.

Deflexion due to H_α (peak). cm.	Deflexion due to background. cm.	Deflexion due to H_α alone. cm.	Current in m.a.
1·03	0·17	0·86	228
1·47	0·22	1·25	298
2·15	0·29	1·86	390
2·90	0·35	2·55	483
4·97	0·50	4·47	680

Fig. 6.

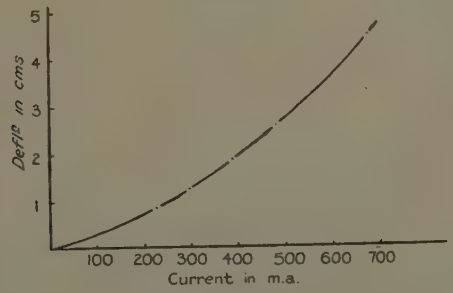

Deflexion due to H_α.

As will be shown later the curve connecting the intensity of H_α with the current is a parabola over the range considered.

(c) *Results for* P_α.

Using the calibration graphs of the spectrometer, the table was turned by means of the screw until it was in the position calculated to make P_α fall on the thermo-element when the collimator and telescope were correctly focussed. Then a survey was made, to cover a considerable range in this region in order to determinate the actual position of P_α.

The following results were obtained and are illustrated in fig. 7.

TABLE III.

Deflexion produced by P_α at different Discharge Currents at a Pressure of 0·30 cm. of Hg.

Deflexion due to P_α (peak). cm.	Deflexion due to background. cm.	Deflexion due to P_α alone. cm.	Current in m.a.
0·86	0·52	0·34	887
0·77	0·51	0·26	667
0·74	0·57	0·17	400

Fig. 7.

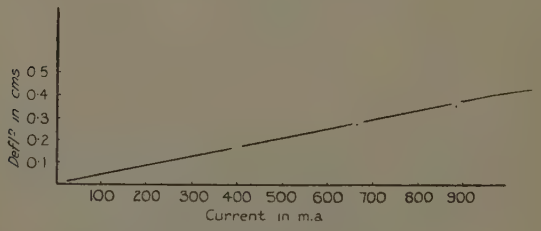

Deflexion due to P_α.

The figure shows this variation to be linear, the line again passing through the origin.

DISCUSSION OF RESULTS.

There are several factors which may affect the above results if intercomparison of intensities is to be made.

(*a*) Reflexion at quartz windows and quartz lenses.

(*b*) Reflexion at quartz prism.

(*c*) Reflexion at silver surface.

The differential true absorption of the quartz parts of the apparatus can be neglected for the wave-lengths involved. These factors will be considered in turn.

(a) *Reflexion of quartz windows and quartz lenses.*

(i.) Window of discharge-tube,

(ii.) Collimator and telescope lenses,

(iii.) Window of housing of thermoelement.

We shall consider these, as far as this effect is concerned, to be the same as four quartz plates. Coblentz * has published data for the reflexion from quartz based on Fresnel's formula. The first two columns of the following table are taken from Coblentz's paper, the third being obtained by raising the figures in the second column to the fourth power.

TABLE IV.

Showing Reduction Factor for Lenses and Windows.

Wave-length in μ.	Reduction factor for 1 plate.	Reduction factor for 4 plates.
0·486	0·9113	0·6893
0·656	0·9130	0·6950
1·873	0·9176	0·7092

Thus to correct for reflexion at these surfaces the observed intensity of H_β would have to be divided by 0·6893. It is not, however, the absolute amount of reduction which concerns us, but the reduction of the intensity of one line relative to the reduction of another line.

(b) *Reflexion at quartz prism surface.*

Two effects are involved here, for not only do we need to consider the change in reflecting power for different wave-lengths, but also we need to take into account the fact that the angle of incidence also alters in order that the light of different wave-lengths should traverse the prism under minimum deviation conditions.

The following values obtained by interpolation from values quoted by Coblentz † for the reflexion from the prism.

* Coblentz, Bull. Bur. St. xi. p. 476 (1914–1915).
† Coblentz, Bull. Bur. St. xi. p. 476 (1914–1915).

TABLE V.

Showing Reduction Factor for Quartz Prism.

Wave-length in μ.	Reduction factor.
0·486	0·8757
0·656	0·8791
1·873	0·8861

(c) *Reflexion at Silver Surface.*

Coblentz * has published a table of values of the reflecting power of silver, after having considered the data of Hagen, Rubens, and Paschen. The table below gives the values interpolated from his table.

TABLE VI.

Showing Reduction Factor for Silver Surface.

Wave-length in μ.	Reduction factor.
0·486	0·896
0·656	0·936
1·873	0·979

Combining all the above data we arrive at the values of the final correcting factor to be divided into the values obtained for the observed intensities of the lines.

TABLE VII.

Showing final Correcting Factor.

Wave-length in μ.	Combined correcting factor.
0·486	0·54
0·656	0·57
1·873	0·62

* Coblentz, Bull. Bur. St. x. p. 43 (1914).

From the graphs connecting the observed intensities of H_α and H_β we can draw up a table showing the relative observed intensities, and by correcting the observed ratio of H_α to H_β for the above factors we arrive at the value of the ratio of the intensities of H_α to H_β for varying discharge currents.

TABLE VIII.

Showing Corrected Values of Ratio $H_\alpha : H^\beta$.

Current in m.a.	Observed intensity of H_α.	Observed intensity of H_β.	Observed H_α/H_β.	H_α/H_β corrected.
200	0·72	0·20	3·6	3·4
300	1·25	0·30	4·2	4·0
400	1·92	0·40	4·8	4·5
500	2·70	0·50	5·4	5·1
600	3·60	0·60	6·0	5·7
700	4·70	0·70	6·7	6·3

Fig. 8.

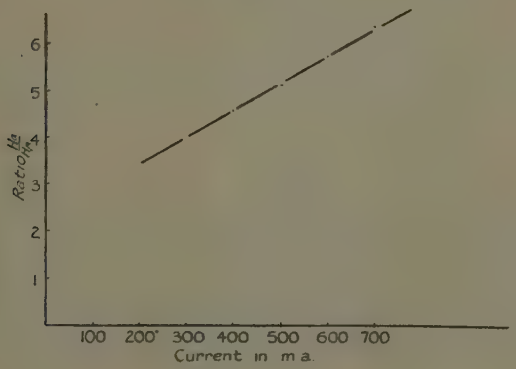

Ratio of H_α/H_β.

As is seen from the graph connecting the ratio H_α/H_β with the current (fig. 8), this ratio increases linearly, and since the intensity of H^β alone increases according to a straight line through the origin, then H_α must increase with the current in such a way that the curve

connecting its intensity with the current is a parabola of the form

$$y=ax^2+bx.$$

Thus, it appears that the different values of the ratio H_α/H_β obtained by different workers must be attributed to the fact that they have been working under different discharge conditions, and therefore on different parts of the above graphs.

On the other hand, since both H_β and P_α increase according to a straight line through the origin, the ratio of H_β to P_α must be a constant at least so far as a variation of the current is concerned. The above two graphs showing H_β and P_α are at different pressures and must not be compared directly, but they serve to show that the ratio is a constant, unlike the ratio of H_α to H_β.

Comparing directly the intensity of H_β with the intensity of P_α under similar conditions, the observed value of the ratio of H_β to P_α was found to be

$$H_\beta : P_\alpha = 2{\cdot}5,$$

and after correcting for reflexions the value becomes

$$H_\beta : P_\alpha = 2{\cdot}9.$$

The conditions under which this was measured were not the best and so the constancy of the ratio is stressed rather than the absolute value, which needs further corroborative support.

Calculation of Relative Transition Probabilities.

Using the above value of the ratio of H_β to P_α we can calculate the ratio of the transition probability involved in the electron jump from a state of total quantum number 4 to a state of total quantum number 3, with that involved in an electron jump from a state of total quantum number 4 to a state of total quantum number 2.

For if

N_4 = No. of atoms with electron in state 4.

A_{ns} = Transition probability between states n and s.

ν_{ns} = Frequency of light due to electron jump from state n to state s.

h = Planck's constant.

Then we have

$$\text{Intensity of } H_\beta = N_4 A_{42} h\nu_{42}.$$
$$\text{,, ,, } P_\alpha = N_4 A_{43} h\nu_{43}.$$
$$\therefore \quad \frac{\text{Intensity of } H_\beta}{\text{Intensity of } P_\alpha} = \frac{A_{42}\nu_{42}}{A_{43}\nu_{43}}.$$
$$\text{giving} \qquad A_{42} : A_{43} = 0{\cdot}7.$$

The values given by Slack are

$$A_{42} = 0{\cdot}845 \times 10^7,$$
$$A_{43} = 0{\cdot}904 \times 10^7.$$

Work is now in progress to extend the investigation by using spectrophotometric methods.

Summary.

The apparatus allows a continuous stream of pure hydrogen to pass through the discharge-tube, and conditions were obtained whereby the atomic spectrum of hydrogen was produced free from background. The variations in the intensities of the lines H_α and H_β in the Balmer series, and of P_α in the Paschen series of the atomic spectrum of hydrogen have been measured as the discharge current through the tube varied from 200 m.a. to about 800 m.a., the pressure in the tube and the potential fall across the tube remaining constant, The intensities of the lines have been measured directly, using a vacuum thermoelement connected to a sensitive galvanometer, and it has been found that the curve connecting the intensity of H_α with the discharge current is parabolic, whilst the variations of both H_β and $P\alpha$ are linear. The ratio of the intensitics of H_α and H_β increases linearly with the current; thus, different experimental values of this ratio obtained by different workers are reconciled. By the comparison of the intensities of H_β and P_α, relative values of transition probabilities have been experimentally determined, and the value obtained is in fair agreement with the values quoted by Slack.

In conclusion, it is a pleasure to express my sincere thanks to Professor Carroll, who suggested this research, and whose interest in the work and whose advice throughout have been most helpful.

Aberdeen.
July 1933.

IV. *The Theory of Electrocapillarity.*—Part II. *The Thermodynamics of Capillarity.* *By* S. R. Craxford, O. Gatty, *and* J. St. L. Philpot *.

Introduction.

In the first paper of this series † the phenomenon of capillarity was discussed and a definition of surface tension was put forward that was in accord with the classical work of Poisson, Laplace, Young, Gibbs, and others. This definition can also be applied to surfaces of finite thickness, and it shows how surface work is actually done on systems of the type used for the measurement of surface tension. The total number of degrees of freedom of a generalized system was investigated, and a modified way of stating the phase rule was proposed. The scope of the present paper is the development of the thermodynamics of capillarity directly from the first and second laws of thermodynamics, together with the conclusions reached in the previous paper. The method adopted is the investigation of the properties of a single system formed by combining the two phases, the interphase, and the containing vessel. In this way attention is focussed on quantities that can be determined directly by experiment, and also on the true number of degrees of freedom of the system. As a result additional terms are introduced into the equations of capillarity if the radii of curvature of the interphase become very small.

1. *The Condition for Equilibrium.*

For any system the first law of thermodynamics may be written

$$dE=\delta Q+\delta W, \quad . \quad . \quad . \quad . \quad . \quad . \quad (1)$$

where dE is an infinitesimal increase in the internal energy, δQ is the heat supplies to the system during this infinitesimal change, and δW is the corresponding work done on the system. The second law of thermodynamics states that for any reversible process

$$Td\mathrm{S}=\delta Q, \quad . \quad . \quad . \quad . \quad . \quad . \quad . \quad (2)$$

* Communicated by Sir Harold Hartley, F.R.S.

† S. R. Craxford, O. Gatty, and J. St. L. Philpot, Phil. Mag. xvi. p. 849 (Nov. 1933).

where dS is the increase in entropy and T the absolute temperature. For a reversible process, therefore,

$$d\mathrm{E}=\mathrm{T}d\mathrm{S}+\delta\mathrm{W}, \quad . \quad . \quad . \quad . \quad . \quad (3)$$

and since all infinitesimal displacements from equilibrium are reversible, this is the condition for equilibrium.

In the first paper of this series a generalized apparatus for making changes in surface area was described, and an expression was obtained for the work done on it by an external pressure p_2 and by a piston called piston 1. Denoting other work done on the system by δW′, the total work is given by

$$\delta\mathrm{W}=-p_2d\mathrm{V}+(p_1-p_2)dv_1+\delta\mathrm{W}' \quad . \quad . \quad . \quad (4)$$

from equation (1) of the first paper. In that paper the following definition of surface tension was also put forward :

$$\gamma_{12}=(p_1-p_2)\Big(\frac{\partial v_{12}}{\partial s_{12}}\Big)_{p_2,\,\mathrm{T},\,\mathrm{N},\,\mathrm{W}',\,s_k}.$$

It was not pointed out, however, that the differential coefficient on the right-hand side is determined uniquely by the single suffix s_k, which in all cases makes the surface expand normally. For example, change of temperature alters the diameter of the capillary tube and the radius of curvature of the meniscus in the same ratio, thereby causing an additional normal contraction or expansion. A similar effect would be observed if the effect of pressure on the diameter of the capillary were to be considered. Thus, provided the suffix s_k is maintained outside it is permissible to write

$$[\gamma_{12}ds_{12}=(p_1-p_2)dv]_{s_k}$$

under all conditions. The same suffix was shown to be sufficient to justify equation (6) in the last paper, so that it is therefore possible to write down the general expression for the work done on the system as

$$[\delta\mathrm{W}=-p_1d\mathrm{V}_1-p_2d\mathrm{V}_2+\gamma ds+\delta\mathrm{W}']_{s_k}, \quad . \quad . \quad (5)$$

where γ is used instead of γ_{12} and s instead of s_{12}. Substituting this in equation (3) above, the general condition for equilibrium becomes

$$[d\mathrm{E}=\mathrm{T}d\mathrm{S}-p_1d\mathrm{V}_1-p_2d\mathrm{V}_2+\gamma ds+\delta\mathrm{W}']_{s_k}. \quad . \quad (6)$$

2. *The Temperature and Pressure Coefficients of Surface Tension.*

It follows from the discussion on degrees of freedom in the first paper that, apart from $\delta W'$, which in this section will be considered to include work necessary for the possible introduction of material particles into the system, expression (6) for dE has three independent degrees of freedom. Taking T, p_2, and s as independent variables, setting $\delta W'=0$, and keeping p_2 constant, the equation can be transformed to

$$\left[dZ=\left[\gamma+V_1\left(\frac{\partial p_1}{\partial s}\right)_T\right]ds-\left[S-V_1\left(\frac{\partial p_1}{\partial T}\right)_s\right]dT\right]_{p_2,\,s_k}, \quad (7)$$

where

$$dZ=d(E+p_1V_1+p_2V_2-TS),$$

and is a complete differential. By cross differentiation, therefore,

$$\left(\frac{\partial\gamma}{\partial T}\right)_s+\left(\frac{\partial V_1}{\partial T}\right)_s\left(\frac{\partial p_1}{\partial s}\right)_T=-\left(\frac{\partial S}{\partial s}\right)_T+\left(\frac{\partial V_1}{\partial s}\right)_T\left(\frac{\partial p_1}{\partial T}\right)_s,$$

and hence

$$\left(\frac{\partial\gamma}{\partial T}\right)_s+\left(\frac{\partial p_1}{\partial s}\right)_T\left(\frac{\partial V_1}{\partial T}\right)_{p_1}=-\left(\frac{\partial S}{\partial s}\right)_T,$$

and this may be written

$$\left[\left(\frac{\partial\gamma}{\partial T}\right)_s\left[1-\left(\frac{\partial p_1}{\partial\gamma}\right)_s\left(\frac{\partial V_1}{\partial s}\right)_{p_1}\right]=-\left(\frac{\partial S}{\partial s}\right)_T\right]_{p_2,\,s_k,\,\delta w'}. \quad (8)$$

The interpretation of this equation is best done term by term. The first, $\left(\frac{\partial\gamma}{\partial T}\right)_{s,\,p_2,\,s_k,\,\delta w'}$, is the rate of change of surface tension of the 12 interphase with temperature, s and p_2 being kept constant. Since s is constant and $\left(\frac{\partial v_{12}}{\partial s_{12}}\right)_{s_k}$ depends only on s if gravity is neglected, this implies that the curvature is also constant. The second term, $\left(\frac{\partial p_2}{\partial\gamma}\right)_{s,\,p_2,\,s_k}$, is equal to $\left(\frac{\partial s_{12}}{\partial v_{12}}\right)_{s_k}$, as may be seen by considering the definition of γ.

The term $\left(\frac{\partial V_1}{\partial s}\right)_{p_1, p_2, s_k}$ is the volume change in phase 1 per unit increase in the surface area s_{12}. Physically this term may be split into two parts. The first is due to the fact that the matter in the interphase may have a slightly different density than in the bulk phases. This part is characteristic of the interphase. The second part is proportional to the bulk of phase 1 and to its coefficient of thermal expansion, and arises from the fact that in order to change s, when p_1, p_2, s_k, and W′ are constant, the temperature must be changed. It therefore has nothing to do with the interphase. Similar irrelevant quantities occur in most of the analogues of equation (8), such as (15) for example, and in the electrocapillary equation which will be given in the next paper. These terms occur in pairs, which form general principles must cancel out, and in any case they can be made as small as desired by reducing the volume of phase 1. In actual experiments the existence of the earth's gravitational field does in effect lead one to take as phase 1 only a thin lamina of material close to the interphase. The rest of phase 1 may then be regarded as a means of applying the pressure, due to its weight, to the imaginary boundary near the interphase. Thus the methods employed by experimenters reduce the second part of $\left(\frac{\partial V_1}{\partial s}\right)_{p_1, p_2, s_k}$ indefinitely. The first part of the term, however, always remains, but can never be much greater than a length τ, which is equal to the thickness of the non-homogeneous region between the two phases. Its product with $\left(\frac{\partial s_{12}}{\partial v_{12}}\right)_{s_k}$ is therefore always small compared to unity, unless the radii of curvature of the interphase are of the same order as the thickness of the interphase.

Corresponding to the bulk part of $\frac{\partial V_1}{\partial s}$ there is a bulk part of $\frac{\partial S}{\partial s}$, namely, the heat of compression when p_1 is altered. As stated above these parts must cancel. The final term to be discussed is best expressed

by considering $T\left(\frac{\partial S}{\partial s}\right)_{T,\, p_2}$ to be the heat supplied to the system during a small increase in surface area at constant p_2, T, s_k, and when $\delta W' = 0$. The previous methods of treatment of the same problem give the expression

$$\left(\frac{\partial \gamma}{\partial T}\right)_{s,\, p_2} = -\left(\frac{\partial S}{\partial s}\right)_{T,\, p_2} \quad . \quad . \quad . \quad . \quad . \quad (9)$$

This is clearly the same as the expression just derived unless the radii of curvature of the surface are of the same order of magnitude as the thickness of the interphase. In this latter case the idea of surface tension is less significant, but by means of the definition of surface tension given in the first paper it is possible, at any rate in theory, to define a surface tension for any one of a series of boundaries in the interphase. Equation (9) is very nearly correct, and shows that surface tension behaves as a free energy term and obeys the Gibbs-Helmholtz equation.

A similar investigation for the pressure coefficients of surface tension may be carried through, and if T, p_1, and s are taken as the independent variables, then

$$\left[\left(\frac{\partial \gamma}{\partial p_1}\right)_s \left[1 - \left(\frac{\partial p_2}{\partial \gamma}\right)_s \left(\frac{\partial V_2}{\partial s}\right)_{p_2}\right] = + \left(\frac{\partial V_1}{\partial s}\right)_{p_1}\right]_{T,\, s_k,\, \delta w'}, \quad (10)$$

and by symmetry

$$\left[\left(\frac{\partial \gamma}{\partial p_2}\right)_s \left[1 - \left(\frac{\partial p_1}{\partial \gamma}\right)_s \left(\frac{\partial V_1}{\partial s}\right)_{p_1}\right] = \left(\frac{\partial V_2}{\partial s}\right)_{p_2}\right]_{T,\, s_k,\, \delta w'}. \quad (11)$$

But since $\left(\frac{\partial p_1}{\partial \gamma}\right)_{s,\, s_k,\, T}$ is no longer simply related to the curvature of the surface, these expressions are not so simple as equation (8), and for this reason (10) is best transformed to

$$\left[\left(\frac{\partial \gamma}{\partial p_1}\right)_s \left[1 + \frac{ds_{12}}{dv_{12}} \cdot \left(\frac{\partial V_2}{\partial s}\right)_{p_2}\right] = \left(\frac{\partial V_1}{\partial s}\right)_{p_1} + \left(\frac{\partial V_2}{\partial s}\right)_{p_2}\right]_{T,\, s_k,\, \delta w'}. \quad . \quad . \quad . \quad (12)$$

This is obtained from equation (10) by introducing

$$\left(\frac{\partial p_2}{\partial \gamma}\right)_{s,\, T,\, s_k,\, \delta w'} = \left(\frac{\partial p_1}{\partial \gamma}\right)_{s,\, T,\, s_k,\, \delta w'} - \frac{ds_{12}}{dv_{12}}.$$

The corresponding equations to (10), (11), and (12), derived by the simple Gibbs method, would be $0=0$. Equation (12) shows directly that for ordinary radii of curvature $\left(\frac{\partial\gamma}{\partial p_1}\right)_{s,\,\mathrm{T},\,s_k,\,\delta\mathrm{w}'}$ is of the order of

$$\left(\frac{\partial \mathrm{V}_1}{\partial s}\right)_{p_1,\,\mathrm{T},\,s_k,\,\delta\mathrm{w}'} \quad \text{and} \quad \left(\frac{\partial \mathrm{V}_2}{\partial s}\right)_{p_2,\,\mathrm{T},\,s_k,\,\delta\mathrm{w}'},$$

that is, of the thickness of the interphase. Similar arguments apply to $\frac{\partial\gamma}{\partial p_2}$.

These expressions can also be made to show the relationship of surface tension to radius of curvature. Thus, if $\left(\frac{\partial v_{12}}{\partial s_{12}}\right)_{s_k} = \alpha$, α is a function of s only, being half the radius of curvature if the surface is spherical. Therefore

$$\left(\frac{\partial\gamma}{\partial \mathrm{T}}\right)_s = \left(\frac{\partial\gamma}{\partial \mathrm{T}}\right)_\alpha = -\left(\frac{\partial\gamma}{\partial\alpha}\right)_\mathrm{T}\left(\frac{\partial\alpha}{\partial \mathrm{T}}\right)_\gamma,$$

so that expression (8) becomes

$$\left[\left(\frac{\partial\gamma}{\partial\alpha}\right)_\mathrm{T}\left[1-\frac{1}{\alpha}\left(\frac{\partial \mathrm{V}_1}{\partial s}\right)_{p_1}\right] = \left(\frac{\partial \mathrm{S}}{\partial s}\right)_\mathrm{T}\left(\frac{\partial \mathrm{T}}{\partial\alpha}\right)_\gamma\right]_{s_k,\,p_2,\,\delta\mathrm{w}'}. \quad (13)$$

This is an expression for $\left(\frac{\partial\gamma}{\partial\alpha}\right)_{\mathrm{T},\,s_k,\,p_2}$ in terms of the quantity $\left(\frac{\partial \mathrm{T}}{\partial\alpha}\right)_\gamma$.

3. *Surface Tension and Free Energy.*

The conception of chemical potential can be developed from this method in a way to extend the recent work of Butler * to interphases that are thicker than a unimolecular layer. For the system shown in fig. 1 of the previous paper the equation

$$d\mathrm{Z} = \mathrm{V}_1 dp_1 + \mathrm{V}_2 dp_2 - \mathrm{S}d\mathrm{T} + \gamma ds + \delta\mathrm{W}'$$

reduces to

$$d\mathrm{Z} = \gamma ds + \delta\mathrm{W}'$$

* J. A. V. Butler, Proc. Roy. Soc. A, cxxxv. p. 348 (1932).

if p_1, p_2, and T are kept constant. Moreover, changes in s and γ can only be brought about by work $\delta W'$, so that the term γds represents an extra work term but no extra degree of freedom. If the whole system contains $N_i \ldots\ldots N_j \ldots\ldots N_s$ moles of chemical components $i \ldots\ldots j \ldots\ldots s$, then

$$\left[\frac{dZ}{dN_r}\right] = \gamma \frac{ds}{dN_r} + \underset{dN_r \to 0}{\text{Lt.}} \left(\frac{\delta W'}{dN_r}\right)_{p_1, p_2, T, N_k, s_k},$$

where N_k means that all the N's except N_r are kept constant.

If we merely consider a system as described in fig. 1 (see Part I.) there is no way of adding particles to the system without dismantling the pistons. But the importance of equation (7) arises if we consider the whole system in between the pistons to be divided up by a series of imaginary planes into a series of subsystems. If the whole system is left subject to the condition that $\delta W'$, dp_1, dp_2, and dT are all zero the system as a whole stays in equilibrium, but small virtual shifts from equilibrium may be supposed to occur by the passage of matter from one subsystem to another. This may be regarded for our present purpose as being brought about by work $\delta W_1'$ being done on a subsystem 1 and work $\delta W_2'$ being done on an adjacent subsystem 2. Since $\delta W'$ for the whole system is zero, it is clear that $\underset{dN_r \to 0}{\text{Lt.}} \left(\frac{\delta W'}{dN_r}\right)_{p_1, p_2, T, N_k, s_k}$ must be the same for every subsystem. For subsystems remote from the physical discontinuity of the interphase, this reduces to the partial molal free energy of component r in one or other or both phases, since $\left[\gamma \frac{ds}{dN_r}\right]_{p_1, p_2, T, N_k, s_k}$ is zero and $\left[\frac{dZ}{dN_r}\right]_{p_1, p_2, T, N_k, s_k}$ becomes the partial molal free energy of r for the bulk phases.

If we still call Z the free energy in the case of that subsystem that includes the interphase, the partial molal free energy of r, $\frac{dZ}{dN_r}$, is equal to the partial molal free energy of r in the bulk phases, namely

$$\underset{dN_r \to 0}{\text{Lt.}} \left(\frac{\delta W'}{dN_r}\right)_{p_1, p_2, T, N_k, s_k},$$

plus the term $\gamma \frac{ds}{d\mathrm{N}_r}$, which represents the additional work that has to be done if r is to be brought up from the bulk phase to the interphase.

The actual magnitude of $\gamma \frac{ds}{d\mathrm{N}_r}$ will depend on the quantity of bulk phase that is being included along with the interphase in the subsystem that contains the discontinuity of the surface, and it vanishes as the bulk phases are allowed to increase in size. Thus $\left[\frac{ds}{d\mathrm{N}_r}\right]_{p_1,\, p_2,\, \mathrm{T},\, \mathrm{N}_k,\, s_k}$ is brought about by changing N_r and so altering the composition of the matter near the surface, which alters γ and so s, until a new value of $\frac{dv_{12}}{ds_{12}}$ is reached where $(p_1-p_2)\frac{dv_{12}}{ds_{12}}$ is again equal to γ.

This expression has previously been obtained by Butler, who only applied it to a unimolecular interphase.

4. *The Gibbs Adsorption Equation.*

The equation

$$dZ=\mathrm{V}_1dp_1+\mathrm{V}_2dp_2-\mathrm{S}d\mathrm{T}+\gamma ds+\delta\mathrm{W}'$$

for a complete system has only three degrees of freedom corresponding to the first four terms on the right-hand side. Taking these three as p_2, T, and s, it is possible to replace $\delta\mathrm{W}'$ by

$$\delta\mathrm{W}''+\sum_{r=1}^{r=s} \underset{d\mathrm{N}_r\to 0}{\mathrm{Lt.}} \left(\frac{\delta\mathrm{W}'}{d\mathrm{N}_r}\right)_{p_2,\, \mathrm{T},\, s,\, s_k,\, \mathrm{N}_k},$$

where the suffix N_k shows that all the N's are kept constant except N_r. If the system be left so that p_2, T, and W'' are kept constant, and N_k is also constant, we have

$$dZ=\gamma ds+\mathrm{V}_1dp_1-\overline{\mathrm{W}}_r'd\mathrm{N}_r,$$

where

$$\underset{d\mathrm{N}_r\to 0}{\mathrm{Lt.}} \left(\frac{\delta\mathrm{W}'}{d\mathrm{N}_r}\right)_{p_2,\, \mathrm{T},\, s,\, \mathrm{W}'',\, \mathrm{N}_k} \equiv \overline{\mathrm{W}}_r'. \quad . \quad . \quad . \quad (14)$$

This may be transformed to

$$dZ'=\gamma ds+\mathrm{V}_1dp_1-\mathrm{N}_rd\overline{\mathrm{W}}_r',$$

where dZ' is a complete differential, and, taking s and W' as the two independent variables, this equation becomes

$$\left[dZ' = \left[\gamma + V_1\left(\frac{\partial p_1}{\partial s}\right)_{\bar{w}_r'}\right] ds - \left[N_r - V_1\left(\frac{\partial p_1}{\partial \bar{W}_r'}\right)_s\right] d\bar{W}_r'\right]_{p_2,\, T,\, W'',\, N_k,\, s_k}.$$

By cross differentiation this yields the equation

$$\left[\left(\frac{\partial \gamma}{\partial \bar{W}_r'}\right)_s \left[1 - \left(\frac{\partial p_1}{\partial \gamma}\right)_s \left(\frac{\partial V_1}{\partial s}\right)_{p_1}\right] = -\left(\frac{\partial N_r}{\partial s}\right)_{\bar{w}_r'}\right]_{p_2,\, T,\, W'',\, N_k,\, s_k}.$$

Clearly from equation (14) W' is equal to $\bar{F}_r$, the partial molal free energy of the species r in phase 2. The equation therefore becomes

$$\left[\left(\frac{\partial \gamma}{\partial \bar{F}_r}\right)_s \left[1 - \left(\frac{\partial p_1}{\partial \gamma}\right)_s \left(\frac{\partial V_1}{\partial s}\right)_{p_1}\right] = -\left(\frac{\partial N_r}{\partial s}\right)_{\bar{w}_r'}\right]_{p_2,\, T,\, W'',\, N_k,\, s_k} \quad . \quad (15)$$

This is the Gibbs adsorption equation generalized for a surface tension that allows interphases of finite thickness and small radii of curvature.

If the volume of phase 1 in contact with the interphase is reduced so that all $p_1 dV_1$ terms are very small compared with γds terms, the surface tension consists only of terms for the interphase that is being investigated, and the terms for the other interphases and the bulk phases become zero. In that case we obtain

$$\left[\left(\frac{\partial \gamma}{\partial \bar{F}_r}\right)_s = -\left(\frac{\partial N_r}{\partial s}\right)_{\bar{F}_r}\right]_{p_2,\, T,\, s,\, W'',\, N_k,\, s_k}, \quad . \quad (16)$$

which is the Gibbs adsorption equation. The exact value of $\left(\frac{\partial N_r}{\partial s}\right)_{\bar{F}_r}$ depends on the position that is taken for the boundary s.

In deducing equation (15),

$$\sum_{r=1}^{r=s}\left(\frac{\partial W'}{\partial N_r}\right)_{p_2,\,T,\,s,\,W'',\,N_k} . dN_r,$$

which represents the chemical work done on the system, was reduced to a single term by imposing the condition that all the N's except N_r were kept constant. Any other set of $(s-1)$ similar restrictions that would reduce it to a single term would be equally effective. Thus for example various partial molal free energies in the system could be kept constant instead of the total number of molecules of a given component. It is necessary, however, to remember that the system is a two-phase one, and so must have two independent variables that correspond to extensive properties quite apart from additional ones corresponding to the walls and pistons of the apparatus. Thus

$$[dZ=\gamma\, ds+[V_1 dp_1]+\bar{W}_r' dN_r]_{p_2,\,T,\,W'',\,N_q,\,L_k}$$

is a complete differential, and may be used if the two extensive variables are taken as N_r and N_q, which latter is kept constant. The suffix L_k denotes that for every chemical component in the system other than r and q either its partial molal free energy $\bar{F}_i$ or its quantity N_i is kept constant. W'' is not a suitable extensive variable, and therefore it is necessary to have at least one N kept constant outside. In order to keep dZ' a complete differential, where

$$[dZ'=\gamma\, ds+[V_1 dp_1]-N_r d\bar{W}_r'',$$

it is necessary to have at least two extensive factors other than W'' kept constant outside. Thus there is only a definite phase relationship between the two intensive factors γ and $\bar{W}_r'$ when the remaining variables contain at least two extensive properties.

Consequently equation (15) becomes in its more general form

$$\left[\left(\frac{\partial\gamma}{\partial F_r}\right)_s\left[1-\left(\frac{\partial p_1}{\partial\gamma}\right)_s\left(\frac{\partial V_1}{\partial s}\right)_{p_1}\right]\right.$$

$$\left.=-\left(\frac{\partial N_r}{\partial s}\right)_{\bar{F}_r}\right]_{p_2,\,T,\,W'',\,N_q,\,N_q',\,L_k}, \quad (17)$$

where L_k means that in the case of all the components excepting r, q, and q' either the partial molal free energy or the total quantity of that component is kept constant. The expression

$$\left(\frac{\partial N_r}{\partial s}\right)_{\bar{v}_r,\, p_2,\, T,\, N_q,\, N_{q'},\, L_k,\, s_k,\, W''}$$

is one that obeys the Gibbs adsorption equation for reasonably large radii of curvature, but it does not agree exactly with the usually accepted meaning of Γr as used by Gibbs. This difference will not be investigated until the discussion of the electrocapillary equations in the third paper of this series.

Summary.

By using the discussion of capillarity published in a previous paper expressions have been deduced for the temperature and pressure cofficients of surface tension. The former contains a term omitted by Gibbs, which would become significant for very small radii of curvature. These expressions have been extended so as to give an equation for the rate of change of surface tension with curvature of the surface. An expression due to Butler, which shows the difference in partial molal free energy of a substance when in the interphase and when in the bulk phases, is extended to a thick interphase by a method that illustrates in a novel way why the partial molal energy of a substance is the same throughout a whole phase. Finally, the Gibbs adsorption equation is rededuced, and the exact conditions under which it is valid are discussed.

One of us (S. R. C.) wishes to thank the Department of Scientific and Industrial Research for a grant to enable this work to be carried out.

Physical Chemistry Laboratory, Balliol & Trinity Colleges, Oxford, and the National Institute for Medical Research, Hampstead.

V. *The Hall Effect and some other Physical Constants of Alloys.* Part II.*—*The Tin-Bismuth Series of Alloys.* *By* W. Rheinallt Thomas, *M.Sc., and* Prof. E. J. Evans, *D.Sc., Physics Department, University College of Swansea* †.

THE effect of the variation of composition of an alloy on its physical properties depends largely on the nature of the constituents of the alloy. In some cases the curve showing the variation of the physical property with composition is continuous, but in others the curve is discontinuous at points corresponding to the presence of intermetallic compounds or phase changes. For the tin-bismuth series of alloys the most interesting and rapid changes in physical properties occur in the region of low tin content. In 1916 Bucher ‡ examined the electrical conductivity, the temperature coefficient of resistance, and the thermo-electrical properties of these alloys, and found in each case a well-defined singular point at a composition corresponding to a small percentage of tin.

The Hall effects of four alloys of low tin content were first examined by Ettingshausen and Nernst § in 1888. They discovered that the value of the Hall potential difference varied in a remarkable manner with increase in intensity of the magnetic field. For small fields the Hall potential difference was in the same direction as in bismuth (negative Hall coefficient), and after reaching a maximum value with increase of field diminished to zero, and finally reversed its direction with further increase in the intensity of the magnetic field. This reversal of the Hall effect for a few alloys of low tin content has since been confirmed by the experiments of A. W. Smith ||.

In the present experiments the Hall coefficients of the tin-bismuth alloys have been measured over a much wider range of composition; and, in addition, determinations of other physical constants, such as resistivity,

* For Part I. see Phil. Mag. xvi. p. 329 (1933).
† Communicated by the Authors.
‡ *Zeit. Anorg. Chemie,* xcviii. p. 97 (1916).
§ Wied. *Ann.* xxxiii. p. 474 (1888).
|| Phys. Rev. x. p. 358 (Oct. 1917).

temperature coefficient of resistance, thermoelectric power, and density have been carried out on the same material.

As the physical properties of alloys depend largely on their state, special attention was paid to annealing, and the final values of the constants given in this paper correspond to the annealed state. The equilibrium diagram of the tin-bismuth series has been the subject of many researches, and a diagram constructed from the results of these investigations is given by Guertler *. At room-temperature there is a solid solution (I.) of tin in bismuth over the small range of composition from 0 to about ·5 per cent. tin at the bismuth end of the series, and a solid solution of bismuth in tin (III.) over the range of composition from 0 to about 6 per cent. bismuth at the tin end of the series.

The remaining compositions consist of a heterogeneous mixture of I. and III. An equilibrium diagram of the system is also given in the 'International Critical Tables' †. According to this diagram at temperatures below 95° C. there exists a solid solution of tin in bismuth (α-phase) over a small range of composition at the bismuth end of the series, and the remaining compositions correspond to mixtures of α+tin.

Solomon and Jones ‡ examined the crystal structure of an alloy containing equal percentages by weight of tin and bismuth by means of the X-ray powder method, and found a mixture of the lattices of the two pure metals. They concluded that the alloys of tin and bismuth are just mixtures of the crystalline phases of the component elements. The curves showing the variation of resistivity and temperature coefficient of resistance with composition indicate the presence of discontinuities at compositions corresponding to small percentages by weight of tin, and these singular points are, in all probability, connected with the formation of a solid solution of tin in bismuth. Solomon and Jones §, however, point out that the solution of a small percentage (about one per cent.) of tin in bismuth is not sufficient to produce a measurable change in the dimensions of the bismuth lattice.

* *Metallographie*, Bd. i. p. 738.
† 'International Critical Tables,' ii. p. 416.
‡ Phil. Mag. xi. p. 1090 (May 1931).
§ *Loc. cit.*

Preparation of Plates.

The alloy plates were prepared from nearly pure specimens of bismuth and tin, the impurities in the bismuth not exceeding 0·1 per cent., and in the tin not exceeding 0·011 per cent. The chief impurities in the bismuth expressed as percentages by weight were :

Silver.....	·01
Lead	·06
Iron	·01

Similarly, the chief impurities in the tin were :

Copper	·0005
Lead	·003
Bismuth	·0005
Iron	·002

The melting-point of a bismuth-tin alloy steadily decreases from about 232° C. as the percentage of bismuth increases, until it reaches a minimum value at the composition of the eutectic. The eutectic consists of 58 per cent. by weight of bismuth and 42 per cent. by weight of tin, and has a melting-point of 137° C. The melting-points of the remaining alloys lie between 137° C. and the melting-point (269° C.) of bismuth. All the alloys could, therefore, be prepared at comparatively low temperatures, and the two metals in the desired proportion by weight were melted in a crucible by the application of a Bunsen flame. A little oxidation of the melt was observed under ordinary conditions, but this was practically eliminated by melting the alloys in a covered crucible in an atmosphere of nitrogen. Although tin and bismuth are known to alloy readily, it was considered advisable to keep the melt well stirred in order to ensure uniformity in the composition of the alloy. The melt was then poured into a heated graphite mould of the required dimensions and allowed to cool. Several plates were prepared with a tin content of between 0 and 6 per cent. by weight, as the most rapid variation in the values of the different physical constants with composition occurs in this region. Furthermore, the values of the Hall coefficients could be more readily measured for alloys of low tin content. The plates as cast had fairly uniform dimensions, but since accurate measurements of the resistivities and Hall coefficients

were desired the plates were filed down until the variations in dimensions were almost eliminated. The specimens finally prepared were approximately 15 cm. long, 2·5 cm. broad, and 0·25 cm. thick.

Chemical Analysis.

The compositions of the various alloys were determined by estimating their tin contents. In the method adopted the tin was converted into the chloride, and the hot solution of the latter was reduced by nickel, then cooled in an atmosphere of carbon-dioxide and titrated with iodine in the presence of starch. The tin content of each alloy was determined several times, and the results agreed to

TABLE A.

Percentage composition by weight.

Per cent.	Per cent.	Per cent.	Per cent.	Per cent.	Per cent.
0 Bi	100 Sn	90·5 Bi	9·5 Sn	98 Bi	2 Sn
20 Bi	80 Sn	92·0 Bi	8·0 Sn	98·5 Bi	1·5 Sn
37 Bi	63 Sn	92·05 Bi	7·95 Sn	99 Bi	1 Sn
46·7 Bi	53·3 Sn	93·87 Bi	6·13 Sn	99·07 Bi	0·93 Sn
58 Bi	42 Sn	94·0 Bi	6·0 Sn	99·46 Bi	0·54 Sn
68 Bi	32 Sn	95·1 Bi	4·9 Sn	99·81 Bi	0·19 Sn
77·8 Bi	22·2 Sn	96·0 Bi	4·0 Sn	100 Bi	0 Sn
88 Bi	12 Sn	97·6 Bi	2·4 Sn		

within 0·2 per cent. The percentage weight of bismuth was found by difference. The values obtained in this way were in good agreement with those calculated from the known masses of the two metals employed in the preparation of the alloys. The percentage composition of the various alloy plates is given in Table A.

Annealing.

According to the equilibrium diagram * a change of phase occurs at 95° C. for alloys containing between 0 and 97 per cent. of bismuth. The alloys were therefore annealed in a vacuum electric furnace over a period of several weeks at a temperature a few degrees below 95° C. At intervals the resistivities of the alloys at 0° C. were

* 'International Critical Tables,' *loc. cit.*

measured, and the process of annealing was continued until the resistivities assumed practically constant values.

The temperature of the annealing furnace was then reduced to about 40° C. in three stages, and was kept

TABLE I.

Composition by weight. Bi.	Resistivity at 0° C. in microhms per cm.³	
	Before annealing.	After annealing.
per cent.		
0	11·4	10·6
20	17·8	16·3
37	24·4	23·3
46·7	32·3	27·9
58	45·4	37·6
68	61·9	57·2
77·8	95·5	86·0
88	157·0	155·0
90·5	198·1	195·0
92	208·0	225·6
92·05	225·4	231·2
93·87	250·8	271·0
94·0	237·0	274·6
95·1	290·4	303·5
96	289·0	333·7
97·6	353·8	362·7
98	341·0	372·7
98·5	356·0	386·5
99	381·0	392·8
99·07	367·7	373·0
99·46	354·9	359·6
99·81	..	152·7
100.....	107·5	108

constant for weeks at each of the three temperatures 80° C., 60° C., and 40° C. The annealing at the lowest temperature (40° C.) was continued until the resistivity of each plate remained constant.

Measurement of Physical Constants.

As the methods employed in the determination of the Hall coefficients and other physical constants of the various alloys have been already described in detail, in a paper dealing with the physical properties of the lead-bismuth series (Part I.) *, it is only necessary to make a brief reference to a few points connected with the measurements.

Graph I.

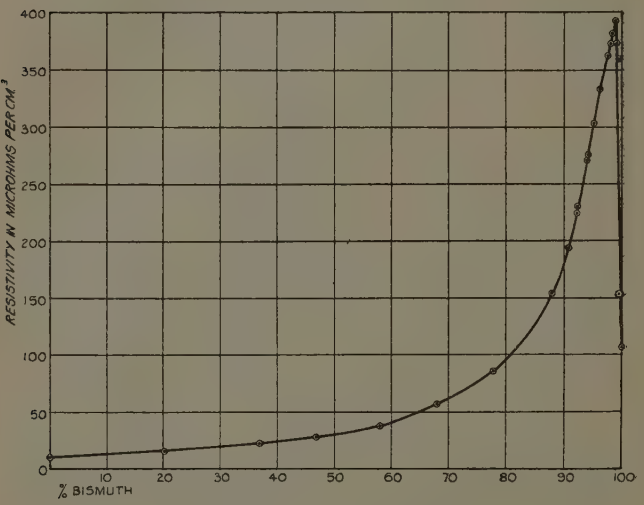

Resistivity.—Composition curve.

Resistivity.

The experimental results are collected in Table I. and plotted in Graph I. It is estimated that on the average the experimental errors are not greater than 0·3 per cent.

Mean Temperature Coefficient of Resistance.

The temperature coefficients of resistance of the alloys were determined over the two ranges of temperature

* Part I. *loc. cit.*

0°–20° C. and 0°–40° C., and the results showed that the temperature coefficient of each alloy was practically independent of the temperature difference. The results are collected in Table II. and plotted in Graph II., and it is estimated that the experimental errors are not greater than 0·4 per cent. on the average.

Thermoelectric Power.

The mean thermoelectric powers of the alloys with respect to pure electrolytic copper have been determined over the temperature range 0°–40° C. Experiments, which were carried out over smaller temperature ranges in the above region, have, however, shown that there exists a linear relation between the E.M.F. and temperature difference. The errors in the determinations are estimated to be not greater than 0·4 per cent. on the average, and the results are given in Table III. and plotted in Graph III.

Density.

The results of the density determinations are shown in Table IV. and Graph IV.

Hall Effect.

The Hall coefficients of both bismuth and tin are negative at room-temperature, but the magnitude of the coefficient is much greater in the case of bismuth. In addition, as previously mentioned, the tin-bismuth alloys exhibit the phenomenon of reversal of the Hall coefficient as the intensity of the magnetic field is increased. The accuracy of the experimental results, therefore, depends on the composition of the alloy and also on the intensity of the magnetic field. In the case of some alloys the error in the determination of the Hall coefficient is less than one per cent.; but for alloys of comparatively large tin content and for others under the influence of magnetic fields of almost sufficient magnitudes to produce a reversal of the Hall coefficient, the error is proportionally greater. The experimental results are given in Table V. and plotted in Graphs V., VI., and VII.

TABLE II.

Composition by weight. Bi.	Mean temp. coeff. of resistance between 0° and 40° C. × 10^4.	Composition by weight. Bi.	Mean temp. coeff. of resistance between 0° and 40° C. × 10^4.
per cent.		per cent.	
0	44·8	94	20·11
20	31·56	95·1	18·72
37	29·91	96	17·63
46·7	29·45	97·6	14·37
58	28·61	98	13·32
68	27·62	98·5	15·45
77·8	26·13	99	17·71
88	23·45	99·46	23·48·
90·5	22·25	99·81	28·12
92	21·50	100	39·7

Graph II.

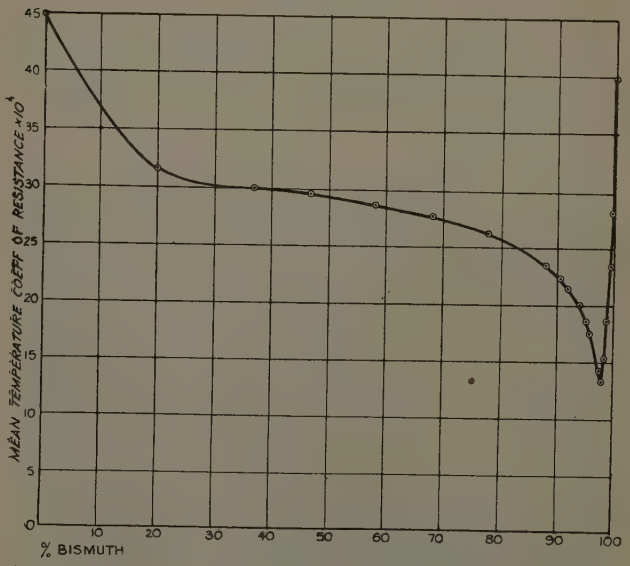

Mean temperature coefficient.—Composition.

TABLE III.

Composition by weight. Bi.	Thermoelectric power with reference to copper in microvolts per degree C.	Composition by weight. Bi.	Thermoelectric power with reference to copper in microvolts per degree C.
per cent.		per cent.	
0.....	− 3·09	94	+22·19
20.....	− 2·01	96	+21·07
37.....	− 2·15	97·6	+19·02
46·7	− 2·51	98	+18·80
58.....	− 2·81	98·5	+17·23
68.....	− 1·78	99	+13·34
77·8	+ 3·04	99·07	+ 6·89
88.....	+13·70	99·46	−18·89
92.....	+18·90	99·81	−25·30
92·05 ..	+20·01	100	−64·80

Graph III.

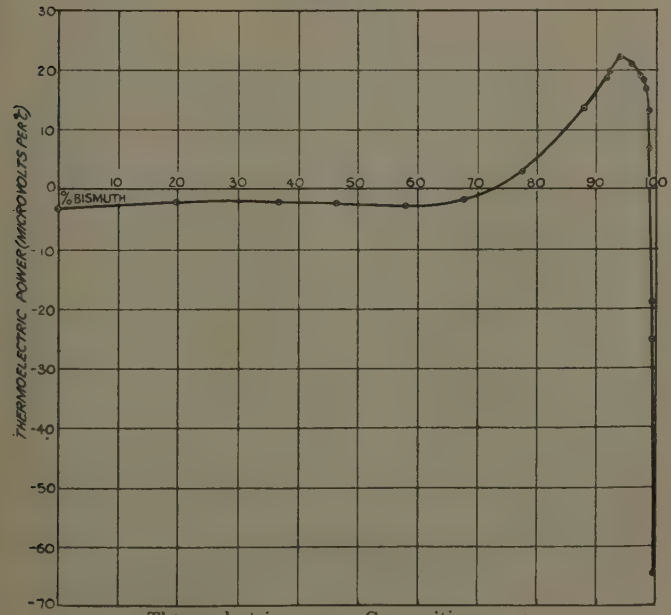

Thermoelectric power.—Composition curve.

TABLE IV.

Composition by weight. Bi.	Density in grams per c.c. at 16° C.	Composition by weight. Bi.	Density in grams per c.c. at 16° C.
0	7·28	93·87	9·56
20	7·72	94	9·58
37	8·11	95·1	9·61
46·7	8·31	96	9·64
58	8·60	97·6	9·70
68	8·84	98	9·72
77·8	9·08	98·5	9·74
88	9·38	99	9·79
90·5	9·45	99·46	9·88
92	9·51	99·81	9·83
92·05	9·53	100.....	9·80

Graph IV.

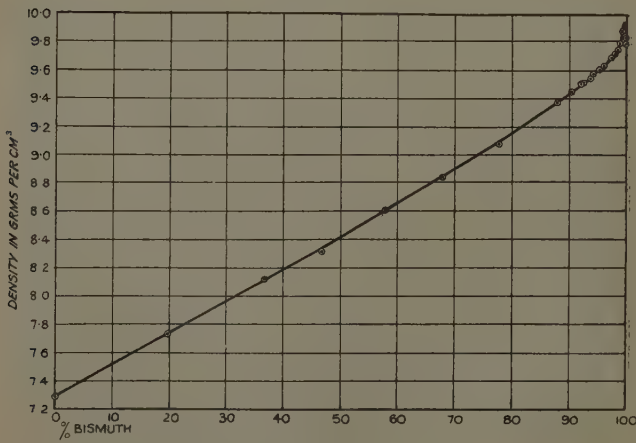

Density.—Composition curve.

Table V.

Composition by weight. Bi.	Hall coefficients. Magnetic fields in gauss. 3096	4630	5787	6795	7661	8424	Temperature in ° C.
per cent.							
100.....	$-7{\cdot}23$	$-6{\cdot}58$	$-6{\cdot}12$	$-5{\cdot}86$	$-5{\cdot}75$	$-5{\cdot}62$	13°
99·8	$-1{\cdot}767$	$-1{\cdot}279$	$-9{\cdot}14\times10^{-1}$	$-6{\cdot}06\times10^{-1}$	$-3{\cdot}37\times10^{-1}$	$-1{\cdot}06\times10^{-1}$	16°
99.....	$-1{\cdot}14\times10^{-1}$	$+7{\cdot}46\times10^{-2}$	$+1{\cdot}89\times10^{-1}$	$+3{\cdot}01\times10^{-1}$	$+3{\cdot}46\times10^{-1}$	$+3{\cdot}95\times10^{-1}$	19°
98·5	$-7{\cdot}98\times10^{-2}$	$+1{\cdot}11\times10^{-1}$	$+2{\cdot}13\times10^{-1}$	$+2{\cdot}92\times10^{-1}$	$+3{\cdot}34\times10^{-1}$	$+3{\cdot}70\times10^{-1}$	17°
98.....	$-5{\cdot}25\times10^{-2}$	$+1{\cdot}34\times10^{-1}$	$+2{\cdot}37\times10^{-1}$	$+2{\cdot}85\times10^{-1}$	$+3{\cdot}17\times10^{-1}$	$+3{\cdot}55\times10^{-1}$	17°
96.....	$+4{\cdot}46\times10^{-2}$	$+1{\cdot}68\times10^{-1}$	$+2{\cdot}10\times10^{-1}$	$+2{\cdot}43\times10^{-1}$	$+2{\cdot}63\times10^{-1}$	$+2{\cdot}87\times10^{-1}$	20°
94.....	$+1{\cdot}23\times10^{-1}$	$+1{\cdot}59\times10^{-1}$	$+1{\cdot}81\times10^{-1}$	$+2{\cdot}00\times10^{-1}$	$+2{\cdot}14\times10^{-1}$	$+2{\cdot}28\times10^{-1}$	19°
92.....	$+9{\cdot}45\times10^{-2}$	$+1{\cdot}20\times10^{-1}$	$+1{\cdot}37\times10^{-1}$	$+1{\cdot}52\times10^{-1}$	$+1{\cdot}62\times10^{-1}$	$+1{\cdot}71\times10^{-1}$	17°
88.....	$+4{\cdot}19\times10^{-2}$	$+5{\cdot}74\times10^{-2}$	$+6{\cdot}80\times10^{-2}$	$+7{\cdot}74\times10^{-2}$	$+8{\cdot}34\times10^{-2}$	$+9{\cdot}03\times10^{-2}$	16°
77·8	$+2{\cdot}62\times10^{-3}$	$+5{\cdot}19\times10^{-3}$	$+9{\cdot}81\times10^{-3}$	$+1{\cdot}37\times10^{-2}$	$+1{\cdot}64\times10^{-2}$	$+1{\cdot}76\times10^{-2}$	17°
68.....	$-4{\cdot}72\times10^{-3}$	$-1{\cdot}23\times10^{-3}$	$+1{\cdot}31\times10^{-3}$	$+3{\cdot}03\times10^{-2}$	$+4{\cdot}02\times10^{-3}$	$+4{\cdot}70\times10^{-3}$	15°
58.....	$-2{\cdot}78\times10^{-3}$	$-8{\cdot}39\times10^{-4}$	$+7{\cdot}14\times10^{-4}$	$+1{\cdot}84\times10^{-3}$	$+2{\cdot}72\times10^{-3}$	$+3{\cdot}35\times10^{-3}$	16°
46·7	$-7{\cdot}83\times10^{-4}$	$-1{\cdot}53\times10^{-4}$	$+3{\cdot}61\times10^{-4}$	$+6{\cdot}78\times10^{-4}$	$+9{\cdot}18\times10^{-4}$	$+1{\cdot}13\times10^{-3}$	16°
37.....	$-3{\cdot}46\times10^{-4}$	— —?	$+2{\cdot}09\times10^{-4}$	$+4{\cdot}24\times10^{-4}$	$+5{\cdot}74\times10^{-4}$	$+6{\cdot}21\times10^{-4}$	16°
100.....		*$-4{\cdot}0\times10^{-5}$ —	—	—	—	—	—

* Campbell, 'Galvanomagnetic and Thermomagnetic Effects,' p. 124.

Experimental Results.

As pointed out in the introduction to this paper, the most rapid variations in the physical properties of the alloys of the tin-bismuth series with composition occur in the region of low tin content. The curves connecting the electrical resistivity, the temperature coefficient of resistance, the thermoelectric power, and the density

Graph V.

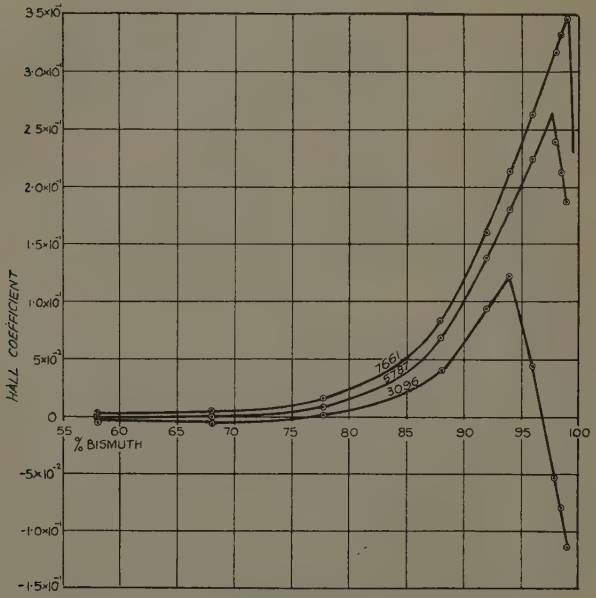

Hall coefficient.—Composition curve for magnetic fields 3096, 5787, 7661 gauss.

with the percentage by weight of bismuth in the alloys, exhibit in the above region either a well-defined maximum or minimum at a composition which depends on the nature of the physical property examined. In this respect the results are in agreement with those previously obtained for the alloys of the lead-bismuth series *.

* Thomas and Evans, Phil. Mag. *loc. cit.*

Since tin and lead belong to the same group in this periodic table, some resemblance in the physical properties of the tin-bismuth and the lead-bismuth alloys is to be expected. This resemblance is well brought out by comparing the two curves, which represent for the above systems the variation of a given electrical property with composition.

Graph VI.

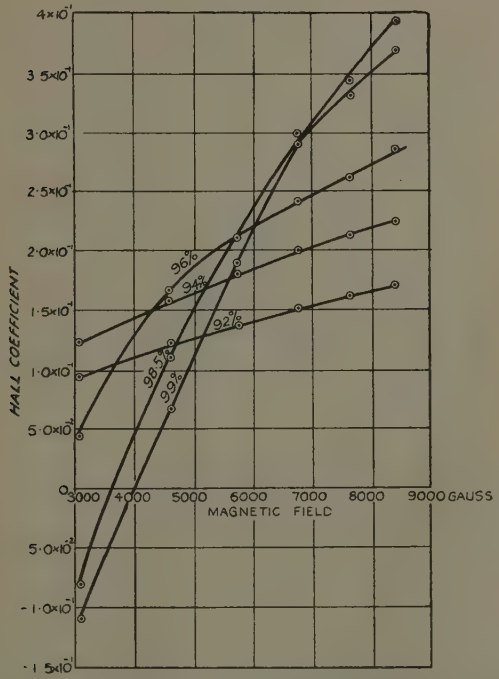

Showing relation between Hall coefficients and field strengths for alloys of high bismuth content.

The resistivity-composition curve (Graph I.) shows that the resistivity increases slowly and approximately linearly as the percentage weight of bismuth is increased from 0 to 50, then more rapidly over the range of composition from 50–85, and finally very rapidly to a maximum for the alloy containing about 99 per cent. of bismuth.

The resistivity then falls very rapidly to the value for pure bismuth. Although the tin-bismuth resistivity-composition curve is very similar to that obtained for lead-bismuth, the variation in the resistivity of the tin-bismuth alloys over the range of composition from 85 per cent. bismuth to the point of maximum resistivity is much more rapid than for the lead-bismuth alloys over the corresponding range. In addition, the point

Graph VII.

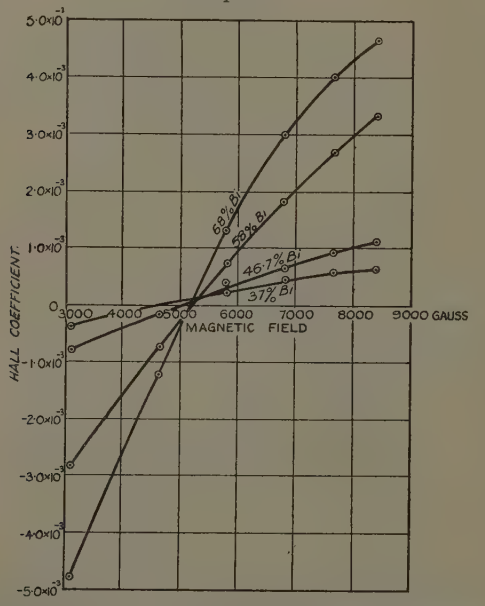

Showing relation between Hall coefficients and field strengths for alloys of lower bismuth content.

of maximum resistivity of the lead-bismuth series occurs at the composition 96 per cent. bismuth.

An account of the earlier experiments on the conductivities of the alloys of the tin-bismuth system is given by Guertler *. The resistivity-composition curve

* Guertler, *Metallographie*, Bd. ii. Eigenschaften, T. II. Hft. 6, pp. 335–340.

obtained in the present investigation is in general agreement with that determined by Bucher, who found that an alloy containing about 1·7 per cent. of tin by weight possessed the maximum resistivity.

According to the equilibrium diagram given in the 'International Critical Tables' there is, below 95° C., a solid solution of tin in bismuth in tin at the bismuth end of the series. There is, however, some uncertainty with regard to the limit of solubility of tin in bismuth at various temperatures, and the diagram is not given below about 70° C. The diagram given by Guertler is much more complete and indicates the presence of solid solutions at both ends of the series. In this diagram also there is uncertainty concerning the limits of solubility at both ends of the series, and the nature of the changes taking place at the tin end of the series at temperatures between 0 and 25° C. In the present experiments no data are available for testing the limit of solubility (if any) at the tin end of the series; but Bucher's results for the conductivities at 20° C. of tin-bismuth alloys of low bismuth content (0 to 21 per cent. by weight) do not show a well-defined discontinuity at the tin end of the series.

The effect of annealing on the resistivities is shown in Table I. The resistivities of the alloys containing from 0 to 90·5 per cent. bismuth were diminished by annealing, and the resistivities of the alloys containing more than 90·5 per cent. of the bismuth were increased.

The main feature of the temperature coefficient of resistance-composition curve (Graph II.) of the tin-bismuth series is the well-defined minimum at the composition corresponding to 98 per cent. by weight of bismuth. The minimum previously determined for the lead-bismuth series of alloys occurs at the same percentage weight of bismuth, and the corresponding curves have the same general characteristics. The temperature coefficient of the tin-bismuth alloys diminishes fairly rapidly over the range of composition from 0–20 per cent. bismuth, then comparatively slowly over the range 20–80 per cent., and finally much more rapidly to the minimum value at 98 per cent. bismuth. The temperature coefficient then rises rapidly to the value for pure bismuth. The variation in the temperature coefficient of the tin-bismuth alloys with composition in the neighbourhood

of the minimum is less rapid than the corresponding variation for the lead-bismuth alloys. In addition, the tin-bismuth alloys do not give negative temperature coefficients in the neighbourhood of the minimum, as is the case for the lead-bismuth alloys.

Bucher plotted the percentage change of conductivity between 25° and 100° C. $\left[i.e., 100\left(\frac{\lambda_{25}-\lambda_{100}}{\lambda_{25}}\right)\right]$ against the atomic percentages of bismuth in the various alloys and found discontinuities in the curve at the compositions 14, 72, and 97·1 atoms per cent. In the present investigation observations were carried out over a smaller temperature range (0°–40° C.), and the temperature coefficient composition curve shows no discontinuities at 14 and 72 atoms per cent. The highest temperature at which measurements were carried out was 40° C., and this is well below the temperature (95° C.) at which a change of phase occurs in the system.

Although Solomon and Jones *, from an X-ray examination of the alloy containing equal percentages by weight of tin and bismuth, concluded that all the alloys of the series are just mixtures of the crystalline phases of the component elements, the resistivity-composition and the temperature coefficient of resistance-composition curves seem to indicate the presence of a solid solution of tin in bismuth at the bismuth end of the series. It is, however, impossible to fix the limit of solubility from the experimental results, as the maximum in the resistivity curve does not occur at the same composition as the minimum in the temperature-coefficient curve. The same difficulty is also encountered when the variation of each of the other physical properties with composition is examined.

The thermoelectric power-composition curve (Graph III.) of the tin-bismuth alloys does not show either a maximum or a minimum at the compositions 98 and 99 per cent. bismuth. The curve rises very rapidly in the region between 100 and 98·5 per cent. bismuth, and then more slowly to a maximum at the composition 94 per cent. bismuth. The general nature of the tin-bismuth curve is very similar to the corresponding

* Solomon and Jones, *loc. cit.*

lead-bismuth curve, but the maximum in the latter occurs at about 68 per cent. bismuth.

The effect of annealing on the thermoelectric powers of some alloys is fairly considerable, and is shown in Table VI. below. In the case of the plates marked with an asterisk the results of the thermoelectric power measurements showed that the annealing was nearly but not quite complete.

The distinctive feature of the density-composition curve (Graph IV.) is the sudden rise and fall in density near the bismuth-end of the series. The rapid change in density occurs over the range of composition from 98·5 to 100 per cent. bismuth, and an alloy containing about

TABLE VI.

Composition by weight. Bi.	Thermoelectric power in microvolts per ° C.	
	Before annealing.	After annealing.
per cent.		
99·46	−19·5	−18·89
99·07	+ 9·62	+ 6·89
97·6	+26·2	+19·02
*95·1	+26·16	+22·43
*93·9	+38·4	+22·91
92·05	+33·6	+20·01
*90·5	+30·1	+18·26

* The values of the other physical properties for plates marked with an asterisk were constant within experimental error.

99·5 per cent. bismuth and 0·5 per cent. tin has the maximum density.

The density-composition curve is almost linear over the range between 0 and 80 per cent. bismuth. The relation between the density and composition of the lead-bismuth alloys is also almost linear over the greater part of the range, but in this case there is a rapid fall and rise in density near the bismuth end of the series, and an alloy containing about 99 per cent. of bismuth has the minimum density.

The Hall coefficients of the tin-bismuth system are of great interest owing to the reversals of sign, which occur when the magnetic field is increased. The Hall

coefficient-composition curves for magnetic fields of 3096, 5787, and 7661 gauss are plotted in Graph V. The three curves are similar in shape and show discontinuities at compositions which depend on the magnitude of the magnetic field. The discontinuity (maximum) occurs at a composition of 94 per cent. bismuth for a magnetic field of 3096 gauss, and shifts towards a composition of higher bismuth content as the intensity of the magnetic field is increased. An examination of Table V. shows that for magnetic fields of 6795, 7661, and 8424 gauss, the maximum on the curves occurs approximately at the composition 99 per cent. of bismuth. Starting from the bismuth end of the series the curves rise rapidly to a maximum and then fall rapidly until the composition 88 per cent. of bismuth is reached. This rapid rise and fall at the bismuth end of the series is also characteristic of the lead-bismuth series, but in this case the maximum always occurs at the same composition for all fields, and is followed by a minimum. An examination of Table V. and Graph V. for the tin-bismuth series shows that the three curves cross the axis of zero Hall coefficient near the bismuth end. The lowest curve also crosses the zero axis at the point corresponding to about 77 per cent. of bismuth. Since the Hall coefficient of tin is negative, it follows that the curves corresponding to 5787 and 7661 gauss must cross the axis at compositions of lower bismuth content than shown in the graph. Therefore, for a given magnetic field there are alloys of definite composition which have a zero Hall coefficient, but a satisfactory explanation of this result is difficult on existing theories.

The variation of the Hall coefficient with magnetic field for alloys of known compositions is plotted in Graphs VI. and VII. The graphs show the reversal of the Hall coefficient for some of these alloys. It is seen, from an examination of the curves showing reversal, that as the magnetic field increases from its lowest value to that required for reversal, the negative value of the Hall coefficient of an alloy of given composition continually diminishes. This result is also true of pure bismuth and of the alloy containing 99·8 per cent. bismuth, but in both cases the Hall coefficient does not reverse for the highest field (8424 gauss) employed in the present experiments. The graphs also show that the magnetic

field required to produce a reversal of the sign of the Hall coefficient depends upon the composition of the alloy. Further experiments are now in progress on the Hall coefficients of the tin-bismuth and lead-bismuth alloys in much weaker magnetic fields. The reversal of the sign of the Hall coefficients of the tin-bismuth alloys with increasing magnetic field has also been observed for a few alloys of low tin content by Ettingshausen and Nernst * and by A. W. Smith †, but their values of the magnetic fields required for reversal are in disagreement with each other and with those obtained in the present experiments.

This discrepancy may, however, be due to differences in the heat treatment of the alloys, as the results of a few experiments carried out on lead-bismuth alloys ‡ seem to indicate. In a subsequent communication experiments on the Hall coefficients on unannealed plates will be described.

The authors are indebted to Mr. R. E. James, M.Sc., who carried out a number of preliminary experiments on the physical properties of the system discussed in this paper.

July 1933.

VI. *Tapered Loaded Submarine Cable.*

By A. T. Starr, *M.A.*, *B.Sc.* (*Faraday House*) §.

Introduction.

In order to obtain duplex working on loaded submarine telegraph cables it is necessary to vary the loading from light (or even no) loading at the ends to a higher loading in the middle. Mr. Fielder has described some cases and some measurements (' Institution of Electrical Engineers,' Jan. 1932, p. 169). His theoretical work on the value of the sea-earth terminating resistance uses a method of approximation due to Rosen. In this paper

* Ettingshausen and Nernst, *loc. cit.*
† A. W. Smith, *loc. cit.*
‡ Thomas and Evans, *loc. cit.*
§ Communicated by the Author.

the solution of the linearly tapered line is used to obtain exact results.

Linearly Tapered Line.

The solution of this problem has been given by the author ('Proceedings of the Institute of Radio Engineers,' June 1932, pp. 1052–1063), and is as follows. Let the series impedance per unit length be

$$\mathrm{Z}=zx \quad . \quad . \quad . \quad . \quad . \quad . \quad . \quad (1)$$

and the shunt admittance per unit length be

$$\mathrm{Y}=\text{a constant}. \quad . \quad . \quad . \quad . \quad . \quad . \quad (2)$$

Then, if v and i are the potential and current at distance x from the origin, we have

$$\left.\begin{aligned} v&=\mathrm{A}f_1(x)+\mathrm{B}f_2(x) \\ \text{and} \qquad i&=\mathrm{A}f_3(x)+\mathrm{B}f_4(x) \end{aligned}\right\}, \quad . \quad . \quad . \quad . \quad (3)$$

where

$$\left.\begin{aligned} f_1(x)&=x\mathrm{J}_{2/3}\left(\frac{2}{3}j\sqrt{\mathrm{Y}z}\,x^{3/2}\right), \\ f_2(x)&=x\mathrm{J}_{-2/3}\left(\frac{2}{3}j\sqrt{\mathrm{Y}z}\,x^{3/2}\right), \\ f_3(x)&=-j\sqrt{\frac{\mathrm{Y}}{z}}\,x^{1/2}\mathrm{J}_{-1/3}\left(\frac{2}{3}j\sqrt{\mathrm{Y}z}\,x^{3/2}\right), \\ \text{and} \qquad f_4(x)&=j\sqrt{\frac{\mathrm{Y}}{z}}\,x^{1/2}\mathrm{J}_{1/3}\left(\frac{2}{3}j\sqrt{\mathrm{Y}z}\,x^{3/2}\right), \end{aligned}\right\} \quad . \quad . \quad (4)$$

J being the Bessel function.

In the actual cable let the inductance per unit length at a distance l from the beginning be

$$\mathrm{L}=\mathrm{L}_0+k_{\mathrm{L}}l \quad . \quad . \quad . \quad . \quad . \quad . \quad (5a)$$

and resistance per unit length be

$$\mathrm{R}=\mathrm{R}_0+k_{\mathrm{R}}l, \quad . \quad . \quad . \quad . \quad . \quad . \quad (5b)$$

and the capacity and leakance per unit length be C and G, so as to agree with the notation of Arnold and Bechberger ('Proceedings of the Institute of Radio Engineers,' Feb. 1931, p. 304).

Then

$$Z=(R_0+k_R l)+jw(L_0+k_L l)$$
$$=(R_0+jwL_0)+(k_R+jwk_L)l \quad . \quad . \quad . \quad (6a)$$

and $$Y=G+jwC. \quad . \quad . \quad . \quad . \quad . \quad (6b)$$

If we put

$$z=k_R+jwk_L \quad . \quad . \quad . \quad . \quad . \quad . \quad (7a)$$

and $$x=l+(R_0+jwL_0)/(k_R+jwk_L) \quad . \quad . \quad . \quad (8)$$

equation (6*a*) gives $Z=zx$, and the solution is given by equations (3) and (4) with the provisions of (7) and (8).

The expression in the brackets of equations (4) is

$$\frac{2}{3}j\sqrt{(G+jwC)(k_r+jwk_L)}\,(Z/z)^{3/2}$$
$$=\frac{2}{3}j\sqrt{(G+jwC)}(R+jwL)^{3/2}/(k_R+jwk_L)=u, \text{ say.} \quad (8a)$$

Line of Length l.

Let us consider the line from $l=0$ to $l=l$ as a four-terminal network, with a pair of input and a pair of output terminals. Then if i_1, v_1 and i_2, v_2 are the input and output currents and voltages

$$\left.\begin{aligned} i_1&=ai_2+bv_2,\\ v_1&=ci_2+dv_2,\end{aligned}\right\} \quad . \quad . \quad . \quad . \quad . \quad . \quad (9)$$

where

$$\left.\begin{aligned} a&=[f_4(x_1)f_1(x_2)-f_3(x_1)f_2(x_2)]/D,\\ b&=[f_3(x_1)f_4(x_2)-f_4(x_1)f_3(x_2)]/D,\\ c&=[f_2(x_1)f_1(x_2)-f_1(x_1)f_2(x_2)]/D,\\ d&=[f_1(x_1)f_4(x_2)-f_2(x_1)f_3(x_2)]/D,\\ D&=[f_2(x_2)f_3(x_2)-f_1(x_2)f_4(x_2)],\end{aligned}\right\} \quad . \quad . \quad (10)$$

and

$$\left.\begin{aligned} x_1&=(R_0+jwL_0)/(k_R+jwk_L),\\ x_2&=l+x_1.\end{aligned}\right\} \quad . \quad . \quad . \quad . \quad (11)$$

a, b, c, d are the parameters of this network. We can obtain the image parameters of the line, and they are

$$\left.\begin{aligned} Z_1&=\sqrt{cd/ab},\\ Z_2&=\sqrt{ac/bd},\end{aligned}\right\} \quad . \quad . \quad . \quad . \quad (12)$$

and $$T=\log_e(\sqrt{ad}+\sqrt{bc}).$$

formulæ derived by the author (*loc. cit.*). Z_1 and Z_2 are the image impedances, which are defined by the conditions that Z_1 is the impedance looking in at $x=x_1$ when $x=x_2$ is terminated by Z_2; and Z_2 is the impedance looking in at $x=x_2$ when $x=x_1$ is terminated by Z_1. When the network is symmetrical Z_1 and Z_2 are equal to one another and to the characteristic impedance. Here Z_1 and Z_2 are not equal: this results in unequal current and voltage attenuation.

Suppose the line is terminated by the impedance Z_t at $x=x_2$. Then

$$v_2 = i_2 Z_t. \quad . \quad . \quad . \quad . \quad . \quad . \quad (13)$$

By equations (13) and (9) we see that the impedance looking in at $x=x_1$ is

$$Z_i = v_1/i_1 = (ci_2 + dZ_t i_2)/(ai_2 + bZ_t i_2),$$

i. e.,

$$Z_i = (c + dZ_t)/(a + bZ_t). \quad . \quad . \quad . \quad . \quad . \quad . \quad (14)$$

For the sake of completeness Z_i will be found in terms of Z_t and the image parameters.

In addition to equations (12), a, b, c, d satisfy

$$ad - bc = 1. \quad . \quad . \quad . \quad . \quad . \quad . \quad (15)$$

(12) gives

$$\sqrt{ad} + \sqrt{bc} = e^{T},$$

and by division

$$\sqrt{ad} - \sqrt{bc} = e^{-T};$$

so that

$$\sqrt{ad} = \cosh T,$$

and

$$\sqrt{bc} = \sinh T,$$

$$Z_1 Z_2 = c/b,$$

and

$$Z_1/Z_2 = d/a;$$

so that

$$\left.\begin{aligned} a &= \cosh T . \sqrt{Z_2/Z_1}, \\ b &= \sinh T/\sqrt{Z_1 Z_2}, \\ c &= \sinh T . \sqrt{Z_1 Z_2}, \\ d &= \cosh T . \sqrt{Z_1/Z_2}. \end{aligned}\right\} \quad . \quad . \quad . \quad . \quad (16)$$

Thus

$$Z_i = Z_1 \frac{Z_2 \sinh T + Z_l \cosh T}{Z_2 \cosh T + Z_l \sinh T} \quad . \quad . \quad . \quad (17)$$

Impedances of a Line of High Attenuation.

Suppose that for the length from 0 to l the attenuation is high. It does not then matter whether the termination Z_l is a short or open circuit, so that the input impedance is

$$Z_i \simeq \frac{c}{a} \simeq \frac{d}{b} \simeq Z_1. \quad . \quad . \quad . \quad . \quad . \quad (18)$$

Before we can apply asymptotic expansions to the Bessel functions we must consider the nature of u as l becomes large.

$$u = \frac{2}{3} j \sqrt{(G + jwC)} (R + jwL)^{3/2} / (k_R + jwk_L)$$

$$= \frac{2}{3} j \sqrt{G + jwC} \sqrt{R + jwL} [l + (R_0 + jwL_0)/(k_R + jwk_L)].$$

This expression increases as $l^{3/2}$, and when l is large the phase angle is

$$\pi/2 + \pi/4 - \tfrac{1}{2} \arctan (G/wC) + \pi/4 - \tfrac{1}{2} \arctan (R/wL)$$

$$= \pi - \tfrac{1}{2} \arctan (G/wC) - \tfrac{1}{2} \arctan (k_R/wk_L).$$

This lies between 0 and π, so that ju has a negative real part. The asymptotic expansion we can use (as a first approximation) is

$$J_n(u) \sim (2/\pi u)^{1/2} \cos (u - n\pi/2 - \pi/4)$$

$$\sim (1/2\pi u)^{1/2} \exp [-j(u - n\pi/2 - \pi/4)].$$

Then

$$(c/a) = [f_2(x_1) f_1(x_2) - f_1(x_1) f_2(x_2)] / [f_4(x_1) f_1(x_2) - f_3(x_1) f_2(x_2)]$$

$$\sim (\sqrt{Z_0/Y}) [J_{-2/3}(u_0) + J_{2/3}(u_0) e^{j\pi/3}] / j [J_{1/3}(u_0) - J_{-1/3}(u_0) e^{j\pi/3}],$$

. . . (19)

where $$Z_0 = R_0 + jwL_0,$$

so that $\sqrt{Z_0/Y}$ would be the characteristic impedance if

the line did not vary from the form at the beginning, and

$$u_0 = \frac{2}{3} j \sqrt{YZ_0}\,(R_0 + jwL_0)/(k_R + jwk_L). \quad . \quad (20)$$

(d/b) is seen to have the same asymptotic value as (c/a). We can put

$$(R_0 + jwL_0)/(k_R + jwk_L) = 1/\alpha, \quad . \quad . \quad . \quad (21)$$

where α is the constant of taper, and

$$\sqrt{YZ_0} = P_0, \quad . \quad . \quad . \quad . \quad . \quad . \quad . \quad (22)$$

the propagation constant at the beginning of the line. Then

$$u_0 = 2jP_0/3\alpha. \quad . \quad . \quad . \quad . \quad . \quad . \quad . \quad (23)$$

Equation (19) gives the exact expression for the input impedance of an infinite length of the tapered line. If it is desired to obtain a simple and approximate expression for this the value of u_0 must be considered. A physical idea of u_0 may be obtained as follows:—j/α is a length, equal to that in which the line would taper from zero series impedance to the series impedance $R_0 + jwL_0$. In general j/α is complex, but this does not affect the conception. The simplest case to imagine is when the line starts from a series impedance R_0 and has tapered inductance only. Then j/α is

$$jR_0/jwk_L = R_0/wk_L,$$

the length of line for the series reactance to build up to the series resistance. Then u_0 is the propagation constant for $\frac{2}{3}$ of this length and may be considered large, so that asymptotic expansions must again be used. If the first approximation is made in equation (19) we get the form 0/0, so that a closer approximation is necessary.

The complete asymptotic expansion for the Bessel function is

$$J_n(u) \sim (2/\pi u)^{1/2}[U_n \cos(u - n\pi/2 - \pi/4) + V_n \sin(u - n\pi/2 - \pi/4)],$$

where $$U_n = 1 - \frac{(4n^2-1^2)(4n^2-3^2)}{2!\,2^6 . u^2}, \quad . \quad . \quad . \quad (24)$$

and $$V_n = \frac{(4n^2-1^2)}{1!\,2^3 . u} - \ldots$$

(Whittaker and Watson, 'Modern Analysis,' 17.5).

We have

$$[J_{-2/3}(u_0)+J_{2/3}(u_0)e^{j\pi/3}](\pi u/2)^{1/2}$$
$$\sim U_{2/3}[\cos(u_0+\pi/3-\pi/4)+e^{j\pi/3}\cos(u_0-\pi/3-\pi/4)]$$
$$-V_{2/3}[\sin(u_0+\pi/3-\pi/4)+e^{j\pi/3}\sin(u_0-\pi/3-\pi/4)]$$
$$\sim \tfrac{1}{2}\exp j(u_0-\pi/4)[e^{j\pi/3}+1][U_{2/3}+jV_{2/3}].$$

Similarly

$$j[J_{1/3}(u_0)-J_{-1/3}(u_0)e^{j\pi/3}](\pi u/2)^{1/2}$$
$$\sim \tfrac{1}{2}\exp j(u_0-\pi/4)[e^{j\pi/3}+1][U_{1/3}+jV_{1/3}].$$

The input impedance of the tapered line is thus

$$Z_i=\sqrt{Z_0/Y}(U_{2/3}+jV_{2/3})/(U_{1/3}+jV_{1/3}). \quad . \quad . \quad (25)$$

From (24) we see that

$$\left.\begin{aligned} U_{1/3}&=1-\frac{5\cdot77}{9^2.2^7u_0^2}+\ldots,\\ V_{1/3}&=-\frac{5}{9.2^3u_0}+\ldots,\\ U_{2/3}&=1+\frac{7\cdot65}{9^2 2^7 u_0^2}-\ldots,\\ V_{2/3}&=\frac{7}{9.2^3u_0}-, \end{aligned}\right\} \quad . \quad . \quad . \quad (26)$$

so that

$$Z_i=\sqrt{Z_0/Y}\left[1+\frac{j7}{72u_0}+\frac{7\cdot65}{9^2.2^7u_0^2}\cdots\right]\Big/\left[1-\frac{j5}{72u_0}-\frac{5\cdot77}{9^2.2^7u_0^2}\right]$$
$$=\sqrt{Z_0/Y}\left[1+\frac{j}{6u_0}+\frac{5}{72u_0^2}\cdots\right]$$
$$=\sqrt{Z_0/Y}\left[1+\frac{\alpha}{4P_0}-\frac{5\alpha^2}{32P_0^2}\cdots\right]. \quad . \quad . \quad . \quad . \quad . \quad . \quad (27)$$

If we wish to find the impedance at the far end, distance l from the beginning, we have to replace

$$\left.\begin{aligned} Z_0 &\text{ by } Z_l=Z_0(1+\alpha l),\\ P_0 &\text{ by } P_l=\sqrt{YZ_l},\\ \text{and} \quad \alpha &\text{ by } -\alpha,\\ \text{so that } u_0 &\text{ is replaced by } u_0'=-2jP_l/3\alpha. \end{aligned}\right\} \quad . \quad . \quad . \quad (28)$$

The impedance from the distant end looking towards the origin is then

$$Z_i' = \sqrt{Z_l/Y}(U_{2\,3}+jV_{2\,3})/(U_{1\,3}+jV_{1/3}), \quad . \quad (25\,a)$$

but here the functions have the argument u_0', not u_0. This gives

$$Z_i' = \sqrt{Z_l/Y}[1-\alpha/4P_l-5\alpha^2/32P_l^2\ldots]. \quad . \quad .(27\,a)$$

Two Tapered Lines, Back to Back.

In practice this expression is not very important, as the line from 0 to l will be joined to a line from l to $2l$ which is the image of the former. If two such lines are put back to back we may find the total result in the following way:—

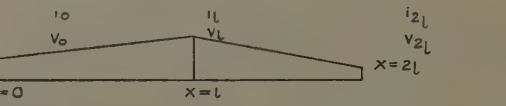

The figure gives a symbolic sketch.

$$\left.\begin{aligned} i_0 &= ai_l+bv_l \\ \text{and} \quad v_0 &= ci_l+dv_l \end{aligned}\right\} \quad . \quad . \quad . \quad . \quad . \quad (29)$$

by equations (9).

Similarly,

$$\left.\begin{aligned} -i_{2l} &= a(-i_l)+bv_l, \\ v_{2l} &= c(-i_l)+dv_l. \end{aligned}\right\} \quad . \quad . \quad . \quad . \quad (30)$$

Remembering that $ad-bc=1$, we find from equations (30) that

$$\left.\begin{aligned} i_l &= bv_{2l}+di_{2l} \\ \text{and} \quad v_l &= ci_{2l}+av_{2l}. \end{aligned}\right\}$$

Substituting in (29), we get

$$\left.\begin{aligned} i_0 &= (ad+bc)i_{2l}+2abv_{2l} \\ \text{and} \quad v_0 &= 2cdi_{2l}+(ad+bc)v_{2l}, \end{aligned}\right\}$$

so that the parameters of the combination of these tapered lines placed back to back are $(ad+bc,\ 2ab,\ 2cd,\ ad+bc)$.

The combination is symmetrical, so that

$$Z_1 = Z_2 = \sqrt{2cd(ad+bc)/2ab(ad+bc)}$$
$$= \sqrt{cd/ab},$$

which is the image impedance at the origin for a single-tapered line, and is given in equations (19), (25), and (27) in various degrees of approximation.

By equation (12) the image propagation constant of the combination is

$$T = \log_e [(ad+bc)+\sqrt{4abcd}]$$
$$= 2 \log_e (\sqrt{ad}+\sqrt{bc}),$$

which is twice the constant for each part. This is a particular case of a general theorem, which states that if two networks of image parameters (Z_1, Z_2, T) and (Z_2, Z_3, T′) are placed in tandem the resulting network has parameters (Z_1, Z_3, T+T′). It is easy to prove this directly from the definition of the image parameters or by the aid of equations (12).

Propagation Constant of the Long Line.

The image propagation constant is given by (12) as

$$T = \log_e (\sqrt{ad}+\sqrt{bc}).$$

For the long line $bc \approx ad$, since both are large and their difference remains equal to 1.

So $$T = \log_e (2\sqrt{ad}) = \tfrac{1}{2} \log_e 4ad. \quad . \quad . \quad . \quad (31)$$

By equations (10) and (4)

$$ad = \frac{[f_4(x_1)f_1(x_2) - f_3(x_1)f_2(x_2)][f_1(x_1)f_4(x_2) - f_2(x_1)f_3(x_2)]}{[f_2(x_2)f_3(x_2) - f_1(x_2)f_4(x_2)]^2}$$

$$= \frac{[J_{1/3}(u_0)J_{2/3}(u) + J_{-1/3}(u_0)J_{-2/3}(u)]}{[J_{-2/3}(u)J_{-1/3}(u) + J_{2/3}(u)J_{1/3}(u)]^2 (x_2/x_1)^{3/2}} \cdot [J_{2/3}(u_0)J_{1/3}(u) + J_{-2/3}(u_0)J_{-1/3}(u)]$$

$$. \quad . \quad . \quad (32)$$

It is rather laborious to derive the asymptotic expression for (32), and there are some pitfalls ; for example, the denominator looks as though it were becoming infinite,

but actually all the exponential terms neutralize one another, and we get

$$[J_{-2/3}(u)J_{-1/3}(u)+J_{2/3}(u)J_{1/3}(u)] \sim \frac{\sqrt{3}}{\pi u}[U_{1/3}U_{2/3}+V_{1/3}V_{2/3}],$$

where U and V are defined in equations (24).

Similarly $[J_{1/3}(u_0)J_{2/3}(u)+J_{-1/3}(u_0)J_{-2/3}(u)]$

$$\sim \frac{\sqrt{3}}{2\pi\sqrt{uu_0}}[(U_{2/3}-jV_{2/3})(U^0_{1/3}+jV^0_{1/3})\exp j(u_0-u) + (U_{2/3}+jV_{2/3})(U^0_{1/3}-jV^0_{1/3})\exp j(u-u_0)],$$

where $U^0_{1/3}$ stands for $U_{1/3}(u_0)$ and so on.

The second factor for the denominator is obtained by interchanging u and u_0.

It has already been shown that the real part of ju is negative, so that we need retain only the $\exp j(u_0-u)$. Equation (32) gives

$$ad = \frac{(U_{2/3}-jV_{2/3})(U^0_{1/3}+jV^0_{1/3})}{4[U_{1/3}U_{2/3}+V_{1/3}V_{2/3}]^2}\exp j2(u_0-u),$$

and (31) then gives

$$T = j(u_0-u)+\tfrac{1}{2}\log_e(U_{2/3}-jV_{2/3})(U^0_{1/3}+jV^0_{1/3}) (U^0_{2/3}+jV^0_{2/3})(U_{1/3}-jV_{1/3})-\log_e[U_{1/3}U_{2/3}+V_{1/3}V_{2/3}]. \quad . \quad . \quad . \quad (33)$$

The last two terms in (33) are small (of the order $1/u$), so that we may write

$$\left.\begin{aligned} T = j(u_0-u) &= \frac{2}{3}\left[lP_l+(P_l-P_0)/\alpha\right] \\ &= \frac{2}{3}\left(P_lZ_l-P_0Z_0\right)\Big/\left(k_R+jwk_L\right). \end{aligned}\right\} \quad . \quad (34)$$

For the two lines placed back to back the attenuation is twice this amount.

Since $P_l=\sqrt{Z_lY}=\sqrt{Z_0(1+\alpha l)Y}=P_0\sqrt{1+\alpha l}$,

we can write

$$T=(2P_0/3\alpha)[(1+\alpha l)^{3/2}-1], \quad . \quad . \quad . \quad (35)$$

It should be noticed that

$$\alpha l = (Z_l/Z_0 - 1).$$

If $\alpha l < 1$, *i. e.*, $Z_l < 2Z_0$, (35) may be written in the form

$$T = P_0 l[1 + \alpha l/4 - \alpha^2 l^2/24 \ldots], \quad . \quad . \quad . \quad (36)$$

which reduces to $P_0 l$ when α is zero.

It is interesting to compare (35) with the propagation constant, which is derived by integrating the constant at each point over the length of the cable. The integrated constant is

$$T' = \int_0^l \sqrt{Z_l Y}\, dl = \sqrt{Z_0 Y} \int_0^l \sqrt{1 + \alpha l}\, dl$$

$$= P_0 \left[\frac{2}{3}\alpha(1+\alpha l)^{3/2}\right]_0^l = (2P_0/3\alpha)\left[(1+\alpha l)^{3/2} - 1\right],$$

which happens to be the same as (35). This is rather a suggestive result.

Summary of Results and Examples.

For a long length of a cable, whose series impedance per unit length varies from

$$Z_0 = R_0 + jwL_0$$

at the beginning to

$$Z_l = Z_0 + (k_R + jwk_L)l$$

at the end, the input impedance is

$$Z_i = \sqrt{Z_0/Y}[1 + \alpha/4P_0 - 5\alpha^2/32P_0^2 \ldots], \quad . \quad . \quad (27)$$

where $Y = G + jwC$ = shunt admittance per unit length,

$$\alpha = (k_R + jwk_L)/Z_0,$$

and $P_0 = \sqrt{Z_0 Y}$.

The impedance at the far end, looking towards the beginning, is

$$Z_i' = \sqrt{Z_l/Y}[1 - \alpha/4P_l - 5\alpha^2/32P_l^2 \ldots], \quad . \quad (27a)$$

where $P_l = \sqrt{Z_l Y}$.

The image propagation constant is

$$\left.\begin{aligned} \mathrm{T} &= \left[\tfrac{2}{3}\mathrm{P}_l l+(\mathrm{P}_l-\mathrm{P}_0)/\alpha\right] \\ &= \tfrac{2}{3}\left(\mathrm{P}_l\mathrm{Z}_l-\mathrm{P}_0\mathrm{Z}_0\right)\Big/\left(k_{\mathrm{R}}+jwk_{\mathrm{L}}\right) \end{aligned}\right\} \quad . \quad . \quad (34)$$

$$= (2\mathrm{P}_0/3\alpha)[(1+\alpha l)^{3/2}-1]. \quad . \quad . \quad . \quad . \quad (35)$$

When $\alpha l<1$, T can be written

$$\mathrm{T} = \mathrm{P}_0 l[1+\alpha l/4-\alpha^2 l^2/12 \ldots]. \quad . \quad . \quad . \quad (36)$$

If another line is placed back to back with this line the impedance at either end is given by (27), and the image propagation constant, which is also the ordinary propagation constant, since the system is symmetrical, is given by twice the value of T in (34) or (35).

If the tapered line is placed behind a length d of unloaded line (constants Z_0 and Y), then the input impedance is

$$\sqrt{\mathrm{Z}_0/\mathrm{Y}}\,[\sqrt{\mathrm{Z}_0/\mathrm{Y}}\tanh \mathrm{P}_0 d+\mathrm{Z}_i]/[\sqrt{\mathrm{Z}_0/\mathrm{Y}}+\mathrm{Z}_i \tanh \mathrm{P}_0 d]$$

$$= \frac{\sqrt{\mathrm{Z}_0/\mathrm{Y}}\,[\tanh \mathrm{P}_0 d+1+\alpha/4\mathrm{P}_0-5\alpha^2/32\mathrm{P}_0{}^2 \ldots]}{1+\tanh \mathrm{P}_0 d[1+\alpha/4\mathrm{P}_0-5\alpha^2/32\mathrm{P}_0{}^2 \ldots]}. \quad (37)$$

If $\mathrm{P}_0 d$ is large, $\tanh \mathrm{P}_0 d \approx 1-2\exp(-2\mathrm{P}_0 d)$, and (37) becomes

$$\sqrt{\mathrm{Z}_0/\mathrm{Y}}\,[1+2\exp(-2\mathrm{P}_0 d)\{\alpha/4\mathrm{P}_0-5\alpha^2/32\mathrm{P}_0{}^2 \ldots\}]. \quad (37a)$$

If $\mathrm{P}_0 d$ is small, $\tanh \mathrm{P}_0 d \approx \mathrm{P}_0 d$, and (37) becomes

$$\sqrt{\mathrm{Z}_0/\mathrm{Y}}\,[1+(1-\mathrm{P}_0 d)(\alpha/4\mathrm{P}_0-5\alpha^2/32\mathrm{P}_0{}^2 \ldots)]. \quad (37b)$$

Equations (37), (37 *a*), (37 *b*) give the correct value for the sea-earth impedance in such a case.

As an example let us consider a cable which has a resistance of 2·61 Ω and natural self-inductance 1·5 mH, capacity C=·38 μF, and conductance G=0·018 wC per mile for the unloaded part.

$$\mathrm{Z}_0 = 2\cdot61+jw.1\cdot5\times10^{-3}$$

and

$$\mathrm{Y} = jw(\cdot38\times10^{-6})(1-0\cdot018\,i).$$

At $w=200$ (a frequency of 31·8 cycles) we have

$$\left.\begin{aligned} Z_0 &= 2{\cdot}61+j(0{\cdot}3)=2{\cdot}63\,/\underline{6^\circ\,36'} \\ \text{and} \\ Y &= j\,76.10^{-6}(1-{\cdot}018\,j)=76.10^{-6}/\underline{88^\circ\,54'}, \end{aligned}\right\} \quad (38)$$

giving

$$\left.\begin{aligned} P_0 &= 14{\cdot}1\times10^{-3}/\underline{47^\circ\,45'} \\ &= (9{\cdot}5+j\,10{\cdot}5)10^{-3} \end{aligned}\right\} \quad (39)$$

and

$$\begin{aligned} \sqrt{Z_0/Y} &= 186/\overline{41^\circ\,9'} \\ &= 140-j\,123. \end{aligned} \quad (40)$$

Let the loading increase to 60 *mh* per mile, with an added resistance of 0·5 Ω per mile at the end of five hundred miles.

Then

$$l=500 \text{ miles},$$

$$\begin{aligned} k_R+jwk &= [{\cdot}5+jw({\cdot}060)]/500 \\ &= 0{\cdot}001+j\,0{\cdot}024 \\ &= 0{\cdot}024/\underline{87^\circ\,36'}, \end{aligned} \quad (41)$$

$$\alpha = 0{\cdot}0091/\underline{81^\circ},$$

and

$$\alpha/P_0 = 0{\cdot}65/\underline{33^\circ\,15'}.$$

Then (27) gives

$$\begin{aligned} Z_i &= 186/\overline{41^\circ\,9'}\,[1+0{\cdot}162/\underline{33^\circ\,15'}-{\cdot}066/\underline{66^\circ\,30'}\ldots] \\ &= 186/\overline{41^\circ\,9'}\,[1{\cdot}109+j\,{\cdot}029] \\ &= (186)(1{\cdot}11)/\overline{41^\circ\,9'}/\underline{1^\circ\,30'} \\ &= 203/\overline{39^\circ\,39'}. \end{aligned} \quad (42)$$

The propagation constant is

$$\begin{aligned} T &= (2P_0/3\alpha)[(1+\alpha l)^{3/2}-1] \\ &= 1{\cdot}02/\overline{33^\circ\,15'}\,[(1+4{\cdot}55/\underline{81^\circ})^{3/2}-1] \\ &= 1{\cdot}02/\overline{33^\circ\,15'}\,[-3{\cdot}52+j\,10{\cdot}3] \\ &= 1{\cdot}02/\overline{33^\circ\,15'}\;10{\cdot}9/\underline{108^\circ\,42'} \\ &= 11{\cdot}1/\underline{75^\circ\,27'}, \end{aligned} \quad (43)$$

so that the attenuation is 2·79 nepers and the phase shift is 10·8 radians.

In order to ascertain the accuracy of these expansions we have to consider the value of u_0, which is

$$u_0 = 1{\cdot}02/56^\circ\,45'.$$

In an asymptotic expansion the error stopping at any term is less than that term. Considering (26), it is seen that the maximum error ratio in the functions of u_0 is then of magnitude

$$\frac{7{\cdot}65}{9^2 2^7 u_0^2} = {\cdot}0437.$$

Thus the maximum error in the impedance is 4·4 per cent., but may be considerably less. It is found that taking the term $1/u_0^3$ in (26) and (27) does not give a closer approximation. In the propagation constant the error is roughly $4{\cdot}4 \times (u_0/u)$ per cent., viz., 0·5 per cent.

Functions in u have an error of only ·04 per cent.

VII. *Investigation of Copper Oxide Films by Electron Diffraction.* *By* C. A. Murison, *M.A.**

THE work described here was carried out to find what influences the crystal structure taken up by heated copper. Small blocks of copper were polished on one face and heated to various temperatures in an electric furnace. The surface was then investigated by electron diffraction. The diffraction apparatus used was very similar to that described by Prof Thomson †. The electrons pass through two pinholes in the anode and are incident at a small grazing angle (about 2°) on the polished surface of the specimen. The diffracted rays are received on a photographic plate. The specimens used being all polycrystalline the patterns are closely analogous to the Debye-Scherrer rings obtained with X-rays.

The powdered oxides of copper were also examined, the powder being rubbed on the smooth surface of a

* Communicated by Prof. G. P. Thomson, M.A., F.R.S.

† Thomson and Fraser, Proc. Roy. Soc. A, cxxviii. p. 641 (1930).

small block of copper. The cuprous oxide was obtained by heating copper turnings in an oxygas flame, the cupric oxide by heating the cuprous oxide for some time at 600° C. or by adding sodium hydroxide solution to a solution of copper sulphate and heating the precipitate. Three types of diffraction pattern were obtained: (1) that due to cuprous oxide, (2) that due to cupric oxide, and (3) a pattern already described by Prof. Thomson * the structure corresponding to which has not been determined. While the cuprous oxide pattern was obtained both from powdered oxide and surface films, the cupric oxide pattern was obtained only from the powder and pattern (3) only from surface films. The three innermost rings of this pattern are very intense, on account of which it may conveniently be called the "3-ring" pattern. The following are its spacings (in 10^{-8} cm.) and intensities:—

2·70 v.s. 2·49 v.s. 2·26 v.s. 1·85 s. 1·74 f. 1·59 f. 1·39 v.s. 1·29 s.
1·26 f. 1·15 s. 1·08 s. ·943 s. ·909 f. ·877 s. ·842 s. ·717 s. ·696 s.

(f.= faint, s.= strong. v.s.= very strong.)

If the copper specimens were heated in air at a temperature between 300° and 500° C., the cuprous oxide and "3-ring" patterns were equally probable, but if air or oxygen was blown through the furnace-tube during the heating of the specimen, the "3-ring" pattern was invariably obtained. On the other hand, if CO_2 or SO_2 was blown into the furnace while the specimen was being heated, the cuprous oxide structure was always formed. Various methods were tried of drying and cleaning the air blown into the furnace, but these made no difference to the pattern. It was found that a cuprous oxide film could be easily changed to give the "3-ring" pattern by reheating the specimen and blowing air through the furnace-tube, but after a "3-ring" specimen had been formed, it was not possible to change it by heating at a temperature under 600° C. Specimens tested at higher temperatures gave such poor diffraction patterns that it was not possible to say which structure caused them.

* Thomson, *loc. cit.*

Chemical Analysis.

A large number of specimens were tested so as to give the " 3-ring " structure, but for a length of time sufficient to make the film ultimately blister off. The substance so obtained was tested by Prof. Baker, who found it to be a mixture of cuprous and cupric oxide, but with cupric oxide greatly predominating. When ground down the substance changed in colour from black to brown and gave the cuprous oxide pattern. It was found that grinding changed the substance almost completely from cupric to cuprous oxide. Prof. Baker suggested that this was an example of the Carey Lea Effect * in which the mechanical energy of grinding can bring about an endothermic chemical reaction. Grinding ordinary cupric oxide made no difference to the pattern obtained.

Conclusion.

It seems clear that the substance giving the " 3-ring " pattern is another crystal form of cupric oxide which is easily changed by mechanical treatment, but unaltered by heat treatment in the temperature range 300°–600° C.

Summary.

The oxide films formed on copper by heating and the powdered oxides of copper were studied by electron diffraction. The powdered oxides give the cuprous or cupric oxide structures, but the surface films give only cuprous oxide or an unknown structure. The treatment necessary for the formation of the unknown structure has been found. Chemical analysis shows it to be a new form of cupric oxide.

My thanks are due to Prof. H. B. Baker for carrying out the chemical analysis of the substance, and to Messrs. Metropolitan-Vickers for permission to publish this paper. I also wish to express my gratitude to Prof. G. P. Thomson under whose supervision this work was done.

* M. C. Lea, Phil. Mag. pp. 31 & 470 (1894).

VIII. *A Unified Field Theory.*—I. *Electromagnetic Field.* *By* D. MEKSYN, *Ph.D., D.Sc., Imperial College of Science, London* *.

§ 1. *Introduction.*

ATTEMPTS to apply the general theory of relativity to electrodynamics began almost immediately after the appearance of Einstein's theory of gravitation.

The wave mechanics has brought out certain new features in dynamics of electrons, which, combined with the idea of general covariancy, suggest a simple way to a unified field theory.

According to Einstein's principle of equivalence, every accelerated motion is equivalent, in a limited region, to a corresponding field of gravitation, *i.e.*, an electron moving with a certain acceleration with an observer at rest relative to it is in its mechanical and electrodynamical properties totally equivalent, for this observer, to an electron at rest in a corresponding gravitational field. The question that arises is only what are the properties of such an equivalent gravitational field. To this end let us briefly remember certain points of Einstein's theory of gravitation.

According to the classical theory the acceleration of a particle m in a field of gravitation due to a mass M is equal to $\frac{M}{r^2}$; or, provided that m is so small in comparison with M that it does not appreciably influence the field due to the latter, the acceleration of m is totally independent of m. Acceleration is proportional to the curvature of the four-dimensional track of a moving particle, and the track itself is a geodesic on a certain surface, if the force is derived from a potential.

According to the general theory of relativity the curving of the track of a mass m in a gravitational field due to M has to be ascribed not to any force exerted on m, but to curvature of space and time in the vicinity of M. Such interpretation becomes possible only because the acceleration of m, or the curvarure of its path, depends on

* Communicated by Prof. R. H. Fowler, M.A., F.R.S.

M and not on m; the latter moves freely in the space-time of M.

Let us now apply these considerations to an electromagnetic field. If an electron of charge e and mass m moves in an electric field due to charge E its acceleration is $\frac{e\mathrm{E}}{m}\frac{1}{r^2}$; or, in contradistinction to the previous case, the acceleration of an electron depends not only on the properties of the extraneous charge, but also on its own charge and mass.

Whereas in the case of gravitation the mass m could be considered as a kind of a test body, in the case of an electromagnetic field the presence of the charge e is a necessary condition for the existence of an electromagnetic acceleration, whose value depends not only upon both charges, but also upon the mass m.

If, therefore, we try to impose a gravitational field equivalent to an accelerated motion, due to an electromagnetic field, this gravitational field must be a conjoint property of both particles; or, *an electromagnetic field must be associated with a many body problem.*

Once we arrived at this conclusion the way to a unified field theory follows almost with logical necessity.

The simplest electromagnetic field is due to two particles, and we consider only this case.

The space-time of two particles must satisfy the following three conditions :—

1. The Special Principle of Relativity.

2. The Law of Dimensions of Space of Two Particles.

According to Schrödinger, the electrons move, in the non-relativistic case, in a seven-dimensional space, *i. e.*, six dimensions of space and one of time. If this space should conform with the special theory of relativity it must have eight dimensions, namely, six of space and two of time.

3. The General Principle of Relativity.

If the charge e tends to zero the electromagnetic field disappears and we are left with a particle m moving in a gravitational field due to M, whose metric is given by Einstein's equations $G\mu\nu=0$; accordingly, in order that the metric of the eight-dimensional space might lead us to Einstein's law of gravitation this metric must satisfy

the same law $G\mu\nu=0$, but only for an eight-dimensional space.

We accordingly arrive at the following conclusion :—

A unified field due to two particles is represented by an eight-dimensional space-time, whose metric satisfies Einstein's law $G\mu\nu=0$.

The following work is merely a mathematical development of this idea ; the summary of the chief results obtained is given at the end of the paper.

I. Motion in an Electromagnetic Field.

§ 2. *Electrostatic Field.*

We shall now consider two spaces which correspond to an electrostatic and electromagnetic field, and show that the motion proceeds along the geodesic of the space ; and, to a first approximation, is equivalent to the motion as given by the special theory of relativity. We shall then prove that these metrics satisfy Einstein's law of gravitation $G\mu\nu=0$.

Let the masses and charges of the two particles be m, M, and e, E, where e, E must be taken with their proper signs, and consider the form

$$ds^2=m(dx_4^2-dx_1^2-dx_2^2-dx_3^2)+2\phi\,dx_4dx_8 \\ +\mathrm{M}(dx_8^2-dx_5^2-dx_6^2-dx_7^2), \quad . \quad . \quad (1)$$

where x_1, x_2, x_3, x_4 are the space and time coordinates of m, and x_5, x_6, x_7, x_8 the corresponding coordinates of M, and

$$\phi=\frac{e\mathrm{E}}{r}, \quad r^2=(x_1-x_5)^2+(x_2-x_6)^2+(x_3-x_7)^2 \quad . \quad (2)$$

if the velocity of light $c=1$; otherwise $\phi=\frac{e\mathrm{E}}{c^2r}$.

The fundamental tensor is accordingly

$$\left.\begin{aligned} &g_{11}=g_{22}=g_{33}=-g_{44}=-m\,; \\ &g_{55}=g_{66}=g_{77}=-g_{88}=-\mathrm{M}\,; \\ &g_{48}=\phi=\frac{e\mathrm{E}}{r} \end{aligned}\right\}, \quad . \quad . \quad . \quad (3)$$

and the contravariant tensor is

$$\left.\begin{aligned} g^{11}=g^{22}=g^{33}=-\frac{1}{m}\ ;\ g^{44}&=\frac{g_{88}}{g_{44}g_{88}-{g_{48}}^2}=\frac{\mathrm{M}}{m\mathrm{M}-\phi^2}\\ g^{55}=g^{66}=g^{77}=-\frac{1}{\mathrm{M}}\ ;\ g^{88}&=\frac{m}{m\mathrm{M}-\phi^2}\\ g^{48}=\frac{-g_{48}}{g_{44}g_{88}-{g_{48}}^2}&=\frac{-\phi}{m\mathrm{M}-\phi^2}\end{aligned}\right\}\ldots\quad(4)$$

The motion of the two particles is now given by the eight equations which follow from

$$\delta\int ds=0.\quad\ldots\quad\ldots\quad(5)$$

These equations are for the particle m

$$\left.\begin{aligned} m\frac{d}{dx_4}\frac{dx_1}{ds}+\frac{\partial\phi}{\partial x_1}\frac{dx_8}{ds}&=0\\ \ldots\quad\ldots\quad\ldots\quad\ldots&\\ m\frac{dx_4}{ds}+\phi\frac{dx_8}{ds}&=\text{const.}=\mathrm{C}_1\end{aligned}\right\},\quad\ldots\quad(6)$$

and for M the corresponding equations are

$$\left.\begin{aligned} \mathrm{M}\frac{d}{dx_8}\frac{dx_5}{ds}+\frac{\partial\phi}{\partial x_5}\frac{dx_4}{ds}&=0\\ \ldots\quad\ldots\quad\ldots\quad\ldots&\\ \mathrm{M}\frac{dx_8}{ds}+\phi\frac{dx_4}{ds}&=\text{const.}=\mathrm{C}_2\end{aligned}\right\}\quad\ldots\quad(6a)$$

The equations (6) and (6*a*) are similar in their appearance to the usual equations of motion, if we remember that ϕ is the potential of the electrostatic force. We have, however, to prove that from them follows also the well-known relativistic increase of mass with velocity; to this end we must find the *connexion between* the *two times*.

We have to solve eight equations (6) and (6*a*) of which only seven are independent, and, hence, there is only one independent time.

In the classical case we have to assign initial values for coordinates and velocities, in our case we have also to assign initial values for $\frac{dx_4}{dx_8}$. We consider the case when the particles start from rest at infinity.

At the initial moment

$$\left(\frac{dx_4}{dx_8}\right)_0 = 1.$$

Consider the equations

$$\left.\begin{aligned} m\frac{dx_4}{ds} + \phi\frac{dx_8}{ds} &= C_1 \\ M\frac{dx_8}{ds} + \phi\frac{dx_4}{ds} &= C_2 \end{aligned}\right\} \quad . \quad . \quad . \quad . \quad . \quad (6b)$$

If ϕ vanishes at infinity, and the particles start there from rest

$$C_1 = \frac{m}{\sqrt{m+M}} \; ; \; C_2 = \frac{M}{\sqrt{m+M}} \quad . \quad . \quad . \quad (6c)$$

We solve our equations by successive approximations. We neglect in (6*b*) the squares of velocities, and, hence, also ϕ, and obtain

$$dx_4 = dx_8 = dt.$$

To this order of approximation

$$ds^2 = m\,dx_4^2 + M\,dx_8^2 = (m+M)dt^2,$$

and (6) and (6*a*) become the usual non-relativistic equations of motion.

Solving them we obtain from the equations of energy and momenta, bearing in mind the initial conditions,

$$\left.\begin{aligned} \frac{m(m+M)}{2M}v_1^2 + \phi &= 0 \\ \frac{M(m+M)}{2m}v_2^2 + \phi &= 0 \end{aligned}\right\}, \quad . \quad . \quad . \quad . \quad (6d)$$

where v_1 and v_2 are the velocities of m and M.

We solve (6*b*) with respect to $\frac{dx_4}{ds}$ and $\frac{dx_8}{ds}$, and obtain

$$\frac{dx_4}{dx_8} = \frac{mM - M\phi}{mM - m\phi} \quad . \quad . \quad . \quad . \quad . \quad (6e)$$

Combining $(6d)$ and $(6e)$ we arrive at the second approximation

$$\frac{dx_4}{dx_8} = \frac{1+\frac{m+\mathrm{M}}{2\mathrm{M}}v_1^2}{1+\frac{m+\mathrm{M}}{2m}v_2^2} \quad \ldots\ldots \quad (6f)$$

In the case when $\mathrm{M} >> m$, and we can neglect v_2^2, $(6f)$ becomes

$$\frac{dx_4}{1+\frac{v_1^2}{2}} = \sqrt{1-v_1^2}\, dx_4 = dx_8.$$

If we do not neglect v_2^2 we find the connexion between the times as follows. Multiplying the numerator and the denominator of $(6f)$ by

$$1-\frac{m}{2\mathrm{M}}v_1^2 = 1-\frac{\mathrm{M}}{2m}v_2^2,$$

we obtain

$$\frac{dx_4}{dx_8} = \frac{1+\frac{v_1^2}{2}}{+\frac{v_2^2}{2}},$$

or to our degree of approximation

$$dx_4^2 - dx_1^2 - dx_2^2 - dx_3^2 = dx_8^2 - dx_5^2 - dx_6^2 - dx_7^2. \quad (7)$$

We now make use of (7) in order to find the corresponding equations of motion.

Each particle must be associated with its own space and time, and their velocities are accordingly

$$v_1^2 = \frac{dx_1^2+dx_2^2+dx_3^2}{dx_4^2}, \qquad v_2^2 = \frac{dx_5^2+dx_6^2+dx_7^2}{dx_8^2}.$$

We have from (1) and (7)

$$ds^2 = \left[(m+\mathrm{M})(1-v_1^2)+2\phi\sqrt{\frac{1-v_1^2}{1-v_2^2}}\right] dx_4^2$$

$$= \left[(m+\mathrm{M})(1-v_2^2)+2\phi\sqrt{\frac{1-v_2^2}{1-v_1^2}}\right] dx_8^2. \quad (8)$$

We now consider the case where

$$\phi << \mathrm{M} \quad \text{and} \quad m << \mathrm{M}, \quad . \quad . \quad . \quad . \quad (9)$$

the equations of motion (6) and (6*a*) become

$$\left.\begin{aligned} m\frac{d}{dx_4}\frac{\dot{x}_1}{\sqrt{1-v_1^2}}+\frac{\partial\phi}{\partial x_1}\frac{1}{\sqrt{1-v_2^2}}&=0 \\ \mathrm{M}\frac{d}{dx_3}\frac{x_5}{\sqrt{1-v_2^2}}+\frac{\partial\phi}{\partial x_5}\frac{1}{\sqrt{1-v_1^2}}&=0 \end{aligned}\right\} . \quad . \quad (10)$$

Let us now consider the last equations in (6) ad (6*a*), namely,

$$m\frac{dx_4}{ds}+\phi\frac{dx_3}{ds}=\mathrm{C}_1, \qquad \mathrm{M}\frac{dx_3}{ds}+\phi\frac{dx_4}{ds}=\mathrm{C}_2.$$

By means of (8) they become

$$\frac{m}{\sqrt{1-v_1^2}}-\frac{m}{m+\mathrm{M}}\frac{\phi}{(1-v_1^2)(1-v_2^2)^{\frac{1}{2}}}+\frac{\phi}{\sqrt{1-v_2^2}}=\text{const.}$$

$$\frac{\mathrm{M}}{\sqrt{1-v_2^2}}-\frac{\mathrm{M}}{m+\mathrm{M}}\frac{\phi}{(1-v_2^2)(1-v_1^2)^{\frac{1}{2}}}+\frac{\phi}{\sqrt{1-v_1^2}}=\text{const.}$$

Adding these two equations

$$\frac{m}{\sqrt{1-v_1^2}}+\frac{\mathrm{M}}{\sqrt{1-v_2^2}}+\phi\{1+\ldots\}=\text{const.} \quad . \quad (11)$$

when the terms in brackets after the unit are of the order of magnitude $\frac{m}{m+\mathrm{M}}$ and v_2^2. According to our assumptions (9) these terms can be neglected, and (11) becomes the usual equation of energy.

We arrive, therefore, at the following conclusion :—

In the case when $\mathrm{M} >> m$, *our equations of motion for m are equivalent to the laws of motion of the Special Theory of Relativity.*

If we do not neglect v_2^2 we obtain the equations of motion of two particles, when the "retardation" is taken into account.

From (6) and (6*a*) follows an important consequence. The first equations of (6) and (6*a*) can be written as

$$m\frac{d^2x_1}{ds^2}+\frac{\partial\phi}{\partial x_1}\frac{dx_4}{ds}\frac{dx_8}{ds}=0,$$

$$\mathrm{M}\frac{d^2x_5}{ds^2}+\frac{\partial\phi}{\partial x_5}\frac{dx_4}{ds}\frac{dx_8}{ds}=0.$$

Adding them together, we obtain

$$m\frac{d^2x_1}{ds^2}+\mathrm{M}\frac{d^2x_5}{ds^2}=0,$$

or

$$m\frac{dx_1}{ds}+\mathrm{M}\frac{dx_5}{ds}=\text{const.}$$

which expresses the law of conservation for the centre of gravity.

Centre of gravity, which loses its importance in the Special Theory of Relativity, *is restored in our case to its former importance.*

As we shall see later, the same takes place in the theory of gravitation.

§ 3. *Electromagnetic Field.*

We consider now a space which can be associated with an electromagnetic field. Its metric is given by

$$\begin{aligned}ds^2=&g_{11}dx_1{}^2+g_{22}dx_2{}^2+g_{33}dx_3{}^2+g_{44}dx_4{}^2+g_{55}dx_5{}^2\\&+g_{66}dx_6{}^2+g_{77}dx_7{}^2+g_{88}dx_8{}^2+2(g_{15}dx_1dx_5\\&+g_{26}dx_2dx_6+g_{37}dx_3dx_7+g_{48}dx_4dx_8),\end{aligned}\quad(12)$$

and the contravariant tensor is

$$g^{11}=\frac{g_{55}}{g_{11}g_{55}-g_{15}{}^2},\qquad g^{15}=\frac{-g_{15}}{g_{11}g_{55}-g_{15}{}^2}.\quad(13)$$

The equations of motion are again given by (5). The equation for the coordinate x, is

$$\begin{aligned}\frac{d^2x_1}{ds^2}+g^{11}\Big\{&\Big(\frac{\partial g_{15}}{\partial x_2}\mathrm{V}_5-\frac{\partial g_{26}}{\partial x_1}\mathrm{V}_6\Big)\mathrm{V}_2+\Big(\frac{\partial g_{15}}{\partial x_3}\mathrm{V}_5-\frac{\partial g_{37}}{\partial x_1}\mathrm{V}_7\Big)\mathrm{V}_3\\&+\Big(\frac{\partial g_{15}}{\partial x_4}\mathrm{V}_5-\frac{\partial g_{48}}{\partial x_1}\mathrm{V}_8\Big)\mathrm{V}_4\Big\}\end{aligned}$$

$$+g^{11}\left\{\frac{\partial g_{15}}{\partial x_5}V_5+\frac{\partial g_{15}}{\partial x_6}V_6+\frac{\partial g_{15}}{\partial x_7}V_7+\frac{\partial g_{15}}{\partial x_8}V_8\right\}V_5$$

$$+g^{15}\left\{\left(\frac{\partial g_{15}}{\partial x_6}V_1-\frac{\partial g_{26}}{\partial x_1}V_2\right)V_6+\left(\frac{\partial g_{15}}{\partial x_7}V_1-\frac{\partial g_{37}}{\partial x_1}V_3\right)V_7\right.$$

$$\left.+\left(\frac{\partial g_{15}}{\partial x_8}V_1-\frac{\partial g_{48}}{\partial x_8}V_4\right)V_8\right\}$$

$$+g^{15}\left\{\frac{\partial g_{15}}{\partial x_1}V_1+\frac{\partial g_{15}}{\partial x_2}V_2+\frac{\partial g_{15}}{\partial x_3}V_3+\frac{\partial g_{15}}{\partial x_4}V_4\right\}V_1=0, \quad \ldots \quad (14)$$

where

$$V_1=\frac{dx_1}{ds}\ldots$$

The values of the fundamental tensor $g_{\mu\mu}$ with two equal subscripts are in this case the same as in (3). We again consider that

$$M>>m, \quad v_1>>v_2.$$

Only the first two terms survive for this case; the third term vanishes because the velocity of the magnetic field is much smaller than the velocity of the electron, and the last two terms vanish because in our case g^{15} tends to zero.

The equation (14) becomes accordingly, after a slight transformation,

$$m\frac{d}{dx_4}\frac{\dot{x}_1}{\sqrt{1-v_1^2}}=\left(\frac{\partial g_{15}}{\partial x_4}u_5-\frac{\partial g_{48}}{\partial x_5}\right)$$

$$+\left(\frac{\partial g_{15}}{\partial x_2}u_5-\frac{\partial g_{26}}{\partial x_1}u_6\right)u_2+\left(\frac{\partial g_{15}}{\partial x_3}u_5-\frac{\partial g_{37}}{\partial x_1}u_7\right)u_3, \quad (15)$$

where

$$u_1=\frac{dx_1}{dx_4}\ldots, \quad u_5=\frac{dx_5}{dx_4}\ldots$$

are the corresponding velocities.

(15) becomes the usual equation of motion if we assume that

$$g_{15}u_5\equiv -eF, \quad g_{26}u_6\equiv -eG, \quad g_{37}u_7\equiv -eH, \quad \ldots \quad (16)$$

where e is the charge of the electron, taken with its proper sign, and F, G, H is the vector potential of the

magnetic field; also $g_{48} \equiv e\phi$ where ϕ is the electrostatic potential.

The magnetic field is thus equal to

$$\alpha = \frac{\partial H}{\partial y} - \frac{\partial G}{\partial z} \cdots$$

If this theory is correct it follows from (16) the important conclusion that the *vector potential has no metrical meaning*, only the electrostatic potential is simply connected with the fundamental tensor.

§ 4. *Gravitation.*

We leave the consideration of gravitation to the subsequent parts of this work, where it will be shown that our equations give us the solution of the two body problem in Einstein's theory of gravitation.

We now consider only a case which will be of use later, namely,

$$ds^2 = m[(1-\gamma)dx_4^2 - (1+\delta_1)(dx_1^2+dx_2^2+dx_3^2)]$$
$$M[(1-\gamma)dx_8^2 - (1+\delta_2)(dx_5^2+dx_6^2+dx_7^2)].$$

To the first approximation the equation of motion is

$$m\frac{d^2x_1}{dt^2} = \frac{\partial}{\partial x_1}\frac{m+M}{2}\gamma,$$

where

$$dx_4 = dx_8 = dt, \quad ds^2 \equiv (m+M)dt^2,$$

or the gravitational force is derived from a potential

$$V = -\frac{m+M}{2}\gamma, \quad \cdots\cdots \quad (19)$$

II. The Metric of an Electromagnetic Field.

§ 5. *First Approximation.*

The fundamental tensor of our space satisfies Einstein's gravitational equations $G_{\mu\nu}=0$.

The tensor $G_{\mu\nu}$, in its usual notation, is equal to

$$G_{\mu\nu} = -\{\mu\sigma, \alpha\}[\rho\nu, \alpha]g^{\sigma\rho} + \{\mu\nu, \alpha\}[\rho\sigma, \alpha]g^{\sigma\rho}$$
$$+\tfrac{1}{2}g^{\sigma\rho}\left(\frac{\partial^2 g_{\rho\sigma}}{\partial x_\mu \partial x_\nu} + \frac{\partial^2 g_{\mu\nu}}{\partial x_\rho \partial x_\sigma} - \frac{\partial^2 g_{\mu\sigma}}{\partial x_\rho \partial x_\nu} - \frac{\partial^2 g_{\rho\nu}}{\partial x_\mu \partial x_\sigma}\right). \quad (20)$$

In the first approximation we take only the last term in (20), and hence

$$G_{\mu\nu}=\tfrac{1}{2}g^{\sigma\rho}\left(\frac{\partial^2 g_{\rho\sigma}}{\partial x\,\partial x_\nu}+\frac{\partial^2 g_{\mu\nu}}{\partial x\,\partial x_\sigma}-\frac{\partial^2 g_{\mu\sigma}}{\partial x_\rho\partial x_\nu}-\frac{\partial^2 g_{\rho\nu}}{\partial x_\mu\partial x_\sigma}\right). \quad (21)$$

The metric of the space is in this case

$$ds^2=m(dx_4^2-dx_1^2-dx_2^2-dx_3^2)+M(dx_8^2-dx_5^2-dx_6^2-dx_7^2)$$
$$+2(g_{15}dx_1dx_5+g_{26}dx_2dx_6+g_{37}dx_3dx_7+g_{48}dx_4dx_8). \quad (22)$$

We assume that

$$M>>m, \quad m>>(|g_{15}\ldots g_{48}|). \quad . \quad . \quad (23)$$

In this case we need to retain in (21) only the terms where $\sigma=\rho$ and, hence,

$$G_{\mu\nu}=\tfrac{1}{2}g^{\sigma\sigma}\left(\frac{\partial^2 g_{\mu\nu}}{\partial x_\sigma^2}-\frac{\partial^2 g_{\mu\sigma}}{\partial x_\nu\partial x_\sigma}-\frac{\partial^2 g_{\nu\sigma}}{\partial x_\mu\partial x_\sigma}\right). \quad . \quad (25)$$

We obtain accordingly

$$\left.\begin{aligned}
G_{11}&=-g^{55}\frac{\partial^2 g_{15}}{\partial x_1\partial x_5}\\
G_{12}&=-\tfrac{1}{2}g^{55}\frac{\partial^2 g_{15}}{\partial x_2\partial x_5}-\tfrac{1}{2}g^{66}\frac{\partial^2 g_{26}}{\partial x_1\partial x_6}\\
G_{15}&=\tfrac{1}{2}\left\{g^{11}\frac{\partial^2 g_{15}}{\partial x_1^2}+\ldots+g^{88}\frac{\partial^2 g_{15}}{\partial x_8^2}\right\}\\
&\qquad -\tfrac{1}{2}g^{11}\frac{\partial^2 g_{15}}{\partial x_1^2}-\tfrac{1}{2}g^{55}\frac{\partial^2 g_{15}}{\partial x_5^2}\\
G_{16}&=-\tfrac{1}{2}g^{55}\frac{\partial^2 g_{15}}{\partial x_6\partial x_5}-\tfrac{1}{2}g^{22}\frac{\partial^2 g_{12}}{\partial x_1\partial x_2}
\end{aligned}\right\}\ldots \quad (26)$$

The general law of formation of these tensors is clear; we have purposely left the two terms outside the brackets in G_{15}, although they can be cancelled out with two terms inside the brackets, in order to make clearer the law of formation of the tensors.

We can make the following inferences from these equations for the tensor g_{15}, and there is no difficulty in framing analogous conclusions for the remaining components $g_{26}\ldots$

(*a*) From the equations $G_{11}=0$, $G_{12}=0$, $G_{16}=0$, we conclude that

$$\frac{\partial g_{15}}{\partial x_1}=\frac{\partial g_{15}}{\partial x_5}=0. \quad . \quad . \quad . \quad . \quad . \quad (27)$$

(*b*) From $G_{15}=0$, we get by making use of (26) that

$$-\left(\frac{1}{m}+\frac{1}{M}\right)\left(\frac{\partial^2 g_{15}}{\partial y^2}+\frac{\partial^2 g_{15}}{\partial z^2}\right)+\frac{1}{m}\frac{\partial^2 g_{15}}{\partial x_4^2}+\frac{1}{M}\frac{\partial^2 g_{15}}{\partial x_8^2}=0.$$

We consider only the particular case when the vector potential is independent of time ; we obtain thus

$$\left(\frac{1}{m}+\frac{1}{M}\right)\left(\frac{\partial^2 g_{15}}{\partial y^2}+\frac{\partial^2 g_{15}}{\partial z^2}\right)=0. \quad . \quad . \quad . \quad (28)$$

1. *Electric field.*—The following components vanish

$$g_{15}=g_{26}=g_{37}=0. \quad . \quad . \quad . \quad . \quad . \quad (29)$$

From (27), (28), we conclude that

$$\left.\begin{aligned} &\frac{\partial g_{48}}{\partial x_4}=\frac{\partial g_{48}}{\partial x_8}=0 \\ &\frac{\partial^2 g_{48}}{\partial x^2}+\frac{\partial^2 g_{48}}{\partial y^2}+\frac{\partial^2 g_{48}}{\partial z^2}=0 \end{aligned}\right\}, \quad . \quad . \quad . \quad (30)$$

or, in the case of an electric field, our equations $G_{\mu\nu}=0$ are identical with the equation for the electrostatic potential in the classical theory.

2. *Magnetic field.*—We assume that $g_{48}=0$. The equations for the remaining tensors g_{16}, g_{26}, g_{37} are from (28)

$$\left.\begin{aligned} &\frac{\partial^2 g_{15}}{\partial y^2}+\frac{\partial^2 g_{15}}{\partial z^2}=0 \\ &\frac{\partial^2 g_{26}}{\partial x^2}+\frac{\partial g^2{}_{26}}{\partial z^2}=0 \\ &\quad . \quad . \quad . \quad . \quad . \end{aligned}\right\} \quad . \quad . \quad . \quad . \quad . \quad (31)$$

It is interesting to compare them with the corresponding equations for the vector potential, although our fundamental tensor is not identical with the vector potential.

If F, G, H, and ϕ is the electromagnetic vector potential, then each component satisfies the wave equation, and they are connected by the following relation :

$$\frac{\partial F}{\partial x}+\frac{\partial G}{\partial y}+\frac{\partial H}{\partial z}+\frac{\partial \phi}{\partial t}=0.$$

Our equations (30) and (31) correspond to the case

$$\frac{\partial F}{\partial x}=\frac{\partial G}{\partial y}=\frac{\partial H}{\partial z}=\frac{\partial \phi}{\partial t}=0. \quad . \quad . \quad . \quad (32)$$

It does not follow, of course, that the unified field theory cannot describe the more general case of the classical electrodynamics, but only that this is impossible to do in eight dimensions.

Our metric, however, can represent, except for the electrostatic force, the important case of a constant magnetic field.

The components of our tensor in this case are

$$\left.\begin{aligned} g_{15}&=a_1(x_2-x_6)\sim -e\mathrm{F}\\ g_{26}&=a_2(x_3-x_7)\sim -e\mathrm{G}\\ g_{37}&=a_3(x_1-x_5)\sim -e\mathrm{H}\end{aligned}\right\}, \quad . \quad . \quad . \quad (33)$$

which, according to (15), give the following magnetic field,

$$\alpha=a_2u_6, \quad \beta=a_3u_7, \quad \gamma=a_1u_5. \quad . \quad . \quad . \quad (34)$$

It is worth while noticing that our equations can also describe a variable electromagnetic field of the kind that is associated with a plane polarized wave.

We come, therefore, to the following conclusion; our eight-dimensional space can describe, among others, an electrostatic and a uniform magnetic field.

§ 6. *The Second Order of Approximation.*

If we solve our equations to the second order of approximation, we obtain the following expression for the fundamental tensor:

$$\left.\begin{aligned} g_{11}=g_{22}=g_{33}&=-m\left[1-\frac{e^2\mathrm{E}^2}{8m(m+\mathrm{M})}\frac{1}{r^2}\right], & g_{44}&=m\left[1+\frac{e^2\mathrm{E}^2}{2m\mathrm{M}}\frac{1}{r^2}\right]\\ g_{55}=g_{66}=g_{77}&=-\mathrm{M}\left[1-\frac{e^2\mathrm{E}^2}{8\mathrm{M}(m+\mathrm{M})}\frac{1}{r^2}\right], & g_{88}&=\mathrm{M}\left[1+\frac{e^2\mathrm{E}^2}{2m\mathrm{M}}\frac{1}{r^2}\right]\\ g_{15}=g_{26}=g_{37}&=-\frac{e^2\mathrm{E}^2}{8(m+\mathrm{M})}\frac{1}{r^2}, & g_{48}&=\frac{e\mathrm{E}}{r}\end{aligned}\right\}. \quad (35)$$

It is valid at least to the $\frac{1}{r^5}$ approximation. We omit the solution for the sake of brevity.

From (35) and (19) we obtain the following result :—

Two particles of charges e, E, and masses m, M, exert on each other a repulsive force with a potential

$$\frac{1}{4}\left(\frac{1}{m}+\frac{1}{M}\right)\frac{e^2E^2}{c^2r^2},$$

where c is the velocity of light.

It was suggested elsewhere that this additional force might account for the stability of Neutrons *.

Summary.

1. A unified field of two particles can be represented by an eight dimensional space, whose metric satisfies Einstein's law of gravitation $G_{\mu\nu}=0$.

2. The electrostatic potential is simply connected with the fundamental tensor, but the vector potential and the electromagnetic force have no metrical meaning.

3. The eight-dimensional space does not describe the most general electromagnetic field, but it includes the cases of an electrostatic and constant magnetic fields.

4. The law of motion and the connexion between the two times is given by the geodesic of space.

5. Two particles of charges e, E and masses m, M, exert on each other a repulsive force with a potential

$$\frac{1}{4}\left(\frac{1}{m}+\frac{1}{M}\right)\frac{e^2E^2}{c^2r^2}.$$

I wish to thank Prof. R. H. Fowler for his interest in this work.

* 'Nature,' cxxxi. p. 366 (1933).

IX. *The Thermal Expansion of the Crystal Lattices of Silver, Platinum, and Zinc.*

By Prof. E. A. Owen *and* E. L. Yates, *M.Sc., University College of North Wales, Bangor* *.

[Plate VII.]

THE accurate determination of lattice parameters over a range of temperature provides a simple and direct method of measuring the coefficient of thermal expansion of a crystal. The main difficulty in carrying out such measurements is the determination of the true temperature of the specimen under investigation. The first part of the present paper is devoted to an examination of the elements silver and platinum, whose thermal expansions have been accurately determined by other methods. By the arrangement adopted, measurements of the crystal parameters of these two elements were made when they were heated *in vacuo* at temperatures ranging from about 20° C. to 600° C. This part of the work, in addition to extending the range of temperature over which the expansion of silver had previously been studied, provided a test on the accuracy of the measurement of temperature in the experiments. Having come to the conclusion that the method yielded accurate values of the temperature, the latter part of the investigation was devoted to an examination of the thermal expansion of zinc. A detailed series of measurements was made from room temperature to temperatures approaching the melting-point of zinc, and the expansion of the zinc crystal studied perpendicular to and in the direction of the hexagonal axis.

1. *Apparatus.*

The high temperature precision camera employed in the work, has already been described †. In this camera the temperature of the specimen is measured with a nickel-nichrome thermocouple, which is soldered into the face of a copper sheet 2 mm. thick, fitting closely over that part of the circumference of the camera occupied by the reflecting material. The couple was carefully

* Communicated by the Authors.

† Owen and Yates, Phil. Mag. xvi. p. 606 (1933).

calibrated; at temperatures above 100° C. by noting the melting-points of tin, lead, zinc, antimony, and aluminium, and below 100° C. by direct comparison with a mercury thermometer.

Two methods of mounting the specimen on the camera were tried. In the first (Method I.) the powder was fixed to thin copper foil (0·05 mm. thick), and this was backed by the thick copper sheet carrying the thermocouple. In the second (Method II.) the powder was fixed directly to the surface of the copper sheet and was thus in close contact with the thermocouple. In both cases the specimen was separated from the circumference of the camera by a sheet of mica 0·1 mm. thick, in which a slot was cut to allow the X-ray beam to fall on the powder. This sheet of mica was found to be necessary to prevent rapid conduction of heat away from the specimen. With this arrangement the main temperature gradient was across the mica and not across the reflecting powder.

The invar back of the camera was insulated from the main body of the camera with silica rods. The temperature of the camera was recorded on a separate thermocouple, the maximum temperature reached being 88° C. when the specimen was maintained at 600° C. Allowance was made for the changes in the fiducial distances on the camera due to changes in temperature. It had previously been found that the films contracted uniformly by about 0·6 per cent. on subjection to a vacuum, and in the present investigation it was observed that they expanded by about the same amount when they were heated to about 80° C. It was essential therefore to be able to correct the measured arcs for changes in the lengths of the films, and for this purpose eight holes were drilled in the circumference of the camera to allow four fiducial distances to be measured on each film. The measurements showed that the films expanded uniformly along their length.

2. *Procedure.*

Before making an exposure, the camera enclosure was first evacuated with an oil-pump to a pressure of about 0·001 mm. Hg, then washed out several times with nitrogen (except when the exposures were made at room temperatures), and again evacuated. The vacuum was

maintained for more than an hour before the X-ray exposure was commenced, in order to allow the film time to attain its maximum contraction. The heating current was then switched on and adjusted until the thermo-couple was recording a steady temperature near which an exposure was desired. The temperature of the main body of the camera seldom varied over more than 5° C. during the course of an exposure. A record was also kept of the temperature of the cold-junction and a correction made when necessary to the readings of the thermo-couple. The vacuum in the enclosure was maintained after the completion of the exposure until the temperature of the reflecting powder had dropped below 50° C. This procedure slowed up the work, as it took over an hour for a specimen to cool from 500° C. to 50° C., but it was necessary in order to be able to examine the actual condition of the specimen during the exposure.

The temperatures of exposure were chosen at random except that exposures at room temperature were made at intervals to test whether the lattice had returned to its original dimensions after heating.

3. *Sources of Error.*

The sources of error in the determination of lattice parameters at ordinary temperatures with the precision camera have already been fully discussed *, and an average accuracy of about 1 in 15,000 was claimed for the measurements. Since in the present work the films change so considerably on subjection to a vacuum and also on exposure to heat, such high accuracy could not be expected. The close agreement, however, between the values of the lattice parameter calculated from each of a pair of lines, and again between the values from different films exposed under similar conditions, showed that the accuracy was still high and of the order of 1 in 10,000.

In estimating the accuracy of the temperature measurement several factors are to be considered. The effect of each factor separately is small, but if they all acted in the same direction the resulting error would be too great. The calibration of the pyrometer and its galvano-

* Owen and Yates, Phil. Mag. xv. p. 472 (1933).

meter depended upon the accuracy of the determination of the melting-points of the metals used for the calibration. The calibration curve was a straight line over the range 100° C. to 660° C., the observed points falling within 3° C. of it. This curve was determined when the cold-junction was at 20° C. During the course of the work this varied between 18° C. and 22° C.; allowance was made for this variation.

The largest error in the temperature measurement arose from fluctuations in temperature during the X-ray exposure. Although strict watch was kept on the galvanometer scale reading during an exposure, which in the initial stages of the work lasted about two hours, fluctuations of about $\pm 5°$ C. did occur at 600° C. owing to small variations in the heating current. The range of temperature fluctuation was proportionately less at lower temperatures. The maximum error in the measurement of temperature above 500° C. was taken to be $\pm 10°$ C.; the error at 300° C. was less than half of this, and below 100° C. an error of more than $\pm 3°$ C. was considered improbable. Later these errors were reduced by diminishing the length of the exposure. This was accomplished with a Levy-West intensifying screen, having previously ascertained that the parameter values were not altered by the introduction of the screen.

4. *Thermal Expansion of Silver and Platinum.*

Exposures were made with silver powder at temperatures ranging from 10° C. to 600° C. and at intervals of temperature of about 50° C. The X-ray tube was furnished with a nickel target; the wave-lengths of the radiations emitted were taken to be $K\alpha_1 = 1{\cdot}65450$ Å. and $K\alpha_2 = 1{\cdot}65835$ Å.*. The reflecting powder was mounted on copper foil, as in Method I. The results of the measurements are shown graphically in fig. 1, from which it will be observed that the experimental values tend to fall below the values calculated from the known coefficient of linear expansion of silver. At high temperatures, too, the experimental values incline towards the temperature axis.

At this stage the method of procedure was slightly modified. A series of photographs was taken when half

* Siegbahn, 'Spectroskopie der Röntgen Strahlen,' 2nd ed.

the copper foil was covered with silver powder and the other half with platinum. To obtain lines from both materials on the same film copper radiation was employed, the wave-lengths being taken to be $K\alpha_1 = 1{\cdot}537395$ Å. and $K\alpha_2 = 1{\cdot}541232$ Å. The same effect as above mentioned was observed both in the platinum and in the silver parameter determinations.

The metallic powders were next cemented directly on the thick copper sheet carrying the thermocouple (Method II.), so that each powder occupied one half of the sheet without mixing and the X-ray beam was arranged to fall symmetrically upon them. The copper sheet was held on the back of the camera in direct contact with the mica sheet, as already described. Copper radiation was again employed. A comparison of the measurements of films taken with the powders at two different temperatures and with the two methods of mounting is given in Table I.

These measurements show that the parameters obtained when the powders are placed on the foil are lower than those obtained when the powders are mounted directly on the copper sheet and therefore in closer contact with the thermocouple. In view of several results of this nature it was decided definitely to abandon the method of fixing the powders on thin foil and to adopt the method of mounting them directly on the copper sheet carrying the thermocouple. The advantage of this method of mounting over the other is evident from fig. 1. There is good agreement between observed and calculated values of the parameter over the range of temperature 20° C. to 300° C., the range over which the coefficient of thermal expansion of silver has been previously determined by accurate methods. The curve obtained with platinum (fig. 2) shows equally good agreement with calculated values * over the range from 20° C. to 600° C. It was concluded from these results that the temperature of the irradiated specimen could be accurately determined by the method adopted. It should be noted that the X-ray beam in these experiments covered only a very limited area of powder directly in the neighbourhood of the thermocouple, and that, consequently, the temperature of the powder contributing to the reflected beam would

* 'International Critical Tables,' ii. p. 459.

TABLE I.—Copper Radiation.

Reflecting Powders on Foil (Method I.).

Temp. (°C.).	Arc (mm.).	Line.	Refl. planes.	Parameter corrected (Å.).	
303....	118·00	α_1	422	$3{\cdot}9257_2$	Pt
	114·42	α_2	422	$3{\cdot}9256_3$	
	93·05	α_1	{511 / 333}	$4{\cdot}0982_2$	Ag
	88·56	α_2		$4{\cdot}0985_1$	
503....	120·67	α_1	422	$3{\cdot}9332_9$	Pt
	117·17	α_2	422	$3{\cdot}9331_9$	
	100·64	α_1	{511 / 333}	$4{\cdot}1163_6$	Ag
	96·21	α_2		$4{\cdot}1158_7$	

Reflecting Powders on Sheet (Method II.).

Temp. (°C.).	Arc (mm.).	Line.	Refl. planes.	Parameter corrected (Å.).	
302....	118·30	α_1	422	$3{\cdot}9265_5$	Pt
	114·65	α_2	422	$3{\cdot}9262_6$	
	94·11	α_1	{511 / 333}	$4{\cdot}1007_0$	Ag
	89·57	α_2		$4{\cdot}1007_2$	
504....	121·13	α_1	422	$3{\cdot}9346_2$	Pt
	117·73	α_2	422	$3{\cdot}9347_6$	
	101·51	α_1	{511 / 333}	$4{\cdot}1185_4$	Ag
	94·41	α_2		$4{\cdot}1187_4$	

Fig. 1.

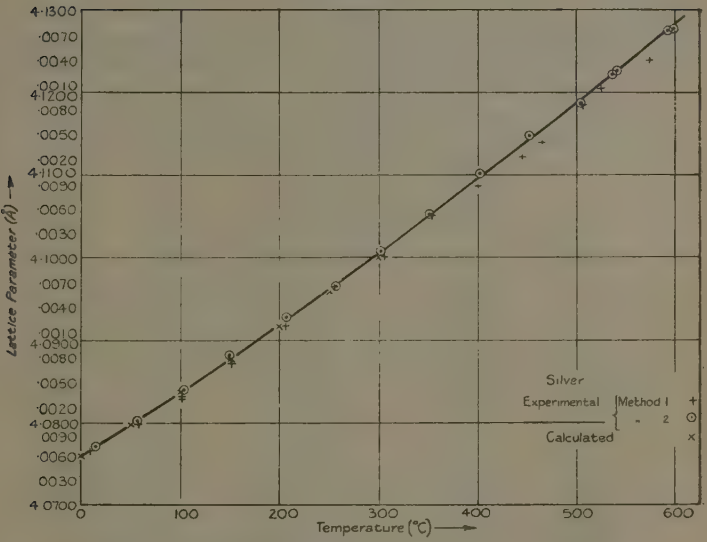

Variation with temperature of the crystal parameter of silver.

Fig. 2.

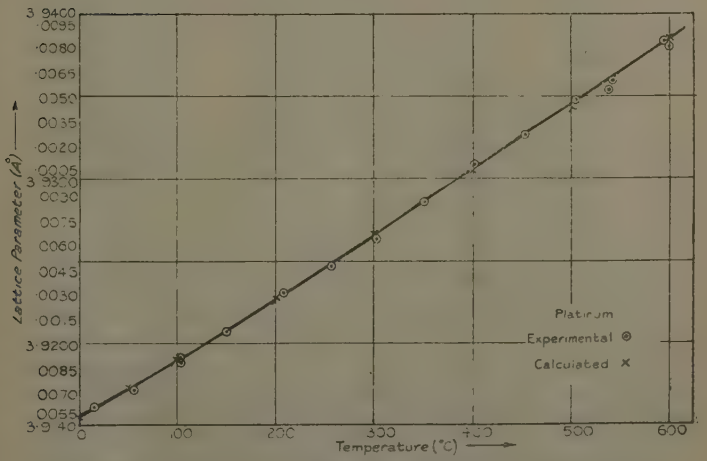

Variation with temperature of the crystal parameter of platinum.

be fairly uniform. The thin layer of adhesive used to mount the powder on the copper sheet may, however, be responsible for a small difference of temperature between the front surface of the powder actually reflecting the radiation and the surface of the copper sheet into which the thermocouple was fixed. The layer of adhesive was made as thin as possible with the object of minimising this difference in temperature.

TABLE II.

Film no.	Temperature (° C.).	Lattice parameter (Å.).	
		Silver.	Platinum.
E 78, E 79, E 91	15	4·0772	3·9161
E 87	56	4·0802	3·9172
E 82	102	4·0839	3·9192
E 81	103	4·0841	3·9189
E 86	150	4·0882	3·9208
E 80	208	4·0928	3·9231
E 83	256	4·0966	3·9247
E 77	302	4·1007	3·9264
E 85	351	4·1051	3·9286
E 76	402	4·1103	3·9309
E 84	453	4·1148	3·9326
E 94	504	4·1186	3·9347
E 93	539	4·1221	3·9354
E 88	543	4·1224	3·9359
E 89	595	4·1274	3·9382
E 92	600	4·1276	3·9380

The results obtained with silver and platinum are collected in Table II.

The filings were prepared from material which was 99·9 per cent. pure; they were freed from possible contamination with iron from the file and degassed by heating under a maintained vacuum for a few minutes in a Bunsen flame. Some of the photographs are reproduced in Pl. VII. An interesting feature of these photographs is the marked decrease in the intensity of the

silver lines with increase in temperature. The effect is not so marked in the platinum lines. A more detailed examination of this phenomenon under definite conditions of photographic development is desirable.

TABLE III.

Temp. (° C.).	Lattice parameter (Å.).			
	X-ray measurements.		International Critical Tables.	
	Silver.	Platinum.	Silver.	Platinum.
0	4·0760	3·9156	4·0760	3·9156
15	4·0772*	3·9161*	4·0772*	3·9161*
50	4·0799	3·9172	4·0799	3·9174
100	$4{\cdot}0838_5$	3·9190	4·0838	3·9191
150	4·0879	3·9207	4·0877	
200	4·0920	3·9226	4·0917	3·9228
250	4·0962	3·9245	4·0958	
300	4·1005	3·9265	4·1000	3·9266
350	4·1049	3·9285		
400	4·1093	3·9304	..	3·9304
450	4·1138	3·9324		
500	4·1184	3·9343	..	3·9343
550	4·1231	3·9363		
600	4·1278	3·9383	..	3·9383

* Experimental.

From the experimental curves the constants in the relation

$$\alpha_t = \alpha_0(1+\alpha t+\beta t^2+\gamma t^3+\delta t^4)$$

were found to be as follows :—

For silver

$$\alpha = 18{\cdot}89_1 \times 10^{-6}\ ;\ \beta = 3{\cdot}81_7 \times 10^{-9}\ ;$$

$$\gamma = \delta = 0.$$

For platinum

$$\alpha = 7{\cdot}908_5 \times 10^{-6}\ ;\ \beta = 6{\cdot}630_6 \times 10^{-9}\ ;$$

$$\gamma = -7{\cdot}94_5 \times 10^{-12}\ ;\ \delta = 2{\cdot}94_3 \times 10^{-15}.$$

Using these constants to calculate the dimensions of the lattices at intervals of 50° C. between 0° C. and 600° C., we have the values shown in columns 2 and 3 of Table III., which agree closely with the values given in columns 4 and 5 of the same table; the latter have been calculated from the accepted constants of silver and platinum published in the 'International Critical Tables,' vol. ii. p. 459.

5. *Thermal Expansion of Zinc.*

Having arrived at a satisfactory method of measuring the temperature of the specimen, attention was directed to zinc, which has a close-packed hexagonal structure. The X-ray method is very suitable for studying the thermal expansion of a metal possessing hexagonal structure, as the expansion perpendicular to the hexagonal axis can be observed independently of the expansion parallel to this axis. Previous work * on zinc had shown that the structure remains close-packed hexagonal over the range of temperature from 20° C. to 400° C. Approximate values of the thermal expansion along and parallel to the hexagonal axis were also deduced from the measurements, but owing to the difficulty of accurately estimating the temperature of the specimen and the inaccuracy in the determination of the parameters, it was desirable to carry out further measurements with the high temperature precision camera, especially in view of the fact that slight irregularities were observed at the highest temperatures of observation.

The method of determining the base side and the axial ratio from precision camera photographs has been described in previous papers †. A slight departure from the method there described had to be made in the present work owing to the fall in the intensity of the lines which occurs when the powder is heated. This decrease of intensity caused lines from the (2130), ($21\bar{3}3$), and (2024) planes to become too faint above about 300° C. for accurate measurement. The remaining pair of lines being the α_1 and α_2 characteristic K-radiation of nickel reflected from the ($21\bar{3}1$) plane, was not sufficient to determine completely

* Owen and Iball, Phil. Mag. xvi. p. 479 (1933).
† Owen and Pickup, Proc. Roy. Soc. cxl. pp. 179 and 344 (1933).

TABLE IV.

Radiation.	Temp. (° C.).	Arc (mm.).	Line.	Refl. planes.	Base side (Å.). Observed.	Base side (Å.). Mean corrected.	Axial ratio.
Nickel	381	119·57	α_1	$21\bar{3}1$	$2{\cdot}6769_2$	$2{\cdot}6769_0$	1·8830
		116·22	α_2	$21\bar{3}1$	$2{\cdot}6767_5$		
Cobalt	384	148·92	α_1	$11\bar{2}4$	$2{\cdot}6771_0$	$2{\cdot}6773_3$	
		146·63	α_2	$11\bar{2}4$	$2{\cdot}6773_8$		
Nickel	300	116·35	α_1	$21\bar{3}1$	$2{\cdot}6709_7$	$2{\cdot}6710_0$	1·8785
		112·95	α_2	$21\bar{3}1$	$2{\cdot}6708_9$		
Cobalt	301	145·45	α_1	$20\bar{2}3$	$2{\cdot}6707_7$	$2{\cdot}6710_2$	
		143·00	α_2	$20\bar{2}3$	$2{\cdot}6708_1$		
		90·04	α_1	$11\bar{2}4$	$2{\cdot}6711_2$		
		85·84	α_2	$11\bar{2}4$	$2{\cdot}6710_6$		

the dimensions of the hexagonal lattice. This difficulty was overcome by employing a cobalt target when repeating exposures at temperatures above 300° C., thus obtaining

TABLE V.

Film no. and radiation.	Temp. (°C.).	Axial ratio.	Base side (Å.).	Height (Å.).	Atomic volume (Å.³).
E 133 Ni	17	1·8560	2·6589	4·9349	15·107
E 132 Ni	19	1·8560	2·6589	4·9349	15·107
E 153 Co	20	1·8560	2·6590	4·9351	15·109
E 146 Ni	21	1·8560	2·6589	4·9349	15·107
E 142 Ni	23	1·8560	2·6591	4·9353	15·111
E 148 Ni	55	1·8590	2·6602	4·9453	15·154
E 135 Ni	100	1·8630	2·6620	4·9593	15·217
E 138 Ni	147	1·8670	2·6639	4·9735	15·283
E 134 Ni	205	1·8715	2·6667	4·9907	15·368
E 149 Ni	253	1·8755	2·6685	5·0048	15·432
E 155 Co	256	1·8760	2·6691	5·0072	15·446
E 157 Co	278	1·8773	2·6701	5·0126	$15{\cdot}474_5$
E 136 Ni	300	1·8785	2·6710	5·0175	15·500
E 161 Co	300	1·8785	2·6712	$5{\cdot}0178_5$	15·504
E 160 Co	301	1·8785	2·6710	5·0175	15·500
E 147 Ni	304	1·8788	2·6715	5·0192	15·511
E 156 Co	323	1·8800	2·6729	$5{\cdot}0250_5$	15·546
E 139 Ni	350	1·8815	2·6741	5·0313	15·579
E 137 Ni	353	1·8815	2·6746	5·0323	15·588
E 151 Ni	380	1·8830	2·6764	5·0397	15·632
E 152 Ni	381	1·8830	2·6769	5·0406	15·640
E 158 Co	384	1·8830	2·6773	5·0425	15·647
E 154 Co	407	1·8840	2·6788	5·0469	15·683
E 150 Ni	409	1·8840	2·6789	5·0470	15·684
E 159 Co	415	1·8842	2·6792	$5{\cdot}0481_5$	15·691

reflexions from the relatively strong reflecting planes $(20\bar{2}3)$ and $(11\bar{2}4)$. To illustrate the use of the two targets in the determination of the lattice dimensions of zinc at high temperatures, the results of the measurements of four films are given in Table IV.

The reflecting powders were prepared from filings of zinc, which was 99·9 per cent. pure. Very little annealing was required. The heating of the material in an evacuated enclosure for about 15 minutes with a Bunsen flame was sufficient to ensure good reflexions. The main difficulty was the fall in the intensity of the lines with rise of temperature.

As in the case of silver and platinum, the powdered zinc was mounted directly on the copper sheet carrying the thermocouple. Photographs were taken *in vacuo* after washing out the enclosure several times with nitrogen. The powders were allowed to cool to a temperature below 50° C. before air was admitted into the chamber. The reflecting powders were changed frequently to ensure freedom from cumulative errors due to possible contamination. The lattice dimensions at ordinary temperatures were measured at frequent intervals to test the camera and powders for errors that might have arisen during the heating process. No such errors were observed. The temperatures at which the photographs were taken were chosen at random ; the order of exposure is indicated by the number of the film in column 1, Table V.

TABLE VI.

Radiation.	α_1.	α_2.	β.
Nickel	1·65450 Å.	1·65835	1·49705
Cobalt	1·78529	1·78919	1·61744

Exposures of about 40 minutes sufficed at low temperatures, but it was necessary to expose for about an hour to obtain sufficient intensity at 400° C. The wavelengths of the radiations used are given in Table VI.

The final figures for the lattice dimensions were deduced by the method of successive approximation. The axial ratio was determined directly from single films at temperatures up to 300° C. Two targets were necessary to determine the axial ratio between 300° C. and 409° C. By plotting these values of axial ratio against temperature

a curve was obtained, which was adjusted to lie smoothly and evenly between the determined points. Small adjustments to the axial ratio were made by taking values direct from the curve. These new values were then used with the film measurements to calculate new values of the base side. In general the adjustment of axial

Fig. 3.

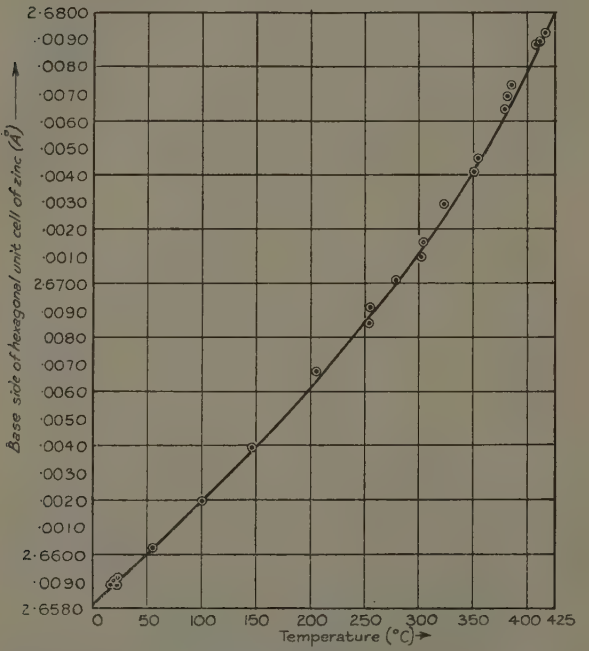

Variation with temperature of the length of the base side of the hexagonal unit cell of zinc.

ratio was so slight that this process yielded values of base side and height of hexagonal unit which were close to the unadjusted values. The same method was employed in two other cases at temperatures of 323° C. and 415° C., to determine the base side from only one pair of lines. The results are summarized in Table V.

Little weight can be given to the result obtained at 415° C. because the only pair of lines recorded on the film at this temperature was very faint on account of the close proximity of this temperature to the melting-point. But the result may be taken as a definite indication that

Fig. 4.

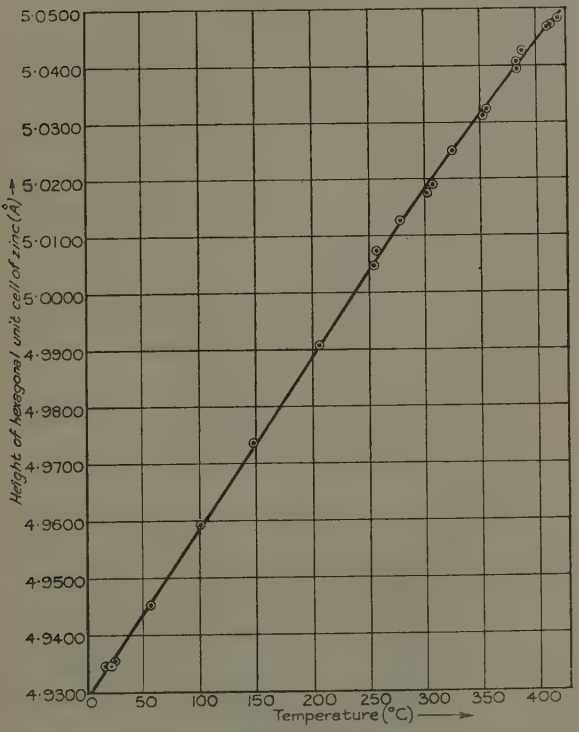

Variation with temperature of the height of the hexagonal unit cell of zinc.

the zinc crystal continues to expand up to a temperature about 4° C. below the melting-point.

The variations with temperature of the base side and the height of the hexagonal unit and of the mean atomic volume are shown in figs. 3, 4, and 5. The figures shown

Fig. 5.

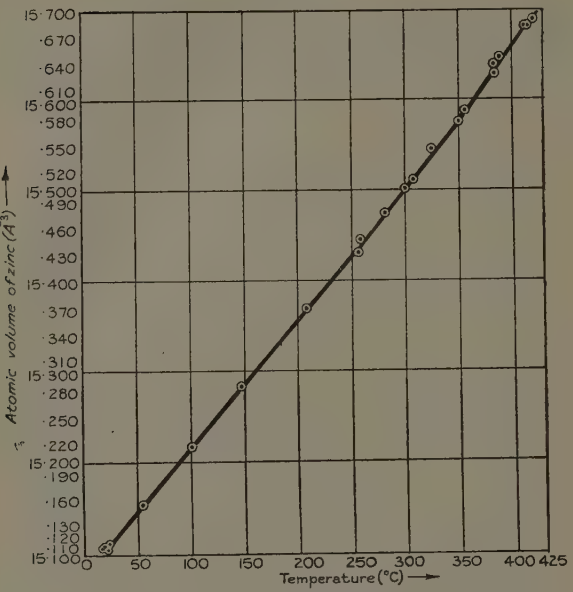

Variation with temperature of the mean atomic volume of zinc.

TABLE VII.

Temp. (°C.).	Base side (Å.).	Height (Å.).	Atomic volume (Å.³).
0	2·6582	4·9290	15·080
20	2·6589	4·9350	15·104
50	2·6600	4·9440	15·145
100	$2{\cdot}6619_5$	4·9590	15·217
150	$2{\cdot}6639_3$	4·9742	15·287
200	$2{\cdot}6661_5$	4·9895	15·358
250	2·6685	5·0043	15·429
300	$2{\cdot}6711_5$	5·0183	15·502
350	2·6742	5·0317	15·580
400	2·6780	5·0448	15·667
410	2·6789	5·0472	15·686

in Table VII. were obtained from these curves; they were used to calculate the values of the coefficients in the relation

$$x_t = x_0(1+\alpha t+\beta t^2+\gamma t^3+\delta t^4)$$

for each quantity. The coefficients are collected in Table VIII.

The accuracy of the determination of the coefficients of expansion is not as high as the figures in Table VIII. would indicate. Calculation shows, for instance, that an error of 0·0001 Å. in the base side as read off the curve, introduces an error in the α-term of $\pm 0{\cdot}3$ at 100° C., this becomes less than $\pm 0{\cdot}1$ at 400° C. The figures in Table VIII. must therefore be considered as determining the slopes of the dimension–temperature curves, and if used to calculate coefficients of expansion, a latitude of

TABLE VIII.

	$\alpha \times 10^6$.	$\beta \times 10^9$.	$\gamma \times 10^{12}$.	$\delta \times 10^{15}$.
Base side	13·04	13·95	− 43·89	109·7
Height	58·06	42·27	−155·54	135·3
Atomic volume ...	86·15	74·33	−326·08	524·9

the order above indicated must be allowed in the decimal figures.

To compare the results with those of Grüneisen and Goens *, who made measurements on single crystal rods of zinc at various temperatures, we give in Table IX., the mean coefficient of expansion between 20° C. and 100° C. based on the present figures. The agreement between the results of the two investigations shows that the thermal expansion of the crystal lattice is the same as that of the material taken as a whole.

The values of the parameters of zinc at different temperatures recorded in a previous paper by Owen and Iball † agree with the present values within the experimental error of the method then employed. The present values, however, are the more accurate, as the temperature measurement is considered to be more reliable.

* *Zeit. f. Physik*, xxix. p. 141 (1924). † *Loc. cit.*

It may be noted here that the temperature measurement could have been carried out through the intermediary of the silver parameter, which had been accurately determined in the first part of the investigation. In this method of temperature measurement the silver would be irradiated at the same time as the zinc, the silver lines supplying information as to the exact temperature of the specimen when under exposure. This method has already been employed in the laboratory for other purposes and has proved most convenient and useful. It was not adopted in the case of zinc because this element volatilizes at the higher temperatures and there was risk of contaminating the silver, thus leading to fictitious values of the temperature. For this reason it was considered more reliable to measure the temperature of the specimen

TABLE IX.

	Mean coefficient of thermal expansion between 20° C. and 100° C.	
	Grüneisen & Goens.	Present work.
Base side ...	$14{\cdot}1 \times 10^{-6}$	$14{\cdot}3 \times 10^{-6}$
Height.....	63·9	60·8
Volume	....	93·5

with the thermocouple as had been done in the case of silver and platinum.

All the parameters recorded in the tables have been corrected for refractivity.

6. *Summary.*

(1) A high temperature precision X-ray camera has been employed to study the expansion of silver, platinum, and zinc. The specimens were heated *in vacuo* when exposed to the X-rays.

(2) Values of the coefficients of thermal expansion of silver and platinum were obtained which agreed closely with previously determined values for these elements. The range of temperature for silver was extended from 300° C. to 600° C.

(3) The thermal expansion of zinc was measured along and perpendicular to the hexagonal axis for temperatures

ranging from 20° C. to 415° C. The zinc lattice was found to continue to expand up to within about 4° C. of the melting-point. Expansion occurred both along and perpendicular to the hexagonal axis up to this temperature, but whereas the rate of change of base side increased, that of the height decreased as the melting-point was approached.

(4) From the results obtained with zinc, it is concluded that the thermal expansion of the crystal lattice is the same as that of the material taken as a whole.

We wish to take this opportunity to thank the Department of Scientific and Industrial Research for a maintenance grant given to one of us (E. L. Y.) to carry out this investigation.

Bangor.
14th September, 1933.

X. *Measurement of Ionic Mobilities in the Positive Column. By* Sidon Harris, *M.A., Fellow in Physics at The Rice Institute, Houston, Texas* *.

Abstract.

Measurements were made on the speed of rotation of the positive column around an annular discharge-tube in air and hydrogen for various values of the strength of the radial magnetic field, of the strength of the electric field, of the pressure of the gas, and of the current through the discharge. Observations were also made on the Hall effect in the positive column under similar conditions of pressure in air and hydrogen. From the two sets of data the ionic velocities in the positive column for various pressures of both air and hydrogen were calculated. The pressure range was from 2 to 5 millimetres of mercury. The values obtained from the Hall-effect measurements for the velocities of the negative ions are in fair agreement with the values obtained by Townsend for free electrons. The mobilities of the positive ions in air and hydrogen were calculated

* Communicated by the Author.

to be 0·71 cm./sec. per volt/cm. and 2·23 cm./sec. per volt/cm. respectively at atmospheric pressure by assuming the mobilities of the positive ions to be inversely proportional to the pressure. The fact that these mobilities are lower than the mobilities of the positive ions produced by X-rays in these gases at atmospheric pressure indicates that the positive ions in the positive column at pressures ranging from 2 to 6 millimetres of mercury are larger than the positive ions produced in these gases by X-rays at atmospheric pressure.

Introduction.

H. A. WILSON and G. H. Martyn * give the linear speed of rotation of the positive column around an annular discharge-tube to be as follows :

$$U = HK_1V_2, \quad . \quad . \quad . \quad . \quad . \quad . \quad (1)$$

where U is the linear speed of rotation of the column in cm./sec., H is the strength of the radial magnetic field at the centre of the column, K_1 and V_2 are the mobility of the positive ions and velocity of the negative ions respectively.

In considering the transverse Hall effect in the positive column, if it is assumed that the concentration gradient is big enough to make the sidewise velocities of the positive and negative ions both zero, the following relation is deduced :

$$Z = 1/2(V_2 - V_1)\,H, \quad . \quad . \quad . \quad . \quad . \quad . \quad (2)$$

where Z is the transverse electric field produced by the Hall effect, V_1 is the velocity of the positive ions along the direction of the discharge, and H is the strength of the magnetic field used to produce the Hall effect. Equation (2) is the result given by H. A. Wilson †. However, if it is assumed that the concentration gradient is negligible, as in the case of a flame, and that the sidewise velocities of the positive and negative ions are equal but opposite in direction, thus producing no transverse current, the following relation is deduced :

$$Z = H(V_2 - V_1). \quad . \quad . \quad . \quad . \quad . \quad . \quad (3)$$

* H. A. Wilson and G. H. Martyn, Proc. Roy. Soc. lxxix. p. 417 (1907).

† H. A. Wilson, Proc. Cam. Phil. Soc. xi. p. 19 (1901).

Equation (3) is given by H. A. Wilson * in a paper on the Hall effect in flames. There is a concentration gradient in the positive column, as the column was observed to be pushed to one side of the discharge-tube when the magnetic field was turned on. It is, however, doubtful that this gradient is big enough to make the sidewise velocities of the positive and negative ions both zero; hence the correct expression for the Hall effect in the positive column is probably given by the following relation:

$$Z = kH(V_2 - V_1), \quad . \quad . \quad . \quad . \quad . \quad . \quad (4)$$

where k is a constant whose value is between 1/2 and 1.

Wilson and Martyn † made measurements on the speed of rotation of the positive column in several gases. Wilson ‡ had previously measured the Hall effect in the positive column in most of these gases, but the pressures at which he had made his measurements were all lower than the lowest pressure at which he and Martyn measured the rotating speed of the discharge. Wilson and Martyn extrapolated the Hall-effect results to higher pressures, and by using equations (1) and (2) calculated the mobilities of the positive ions in air and hydrogen to be 2·2 cm./sec. per volt/cm. and 25 cm./sec. per volt/cm. respectively at atmospheric pressure. They, however, remark that on account of the extrapolated values of the Hall effect the above results are not very significant.

It was thought that it would be of interest to repeat Wilson and Martyn's experiment with a much larger discharge-tube, and to observe at the same time the Hall effect in the positive column produced in a discharge-tube which is in the same vacuum system as the rotating effect discharge-tube. Thus it would be possible to calculate the ionic mobilities in the positive column without extrapolating the Hall-effect results.

Apparatus.

A sketch of the rotating-effect tube is shown in fig. 1. The tube was constructed similarly to the one used by Wilson and Martyn § except that it was much larger.

* H. A. Wilson, Phys. Rev. iii. p. 375 (1914).
† *Loc. cit.*
‡ *Loc. cit.*
§ H. A. Wilson, Phys. Rev. iii. p. 375 (1914).

The mean diameter of the annular tube formed by the two concentric pyrex cylinders GG and G′G′ was 5 inches, and the total distance between the anode ring AA and the cathode ring CC was 12·7 centimetres. The width of the annular tube was 1 inch. The pyrex cylinders were sealed to the aluminium plates PP and P′P′ at the ends as shown in the figure. The tube was

Fig. 1.

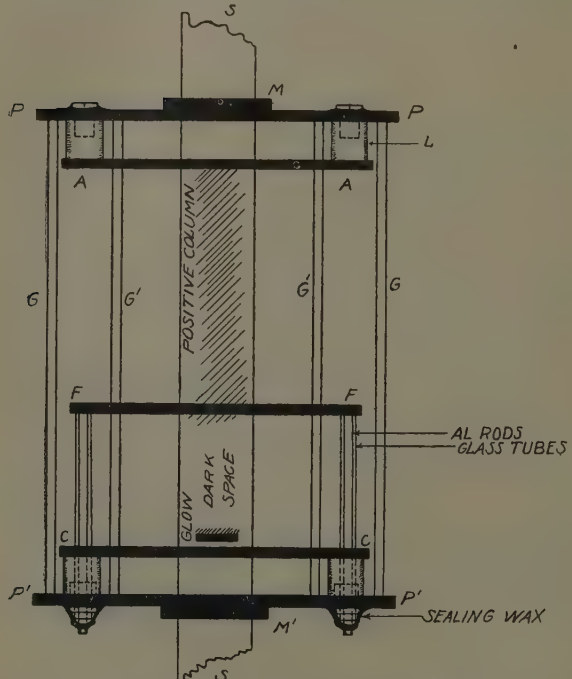

Sketch of the discharge-tube used in making observations on the rotating positive column. GG and G′G′, concentric pyrex cylinders sealed to the aluminium plates PP and P′P′; AA, FF, and CC, chromium-plated brass ring electrodes; L, lugs braised on to AA and CC; M, M′, hard rubber bushings to insulate the steel shaft SS from the aluminium plates PP and P′P′.

evacuated and filled through an aluminium jet (not shown in the figure) which screwed into the plate PP. The chromium-plated brass ring electrodes AA and CC

were fastened to the plates PP and P′P′ by means of three lugs each (only two of which are shown in the figure). The third chromium-plated brass ring electrode FF was held in place by aluminium rods which were run through the lugs supporting CC and CC itself, as is shown in the figure. The ring FF was insulated electrically from the rest of the tube, so that it would assume the approximate potential of the gas at its surface. An electrostatic voltmeter was connected across AA and FF; thus the electric field along the positive column could be measured approximately by dividing the reading of this voltmeter by the distance between AA and FF, which was 8 centimetres. The seven-foot steel shaft SS, 2 inches in diameter, was passed through the centre of the tube; the aluminium plates were insulated from the shaft by the hard rubber bushings M and M′. Two large solenoids were placed at each end of the steel shaft and connected, so that a common magnetic pole was produced in the middle of the shaft; thus a radial magnetic field was produced in the vicinity of the discharge-tube. The magnetic field in this vicinity was examined with search-coils and a compass, and found to be very uniform and radial. The magnetic field was measured at each reading of the speed of rotation of the positive column by reversing the position of a search-coil, the mountings of which were fastened to a wood framework which supported the tube and shaft. The magnetic field intensity at the positive column could be calculated in each case from the deflexions of a calibrated fluxmeter, which were produced when the search-coil was reversed. The wood framework was so tilted that the shaft SS pointed in the direction of the earth's magnetic field. A two thousand volt D.C. generator in series with a milliammeter and a variable water resistance was put across AA and CC. The discharge obtained resembled the one shown in fig. 1. When the magnetic field was turned on the column could be seen to rotate uniformly. The speed of rotation of the positive column was observed through a stroboscopic disk driven by a variable speed motor connected to an electric tachometer.

The tube used to measure the Hall effect was made similar to the one used by Wilson * in his experiments

* *Loc. cit.*

in 1901. A sketch of the tube is shown in fig. 2. The discharge was maintained between the chromium-plated brass disks A and C, and the Hall effect was measured by the probes J which were sealed into the ground-glass joint K. The leads H were connected to a quadrant electrometer. The tungsten wire F was electrically insulated from the rest of the tube; thus the electric field along the positive column could be approximately measured by dividing the potential drop between A and F by the distance between them. The distance between electrodes was the same as in the rotating-effect tube.

Fig. 2.

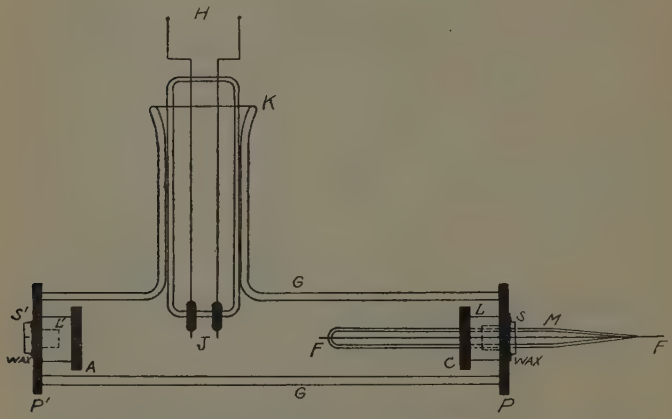

Sketch of the discharge-tube used in making observations on the Hall effect in the positive column. GG, glass cylinder sealed to aluminium plates P and P′; A and C, chromium-plated brass disks supported by lugs L′ and L, which are screwed on to plates P′ and P by screws S′ and S; FF, tungsten wire sealed through the glass tube M; K, ground glass joint, through the male of which is sealed the tungsten probes J; H, leads connecting the probes J to an electrometer.

The tube was evacuated and filled through a small glass tube blown on to the cylindrical glass tube GG. The magnetic field to produce the Hall effect was furnished by two Helmholtz coils accurately centred about the probes J. One coil was placed under the tube and the other was placed around the ground-glass joint K. The distance between the centres of the coils was so

determined that a uniform magnetic field was obtained within a fairly large region around the probes when a current was passed through the coils.

The vacuum system consisted of the two discharge-tubes connected by means of glass tubing to a McLeod gauge and to a two-way stopcock. One side of the cock was connected with a pump and the other with a gas-container. The air was thoroughly dried before it was allowed to pass into the apparatus. The hydrogen was prepared by the action of dilute hydrochloric acid on zinc, and was purified and dried before using.

Experimental Results and Discussion.

When the discharge rotates around the annular tube it imparts to the gas a velocity which is a small fraction of the velocity of rotation of the discharge. This velocity of the gas around the tube is the result of the viscous drag of the discharge on the gas, and can be calculated in the usual manner to be as follows :

$$u=\frac{\mathrm{HC}.ab}{2\pi\mathrm{M}(a^2-b^2)}, \quad . \quad . \quad . \quad . \quad . \quad . \quad . \quad (5)$$

where u is the velocity of the gas in the centre of the discharge-tube, H is the strength of the radial magnetic field producing the rotation of the discharge, M is the coefficient of viscosity of the gas, C is the total current through the discharge, a is the radius of the larger cylinder forming the annular tube, and b is the radius of the smaller cylinder. Equation (5) may be written in the following form :

$$u=\mathrm{GHC}, \quad . \quad . \quad . \quad . \quad . \quad . \quad . \quad (6)$$

where G is a constant depending upon the dimensions of the annular tube and the coefficient of viscosity of the gas. The quantity U in equation (1) is the linear speed of the discharge relative to the gas in the tube ; consequently U is the observed linear speed of rotation of the positive column minus the calculated linear speed of the gas, and consequently

$$\mathrm{U_0}=\mathrm{H(K_1V_2+GC)}, \quad . \quad . \quad . \quad . \quad . \quad (7)$$

where $\mathrm{U_0}$ is the observed linear speed of rotation of the discharge. The dimensions of the annular tube used by Wilson and Martyn * were so much smaller than

* *Loc. cit.*

the dimensions of the tube used in the experiment described in this paper that the drag velocity of the gas (u) in their experiments was negligible.

Table I. shows the variation of the observed speed of rotation of the discharge with total current through the discharge for both air and hydrogen. It is seen from the table that the speed of rotation increases with total current up to a current of about 20 milliamperes,

TABLE I.

Variation of the observed Speed of Rotation of the Positive Column with the Total Current through the Discharge.

Gas.	C.	N.	H.	P.	X.
	m.a.	turns/sec.	gauss.	mm. of Hg.	volts/cm.
Dry air	5	111	151	1·33	42·0
	10	117	151	1·33	40·6
	20	136	151	1·33	40·0
	30	140	151	1·33	39·2
	40	136	151	1·33	39·0
	5	41	58	0·88	33·1
	10	70	58	0·88	31·5
	20	73	58	0·88	31·0
	30	70	58	0·88	30·2
	40	68	58	0·88	29·7
Hydrogen..	20	86	243	6·12	78·1
	35	90	243	6·12	77·7
	50	95	243	6·12	76·8
	20	35	146	6·12	78·8
	35	41	146	6·12	77·5
	50	47	146	6·12	76·9

and then becomes practically independent of the total current. The speed of rotation of the discharge is proportional to Hi, where i is the current density in the discharge; hence the above result may be explained by supposing that the area of the discharge remains practically constant up to a total current of about 20 milliamperes, and that for total current values above 20 milliamperes the area of the discharge increases with the current in such a manner that the current density remains practically constant. The values of the observed speed of rotation of the positive column

used in calculating the ionic mobilities are taken from the current range of 20 to 40 milliamperes.

Figs. 3 and 4 show the variation of the observed speed of rotation of the discharge with the strength of the radial magnetic field at various pressures of the gas for air and hydrogen respectively. It is seen from the

Fig. 3.

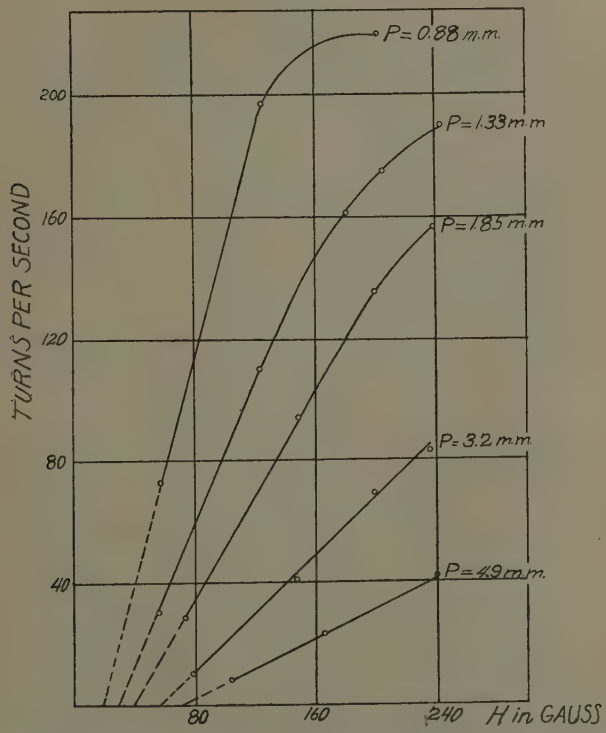

Curves showing the variation of the observed speed of rotation of the discharge, with strength of the radial magnetic field in various pressures of dry air.

curves that the observed speed of rotation is not proportional to H as indicated by equation (7), but that if the curves are extrapolated to intersect the H-axis, and if this intercept is termed H_0, then the observed speed of rotation is proportional to $H - H_0$ at a particular

pressure for a considerable range of H. The value of this H_0 is seen to increase with pressure and to be greater at the same pressure for air than for hydrogen. The discharge could not be made to rotate for very weak magnetic fields, and as the field strength was gradually increased the positive column could be observed to twist with the anode end further advanced than the

Fig. 4.

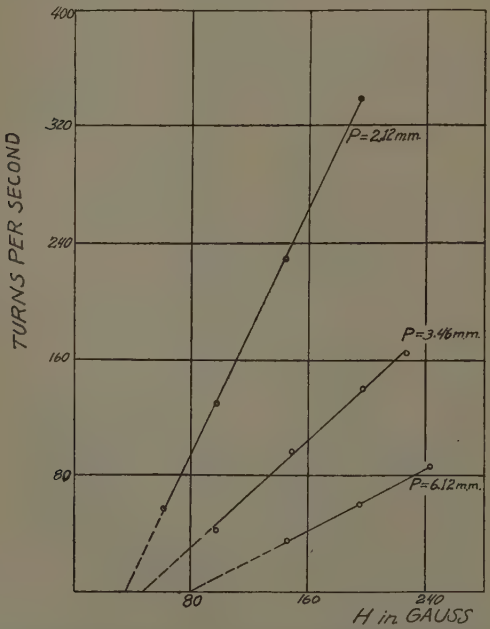

Curves showing the variation of the observed speed of rotation of the discharge, with strength of the radial magnetic field in various pressures of purified hydrogen.

cathode end. For magnetic fields greater than the H_0 corresponding to the particular pressure of the gas used the entire discharge could be observed to rotate uniformly with the positive column in a position at right angles to the electrodes. It thus appears that the presence of the H intercept may be explained by supposing that a certain constant force is required to

overcome a constant sticking force on the discharge at the cathode. In deducing equation (1) Wilson and Martyn assumed no retarding forces on the discharge at the electrodes. It therefore seems permissible to write

$$U_0=(H-H_0)\,(K_1V_2+GC). \quad . \quad . \quad . \quad . \quad (8)$$

It appears that the sticking of the discharge to the cathode ring increases with pressure of the gas and that it is greater at the same pressures in denser gases than in lighter gases. Values of K_1V_2 at various values of the pressure of the gas for both air and hydrogen were calculated from equation (8) by substituting the observed values of U_0, $H-H_0$, G, and C.

In making observations on the Hall effect in the positive column the probes (J, fig. 2) were first rotated across the discharge until the electrometer showed no deflexion when there was no magnetic field present. The probes were then at equal potentials. The magnetic field was then turned on and the resulting deflexion of the electrometer observed; the magnetic field was then reversed and the deflexion of the electrometer in the opposite direction recorded. The average of the two deflexions was taken as the effect caused by the magnetic field employed in the experiment. The average electric field strength along the positive column was determined approximately by dividing the reading of the electrostatic voltmeter, which was across the electrodes F and A (fig. 2), by the distance between them. The electric field strength along the positive column was also measured by rotating the probes parallel to the column until the electrometer showed maximum deflexion; then this reading was divided by the distance between the probes (6 mm.) to obtain the field intensity. The two methods agreed within 4 per cent. of each other. It might be well to remark here that the maximum error introduced in the determination of the electric field strength along the positive column (by the first-mentioned method above) by the anode drop and the Langmuir sheaf was calculated to be less than 7 per cent. The Langmuir sheaf should introduce no error in the measurements made by the probes J (fig. 2) if the positive column is considered to be uniform, for if the column is uniform the sheaf around each probe will

be the same, and as the difference in potential of the two probes is measured the presence of the sheaves should have no effect on the measurements.

Table II. shows the variation of the Hall effect with total current through the discharge. It is seen that the Hall effect is practically independent of current up to a total current of around 10 milliamperes. Measurements at higher current values were not used in computing the ionic mobilities, as the heating effect in the Hall tube became very pronounced at high currents, which action introduces considerable complications in the theory. The heating effect in the larger rotating-effect tube was not so pronounced at currents of about 20 milliamperes as it was in the Hall-effect tube. A strong

TABLE II.

Variation of Hall effect with Total Current through the Discharge.

Gas.	C.	Z.	H.	P.	X.
	m.a.	volts/cm.	gauss.	mm. of Hg.	volts/cm.
Dry air	1	2·282	29·4	3·32	47·5
	5	2·371	29·4	3·32	52·5
	7	2·371	29·4	3·32	52·5
	2	0·408	10·0	6·33	75·6
	5	0·510	10·0	6·33	73·0
	8	0·426	10·0	6·33	74·3
	10	0·426	10·0	6·33	74·3

blast of cool air was blown on the discharge-tubes during operation.

The value of V_2 is so much larger than the value of V_1 at the same pressure that equation (4) may be written in the form

$$Z = kHV_2 \quad . \quad . \quad . \quad . \quad . \quad . \quad . \quad (9)$$

Table III. gives the results of the Hall-effect measurements made at a total current value of 5 milliamperes. The values of V_2 were calculated from equation (9) by substituting the observed values of H and Z. The value of k was assumed to be 1. The fact that the values of V_2 obtained in this manner are in good agreement with the values obtained by J. S. Townsend for free electrons is used as the justification for assuming the value of k to

be 1. Of course no high precision is claimed in the determination of the values of V_2. A good value of k

TABLE III.

Hall-effect Measurements.

Gas.	Z.	H.	P.	X.	$V_2 \cdot 10^{-6}$.	Av. $V_2 \cdot 10^{-6}$.
	volts/cm.	gauss.	mm. of Hg.	v./cm.	cm./sec.	cm./sec.
Dry air	2·975	58·50	5·56	77·1	5·10	
	2·405	48·85	5·56	76·0	4·94	
	1·945	39·15	5·56	74·8	4·97	4·87
	0·975	20·00	5·56	72·5	4·86	
	0·510	10·00	5·56	72·5	5·10	
	3·705	48·85	4·45	68·0	7·56	
	2·965	39·15	4·45	67·0	7·56	
	2·225	29·85	4·45	60·3	7·56	7·63
	1·630	20·00	4·45	61·5	8·13	
	0·740	10·00	4·45	59·1	7·40	
	4·800	48·85	2·50	49·5	9·80	
	3·850	39·15	2·50	46·0	9·80	
	3·025	29·85	2·50	41·5	10·30	9·80
	1·925	20·00	2·50	39·5	9·62	
	0·950	10·00	2·50	38·5	9·50	
	5·650	48·85	1·90	45·7	11·60	
	3·945	39·15	1·90	43·6	10·10	
	2·970	29·85	1·90	40·6	10·15	10·40
	1·950	20·00	1·90	38·1	9·75	
	1·025	10·00	1·90	36·2	10·30	
Hydrogen....	2·040	39·15	6·33	74·3	5·22	
	1·530	29·85	6·33	74·3	5·20	5·15
	1·020	20·00	6·33	73·0	5·10	
	0·510	10·00	6·33	73·0	5·10	
	3·915	48·85	3·85	70·0	8·02	
	2·935	39·15	3·85	69·3	7·50	
	2·315	29·85	3·85	69·3	7·86	7·69
	1·530	20·00	3·85	68·5	7·68	
	0·745	10·00	3·85	68·0	7·45	
	3·770	39·15	1·98	52·1	9·65	
	2·885	29·85	1·98	51·0	9·84	9·60
	1·900	20·00	1·98	50·5	9·50	
	0·950	10·00	1·98	49·7	9·50	

may be computed by taking Townsend's values for V_2 and solving for k in equation (9). The average value of k obtained in this manner differs only slightly from unity. Table IV. compares the values of V_2 obtained from the

Hall-effect measurements with the values given for free electrons by J. S. Townsend.

A curve was plotted showing the variation of K_1V_2 with pressure for both air and hydrogen, and another curve was plotted from the data given in Table III. showing the variation of V_2 with pressure for both air and hydrogen. It was then possible to pick any pressure within the range given in the tables, and then read the values of K_1V_2 and V_2 from the curves for either air or hydrogen.

TABLE IV.

Comparison of the Values of V_2 obtained from the Hall-effect Measurements with the Values of the Velocity of Free Electrons given by J. S. Townsend.

Gas.	X/P.	Values of V_2 (cm./sec.). Townsend.	Harris.
Dry air	14	$8{\cdot}0.10^6$	$7{\cdot}5.10^6$
	17	8·8	9·5
	20	9·4	10·3
Hydrogen..	12	$4{\cdot}6.10^6$	$5{\cdot}6.10^6$
	15	5·6	6·5
	20	7·2	8·0
	25	8·8	9·6

Table V. gives the values obtained for V_2 and K_1 for air and hydrogen within a pressure range of from 2 to 5 millimetres of mercury. It is seen from the table that the product of the pressure and the corresponding values of K_1 may be considered as constant for a given gas within a pressure range of from 2 to 5 millimetres of mercury. By assuming this relation to hold for pressures up to atmospheric pressure, the values of K_1 for air and hydrogen at atmospheric pressure were calculated to be as follows :—

For dry air .... $K_1 = 0{\cdot}71$ cm./sec. per volt/cm.

For hydrogen .. $K_1 = 2{\cdot}23$ cm./sec. per volt/cm.

The accepted values for K_1 at atmospheric pressure for positive ions produced by X-rays are as follows :—

For dry air .... $K_1 = 1{\cdot}5$ cm./sec. per volt/cm.
For hydrogen .. $K_1 = 6{\cdot}0$ cm./sec. per volt/cm.

TABLE V.

Values of K_1 and V_2.

Gas.	P.	K_1V_2.	V_2.	K_1.	$P.K_1$.
Dry Air	2·0	$2{\cdot}97\ 10^9$	$10{\cdot}30.10^6$	288	576
	3·0	1·78	9·45	188	564
	4·0	1·10	8·47	130	520
	5·0	0·68	6·82	100	500
					540 = Av.
Hydrogen....	2·0	$9{\cdot}32.10^9$	$9{\cdot}72.10^6$	970	1940
	3·0	4·39	8·64	507	1521
	4·0	2·97	7·69	387	1548
	5·0	2·31	6·54	354	1770
					1695 = Av.

Conclusions.

While the inaccuracy in determining the ionic mobilities in the positive column by the method just described cannot be said to be less than about 10 per cent., it may be said that the method is at least novel and provides a new way of measuring ionic velocities in the positive column. If the theory of the rotation of the positive column as given by Wilson and Martyn is accepted, then it appears that the positive ions in the positive column at pressures of a few millimetres of mercury are about twice as slow, and consequently must be larger than the positive ions produced in the gases used at atmospheric pressure by X-rays. The result of the Hall-effect measurements indicate that the negative ions in the positive column at a few millimetres of pressure in air and hydrogen are free electrons.

The author wishes to express his appreciation to Dr. H. A. Wilson for his very helpful suggestions throughout the performance of this experiment.

XI. *Negative Sections of the Cold-Cathode Glow Discharge in Helium.*

By K. G. Emeléus, *M.A., Ph.D., University of Michigan, and* W. L. Brown *and* H. McN. Cowan, *Queen's University, Belfast* *.

Abstract.

An outline is presented of the results of the first part of an investigation of a cold-cathode low-voltage glow discharge in He at about 1 mm. pressure made chiefly by collector methods supplemented optically. Data so obtained are less exact than with discharge forms passing heavier currents, but represent an advance on older methods in enabling outstanding problems to be defined more precisely even when not yet solved. Neglecting the negative glow and Faraday dark-space plasmas, analysis of which is being continued, attention is particularly directly to (1) the collector evidence for emission of fast electrons from the cathode (this illustrates the difficulty of deciding between macroscopic and atomic effects in a discharge); (2) the uncertainty as to the electrical conditions in the gas close to the cathode in the primary dark-space and cathode glow; (3) the fact that analysis of cathode dark-space collector characteristics would possibly yield data for a region of space-charge similar to data obtained with collectors in a plasma; (4) the factors controlling the sharpness of the boundary between negative glow and cathode dark space, viz., the abruptness of the change in slope of the potential curve at the boundary and the mean energy of the slow electrons in the negative glow.

1. *Aim of Experiments and Procedure.*

THE study of the cold-cathode glow discharge may be approached optically [1], from the collision properties of the particles involved [2], and from collector analysis. This paper is the first part of a survey of the discharge in helium at a pressure of about 1 mm. made primarily by the third method, and is a sequel to Seeliger's summary [3] and two earlier papers [4] [5]. Although to

* Communicated by the Authors.

some extent our results are tentative, they serve to define outstanding problems and are presented in outline for this reason and because they have a bearing on the application of collector analysis to other discharge forms.

The sections of the discharge are shown in fig. 1. The colours of all parts—3, pink, 4, green, 5, whitish green, 7, purple (extended) or yellow (localized)—are due to the lines of He I. appearing with different relative intensities, excepting 6—peach, near 5—where there are helium bands. 2 and 3 are often repeated several times in parts of 4 more remote from 1; 4, and probably 2 and 3, have positive space-charge. 5 and 6 together, and probably 7 separately, are plasmas.

TABLE I.

Details of Principal Discharge-tubes.

A. Soda-glass. Diameter 3·5 cm. Collector, Fe, 2·5 cm. long, 0·055 cm. diameter. Ni cathode. Anode-cathode 3·5 cm.

B. Soda-glass. Diameter 3·5 cm. Collector, Cu-clad Ni, 0·53 cm. long, 0·03 cm. diameter. Ni cathode. Anode-cathode 4·6 cm.

C. Pyrex. Diameter 3·6 cm. Collector, Mo, 0·8 cm. long, 0·0113 cm. diameter. Na cathode. Anode-cathode distance variable.

D. Pyrex. Diameter 3·7 cm. Collector, Mo, 1·28 cm. long, 0·0115 cm. diameter. Ba cathode. Anode-cathode distance variable.

E. Pyrex. Diameter 4·7 cm. Collector, Fe, 4·14 cm. long, 0·058 cm. diameter. Na cathode. Anode-cathode distance variable.

The dimensions of the principal tubes used are given in Table I. They were cylindrical with closely fitting nickel disk electrodes, attached to pieces of iron so that they could be moved with a magnet.

The collector was fixed radially in the main tube in all cases except B and E. All collectors were cylindrical. In some tubes the electrodes were connected by a thin glass rod resting on the wall. Nickel cathodes were polished with fine emery paper before mounting. Sodium cathodes were made by distilling on a nickel base a layer of sodium, generated from sodium azide, in a part of

the tube not used for measurements, and barium coated electrodes by exploding a film of barium azide on a nickel base in a similar part of a tube. The least cathode fall realized was 85 volts, with sodium. The collectors, sheathed with fine glass tubes, not in contact with the metal where the latter emerged, entered from side tubes ; the movable collectors were attached to enclosed iron slugs in the side tubes. The helium showed no spectroscopic impurity ; a large charcoal trap was in close connexion with the tubes and kept cooled in liquid oxygen during the measurements. No tube was used after it had become more than slightly clouded by sputtering. The circuits were those usual for collector work, but two precautions have been found to improve the characteristic curves. The first is the plan of making all voltage changes and meter readings in the collector circuit with the latter negative (except when slow electrons were contributing a large part of the current) according to a regular time schedule ; in this way any slight drift of the collector current at constant collector potential still leaves the characteristic curve smooth, facilitating particularly determination of the numbers and velocities of the few fast (primary [5]) electrons in the plasma. The second is the introduction of a short-circuiting key in parallel with the reversing switch used when the collector potential is taken through the reference zero (that of anode or cathode) ; this key is depressed while the reversing switch is being thrown over, so avoiding the momentary return of the collector to its floating potential, which would have usually resulted in some distortion of the characteristic through almost inevitable slight hysteresis. Tube-currents remained sufficiently constant with the collector negative to the space to make it unnecessary to apply corrections on this account. The electron currents received in retarding fields for the plasma sections of the discharge have been analyzed for Maxwellian groups and space potential. For reasons already given [4] [5], and now for the additional reasons that a collector disturbs a discharge more than was at first suspected [6], whilst an alternative interpretation may be put on some of the characteristics [7] [8], the concentrations and, to a less extent, the velocity distributions are subject to considerable error. This cannot be evaluated exactly owing to the complicated discharge

form, but it is possible that, always assuming the validity of the temperature analysis, absolute concentrations may be in error by a factor of two; electron temperatures and relative values of concentrations in different parts of any one tube, which is all that is required for many purposes, are probably accurate to 15 per cent. or better. Typical data for the plasma are contained in Tables II.–IV.

Electron Data.

Table II.

Tube B.—Pressure 1·25 mm. Tube volts 387. Current density * $3{\cdot}5\ 10^{-5}$ amp./cm.^{2}. No anode glow. Thickness of cathode dark space about 1 cm. Collector in middle of tube. Cathode dark space—negative glow boundary—fairly well defined visually.

Run 119. Collector in middle of negative glow. Cathode to collector 1·28 cm. Space potential 1·4 volts positive to anode.

	Concentration.	Temperature.
Primary electrons	8·3 10^6/c.c.	39 volts †.
Secondary	5·7 10^7/c.c.	6·9 volts.
Ultimate	1 10^9/c.c.	0·64 volt.

Run 116. Collector in middle of Faraday dark space. Cathode to collector 3·00 cm. Space potential 1·0 volt positive to anode.

	Concentration.	Temperature.
Primary electrons	9 10^6/c.c.	50 volts.
Secondary	2·6 10^7/c.c.	6·5 volts.
Ultimate	6·4 10^8/c.c.	0·66 volt.

Run 113. Collector near anode. Cathode to collector 4·05 cm. Space potential 0·65 volt positive to anode.

	Concentration.	Temperature.
Primary electrons	6·9 10^6/c.c.	42 volts.
Secondary	Trace.	6 volts.
Ultimate	7·2 10^8/c.c.	0·39 volt.

* Current to the cathode divided by area of cathode.

† 1 volt $\equiv$ 7730° K.

TABLE III.

Tube B.—Pressure 1·23 mm. Tube volts 245. Current density 10^{-5} amp./cm.^{2}. Purple anode glow present. Thickness of cathode dark space about 1·3 cm. Discharge in helium. Collector in middle of tube. Cathode dark space—negative glow boundary—very diffuse.

Run 121. Collector to anode side of negative glow. Cathode to collector 2·42 cm. Space potential 14·8 volts negative to anode.

	Concentration.	Temperature.
Primary electrons	1 10^6/c.c.	14·8 volts.
Ultimate	4·0 10^7/c.c.	6·7 volts.

Run 122. Collector nearer cathode. Cathode to collector 2·02 cm. Space potential 13·3 volts negative to anode.

	Concentration.	Temperature.
Primary electrons	3 10^6/c.c.	25 volts.
Ultimate	4·9 10^7/c.c.	6·9 volts.

This discharge was on the point of extinction and disturbed for large negative potentials on the collector; data for the primary electrons are thus not very reliable. This also illustrates the arbitrary nature of the designations primary, secondary, and ultimate [5] as applied in this work.

TABLE IV.

Tube C.—Run 149. Collector in negative glow. Pressure 2·50 cm. Tube volts 92. Current density 7·5 10^{-5} amp./cm.^{2}. No anode glow. Thickness of cathode dark space about 0·22 cm. at axis of tube, about 0·3 cm. at periphery. Cathode to collector 0·32 cm. Anode to cathode 2·1 cm. Space potential 0·45 volt negative to anode.

	Concentration.	Temperature.
Primary electrons	6·7 10^7/c.c.	13·2 volts.
Secondary	2·8 10^8/c.c.	2·14 volts.
Ultimate	1·3 10^{10}/c.c.	0·10 volt.*

* Uncertain to at least 0·03 volt.

TABLE IV. (*cont.*).

Tube E.—Run 158. Collector to anode side of brightest part of negative glow. Pressure 1·35 mm. Tube volts 122. Current density $4 \cdot 10^{-5}$ amp./cm.^{2}. No anode glow. Thickness of cathode dark space 0·7 cm. Cathode to collector 1·35 cm. Anode to cathode 3·7 cm. Space potential 2·0 volts negative to anode.

	Concentration.	Temperature.
Secondary electrons	1·55 10^7/c.c.	9 volts.
Ultimate	7·3 10^7/c.c.	1·7 volts.

2. *Primary Dark Space and Cathode Glow.*

There is strong evidence that this dark space (2, fig. 1) has its origin in the failure of slow electrons from the

Fig. 1.

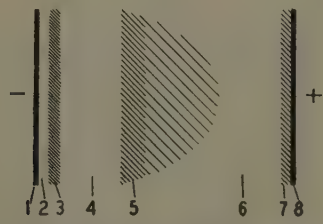

Sections of discharge.

1, cathode; 2, primary dark space; 3, cathode glow; 4, main cathode dark space; 5, negative glow; 6 Faraday dark space; 7, anode glow; 8, anode.

cathode to excite light until they reach an equipotential surface critical for the gas in front of the cathode [9] [10], a process which may be repeated farther out by electrons brought to rest in the first bright layer. The first dark space is probably a general phenomenon [11]; with high cathode fall in potential it may disappear through excitation of light by incoming positive ions, in whose motion resonance interchange of electrons is of importance [12] [13] [14]. Information might be obtained with collectors about (i.) the potential curve in the primary dark space and cathode glow, (ii.) the velocity distribution of the electrons from the cathode.

(i.) Measurements of potential made by adjusting that of a collector set parallel to the cathode until it throws equal shadows towards anode and cathode [15] have been extended to the helium discharge (3). The potential of the boundary between the primary dark space and cathode glow is found to be close to the resonance and ionization potentials of neutral helium, but the measurements are insufficiently accurate to decide between these. The otherwise smooth potential curve for the cathode dark space is often irregular in this region, but great weight cannot be attached to this result on account of the difficulty of making observations when the shadow towards the cathode is short. If there were serious modification of the potential curve it might be possible to consider the cathode glow as a thin plasma, acting as a gaseous cathode for the main part of the cathode dark space, and separated from the cathode by a positive ion sheath (the primary dark space). Some consequences of this view have been examined on rather inadequate data [16], but the weight of evidence is against the idea that the cathode glow is a plasma. It is to be emphasized, however, that some departure from electrical as well as optical properties of the main cathode dark space is to be looked for here.

(ii.) The fact that the primary dark space can be seen in the vapour from sputtering cathodes [17] requires, on the excitation theory, that most of the electrons from the cathode should have small initial speeds. From direct measurements it is, however, known that many secondary electrons formed by ions and metastable atoms of helium at metal surfaces have energies of the order of 10 electron volts [18] [19], a result possibly confirmed by the characteristic curve for a fine wire near the cathode [20]. A collector might, however, fail to receive slow electrons from the cathode, but record fast electrons. The shadows thrown by the collector, not much different from tubes of force (3), will both shield from at least positive ions those parts of the cathode nearest the collector, and direct most electrons from other parts past the collector; only those secondary electrons least guided by the lines of force—that is, those with greatest initial speed—will be able to reach the collector from unshielded parts of the cathode if they have the proper direction of emission [21].

Characteristics have been taken with the collector very close to the cathode. Fig. 2 shows one for Tube B, with the centre of the collector 0·94 mm. from the cathode, at the positive edge of the primary dark space. The tube current was $4{\cdot}7\ 10^{-5}$ amp., pressure 1·3 mm., cathode fall in potential 220 volts, and cathode dark space about

Fig. 2.

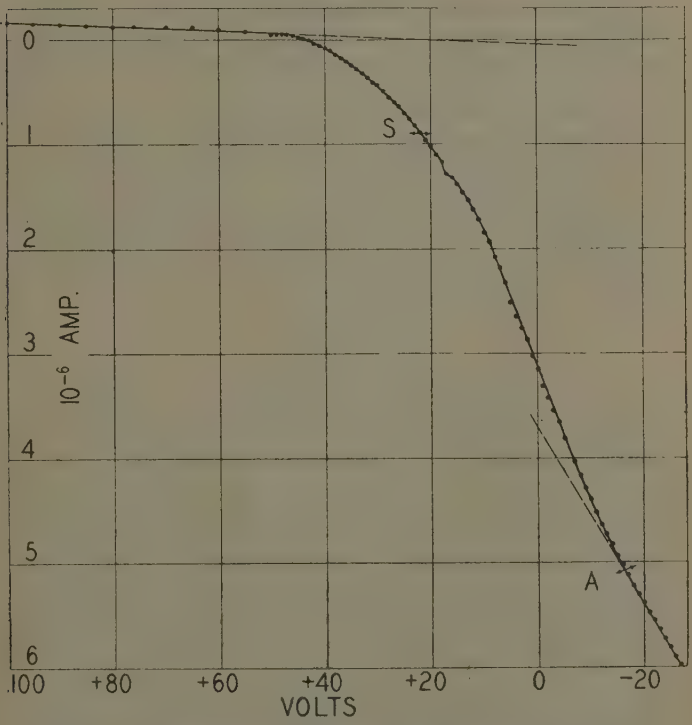

Characteristic for collector near cathode.

Currents below the zero line represent a net flow of positive electricity to collector from the gas. S is the space-potential from position of primary dark space; the reality of the break near S is very doubtful. The lower r.h. straight continued through accurately to −60 volts negative to the cathode.

15 mm. across. The break A may indicate that electrons with initial speed are emitted from the cathode [20].

Taking 4 volts as the work function of the cathode material, the available internal energy of the ion, metastable atom or radiation quantum responsible for the electron emission is the potential of A negative to the cathode, plus 4 or 8 volts [18], and probably lies within the 20–25 volt range of critical potentials of helium. As the collector is moved farther from the cathode A moves closer to the cathode potential and becomes less marked. This furnishes a good example of the difficulty of deciding if an effect in the glow is due to atomic phenomena or to an alteration in macroscopic electrical conditions. The alternatives are to suppose the shift of A due to electron scattering, or that A marks some change in the electric field of cathode and collector. If A became positive to the cathode it could not be due to secondary emission. Examination of all characteristics taken so far [22] shows no case of this. We have also examined how the shadows change for potentials near that of A, but have been unable to obtain help in interpretation of the break.

3. *Cathode Dark Space.*

Fig. 3 gives typical results for the potential in the cathode dark space. Curves 1 and 2 refer to tube A, curve 3 to tube E. All data for the first two, except those given by crosses in 1, which were obtained by plasma collector analysis for the negative glow, are from shadow observations [15]. In 3 circles represent shadow measurements and crosses potentials deduced by assuming the negative faces of the bright cathode striations correspond to 20, 40, and 60 volt equipotentials positive to the cathode [10]. The plasma was too disturbed by the collector in 2 to obtain potential data in the negative glow. For 1 the disturbance was less with the heavier ionization, but sufficiently great for the higher negative voltages to prevent study of the primary electron group. For the two points nearest the anode the semi-log plot was not good, but gave the space potential within about a volt, and an average electron temperature of 3·5 volts and concentration of 7.10^7 per c.c. in each case. For the point nearest the cathode an ultimate group was found with temperature 0·7 volt and concentration $1{\cdot}3.10^8$ per c.c., and a secondary group with temperature 5·7 volts

and concentration $2{\cdot}5.10^6$ per c.c. For continuity with earlier work [15] potential curves have been fitted to the data of 1 and 2 for the Morse formula $V_0(1-e^{-k_1 x}+k_2 x)$ [23], although the empirical nature of this is shown by the fact that, instead of being close to the normal cathode

Fig. 3.

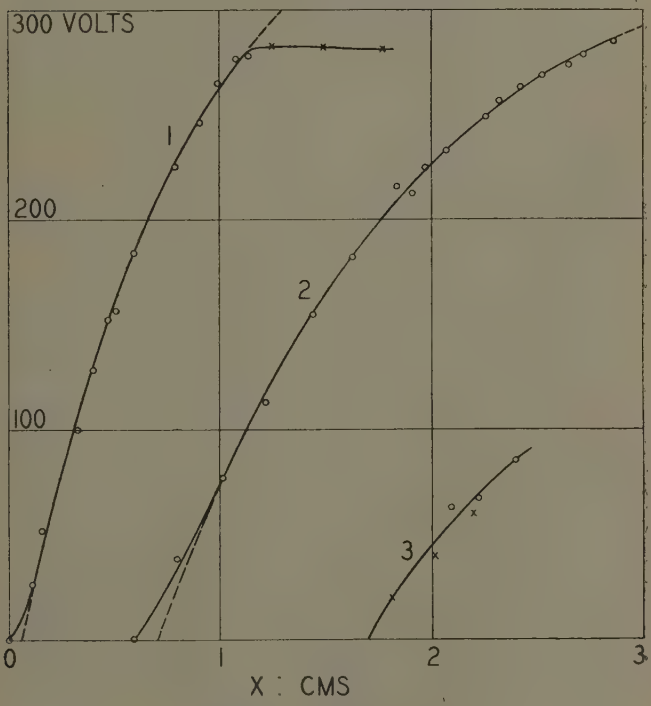

Potentials in cathode dark space.

The zeros of x are displaced in 2 and 3. For 1, $p=1{\cdot}16$ mm., $i=1{\cdot}5$ 10^{-4} amp., cathode fall $=280{\cdot}5$ volts. For 2, $p=0{\cdot}83$ mm., $i=2$ 10^{-5} amp., cathode fall $=286$ volts. For 3, $p=1{\cdot}45$ mm., $i=2{\cdot}6$ 10^{-4} amp., cathode fall $=121$ volts.

fall, V_0 must be much higher to obtain a fit with the data, and has been taken as 500 volts arbitrarily. For 1 $k_1=1{\cdot}00$, $k_2=-0{\cdot}0897$, and for 2, $k_1=0{\cdot}613$ and $k_2=-0{\cdot}075$; the effective zeros for distance (x) from

the cathode were taken 0·02 and 0·12 cm. out respectively. The computed curves are those shown continued as broken lines where they diverge from the experimental points. Measurements could not be made farther from the cathode in 3 on account of the strong light emission from the positive side of the cathode dark space; there was also a layer of sodium D light on the cathode, hindering shadow measurements close in.

An important feature of these measurements and of those of Brown and Thomson is the heavy concentration of positive ions at the positive boundary of the cathode dark space, shown by the large value of the second differential coefficient of the potential with respect to distance from the cathode [24]. The existence of the abrupt field change implies that there is a flux of positive ions from the negative glow into the cathode dark space, since a cathode dark space developing normally outwards from the cathode according to the ionization and space-charge laws could—subject to certain stability conditions—be curtailed at any point if there were injected into it from the anode side a flux of positive ions equivalent to that which would enter there in a fully developed dark space. The actual extension of the dark space, not exceeding a maximum corresponding to zero positive ion current from the negative glow, is a question of setting up equilibrium between this flux and the electron stream entering the negative glow from the cathode dark space, the denser layer of positive ions at the boundary being somewhat analogous to the electron cloud round the filament of a space-charge limited thermionic diode [25]. Considering the difficulty of locating the edge of the negative glow visually, it is doubtful if there was not a similar abrupt transition in the classical work of Aston [26], with higher cathode fall in potential.

Theoretical justification for the choice of potential in the shadow method goes with analysis of the cathode dark-space collector characteristics, not yet accomplished. Some experimental justification occurs in the quite abrupt change in type of shadow [15] and the fair accord between shadow and striation measurements [27]. It is also interesting to notice the similarity between the shadows and the lines of force for a charged cylinder

in an otherwise uniform field [28]. The difficulty in analyzing the curves comes from the fact that the collector is largely responsible for the ionization which it records.

At the negative glow boundary the characteristic curves, previously similar to fig. 2, transform to the ordinary plasma curves for the negative glow, through an intermediate stage [29], in which the negative glow can be seen to be attracted out round the collector and the plasma analysis is completely unreliable [7]. The association of the dark-space form of characteristic with the pre-existing positive space-charge has been shown by inserting two parallel wires, 0·01 mm. diameter, 6 mm. long, 1 mm. apart, in the plasma, forming a positive ion sheath on one and taking the characteristic of the other. For various extensions of the positive ion sheath on the first we obtained for the second all stages from the dark-space characteristic through the boundary characteristic to the plasma form. Penning has reported a similar effect of space-charge [30]. Our measurements were made both in the negative glow and in the Faraday dark space, and with the fixed positive ion sheath both to anode and cathode sides of the collecting electrode ; similar characteristics were obtained in all cases.

Experiments to find if the position of the shadow space potential or changes in the current to the cathode gave any clue to the interpretation of the collector characteristics were inconclusive. The shadow potential occurs near where there is considerable curvature of the characteristic, but no definite singularity. The current to the cathode passes through a weak maximum as the potential of the collector is altered, but this occurs at the shadow space potential only with the collector in the middle of the cathode dark space.

4. *The Cathode Face of the Negative Glow.*

There has been much controversy as to conditions here [3], and it has been seen (3) that this region cannot be explored with a collector. Our dark-space and negative-glow measurements, together with the theory of the transition from a plasma to a sheath [6] account

for its main properties. The transition theory, taken over qualitatively, shows that the edge will be electrically diffuse on account of back diffusion of electrons from the negative glow towards the cathode, and the optical diffuseness of the edge can be referred to the greater extension of the region in which fast electrons from the cathode dark space are losing energy [7]. A full theory of the edge will have to include correlation of the complete potential curve and velocities of the particles in this neighbourhood, and is not yet available. The experimental data show two points, however; (i.) with decrease in current density the transition from the cathode dark space to the negative glow plasma becomes less abrupt [31]; (ii.) simultaneously the mean energy of the slowest electrons in the negative glow increases considerably (Tables II. and III.).

Both (i.) and (ii.) will operate in the same sense, and together produce a rapid increase in diffuseness of the edge with decrease in current, probably accounting for a large part of the changes actually observed in the cases to which reference has just been made. Both will also tend to increase diffuseness with decrease in pressure, which is accompanied by increase in thickness of the dark space at constant cathode fall in potential and by increased mean electron speed in the negative glow [4]. The very low electron temperatures in oxygen [32] must be largely responsible for the extreme sharpness of the edge in this gas. Changes similar to those reported for helium have also been found for neon in unpublished work.

All gases which have long lived excited states will also tend to have diffuse edges, for causes similar to those operating in the positive column [33], but the importance of this diffusion effect in the negative glow is quite unknown.

5. *Negative Glow, Faraday Dark Space, and Anode Glow.*

The main features of the spectra from these regions can be accounted for in terms of the observed velocity distribution of the electrons [34]. Finer details of the spectra are at present under investigation, and fuller treatment of the electrical properties of the plasma is also postponed until these are available. The data

presented in Tables II.–IV. show that the Faraday dark space and negative glow form a typical plasma; the data for Table II. have been completed by radial measurements, showing a similar close constancy of potentials and electron temperatures for the two slowest electron groups. The tendency to reversal of the electric field appears less in helium than in argon [4] [7]; otherwise the two gases behave similarly.

6. *Summary.*

It will be apparent that much remains to be done [35]. The new work is an advance on the old probe methods, but information obtained less exact than with other discharges, particularly those passing heavy currents. The greatest lacuna at present is our inability to interpret the collector characteristics throughout the cathode dark space. Accomplishment of this would probably, as in a plasma, give a quantity of information not otherwise accessible. At present there are no direct measurements of the numbers and speeds of the positive ions and electrons there, only questionable information about the emission from the cathode (2, ii.) and more reliable but still somewhat uncertain data for the potential curve (2, i., and 3). At the negative-glow boundary direct collector analysis seems hopeless, but the interpolated potential curve and theoretical considerations (3, 4) indicate, firstly, that there is a heavy local concentration of positive space-charge, the effect of which is to alter the potential curve for the dark space towards a linear form at higher currents from a parabolic form with apex at the boundary at lower currents; and, secondly, that there is blurring of the edge electrically and optically through back diffusion of electrons from the negative glow. The main plasma properties of the negative glow and Faraday dark space, to be dealt with in detail later, are again obvious.

Experimental data for this paper were obtained at Belfast; we are indebted to Professor Morton for provision of facilities, and to the Government Grant Committee of the Royal Society for defraying the cost of voltmeters. Analysis of data has been completed by K. G. E. at the University of Michigan, where the work has been continued, through the courtesy of

Professor O. S. Duffendack. We are also greatly indebted to Mr. E. W. Pike for discussion of all points involved in the paper.

References.

(1) Druyvesteyn, ' Physica,' xi. p. 129 (1931).
(2) Pike, *Phys. Zeits.*, xxxiii. p. 457 (1932), and a forthcoming publication.
(3) Seeliger, ' Einführung in die Physik der Gasentladungen ' (1927).
(4) Emeléus & Harris, Phil. Mag. iv. p. 49 (1927).
(5) Emeléus & Brown, Phil. Mag. vii. p. 17 (1929).
(6) Tonks & Langmuir, Phys. Rev. xxxiv. p. 876 (1929).
(7) Emeléus & Sloane, Phil. Mag. xiv. p. 355 (1932); we believe, however, now that the secondary emission effect is not of predominant importance.
(8) Druyvesteyn, *Zeits. f. Physik*, lxiv. p. 781 (1930).
(9) Aston, Proc. Roy. Soc. A, lxxx. p. 45 (1908).
(10) Kossel, *Jahrb. Radioakt. Elekt.* xviii. p. 326 (1921).
(11) Güntherschulze & Keller, *Zeits. f. Physik*, lxxi. p. 238 (1931).
(12) Penning & Veenemans, *Zeits. f. Physik*, lxii. p. 746 (1930).
(13) Seeliger, *Naturwiss.* xviii. p. 155 (1930).
(14) Emeléus & Hall, Proc. Roy. Irish Acad. A, xl. p. 1 (1931).
(15) Brown & Thomson, Phil. Mag. viii. p. 918 (1929).
(16) Emeléus & Carmichael, Phil. Mag. v. p. 1039 (1928).
(17) Güntherschulze & Keller, *Zeits. f. Physik*, lxxi. p. 246 (1931).
(18) Oliphant & Moon, Proc. Roy. Soc. A, cxxvii. pp. 373, 388 (1930).
(19) Harrington, Phys. Rev. xxxviii. p. 1312 (1931).
(20) Carmichael & Emeléus, Phil. Mag. viii. p. 909 (1929).
(21) See J. J. Thomson, ' Rays of Positive Electricity,' p. 141, for a similar effect with retrograde rays.
(22) Including those of ref. 20.
(23) Morse, Phys. Rev. xxxi. p. 1003 (1928).
(24) This has now been confirmed optically, ref. 2.
(25) Emeléus, Proc. Roy. Irish Acad. A, xxxix. p. 49 (1930).
(26) Aston, Proc. Roy. Soc. A, lxxxiv p. 526 (1910).
(27) In addition to agreement for the first layer (fig. 1, 3) for the higher cathode falls on Ni (2, i.), and the data of fig. 3 (3), agreement was obtained within about 5 volts for Na cathodes and cathode fall 100–150 volts between the first and third bright cathode striations in several cases.
(28) Clerk-Maxwell, ' Elementary Treatise on Electricity,' pl. iii.
(29) Emeléus & Sloane, ref. (7), fig. 1.
(30) Penning, *Zeits. f. Physik*, lxxviii. p. 454 (1932).
(31) Fig. 3 (1, 2) and ref. (15).
(32) K. G. Emeléus & F. M. Emeléus, Phil. Mag. viii. p. 383 (1929). The case of oxygen is complicated by an increase in light emission on passing a short distance into the cathode dark space (Carmichael, Phil. Mag. viii. p. 362 (1929)), perhaps an effect of the electric field on metastable atoms or molecules (ref. (2)). It is possible that the sharpness of the edge in oxygen and carbon monoxide and the low electron temperature in the negative glow in oxygen (data are lacking for CO) are connected with presence of negative ions.
(33) Compton, Turner, & McCurdy, Phys. Rev. xxiv. p. 597 (1924).
(34) Emeléus, Brown, & Cowan, ' Nature,' cxxvii. p. 593 (1931).
(35) See also K. K. Darrow, ' Electrical Phenomena in Gases,' chapter vii.

XII. *The Combustion of Colloidal Propellants.* *By* A. D. Crow, *O.B.E., Sc.D., and* W. E. Grimshaw, *O.B.E., M.A.* *.

Introduction.

WE have recently proposed a rate of burning law for stabilized colloidal propellants †, based on the hypothesis that the vibrational energy of the incident gas molecules is the factor primarily operative in causing breakdown at the propellant grain surface during the explosion. The experimental evidence adduced by us in support of the theory has been re-examined by Hunt and Hinds ‡ from a standpoint involving the introduction of a criterion for estimating the temperature at any instant during the explosion, based on a formula given by us § for computing the energy losses at the end of combustion. They reach the conclusion that a temperature-density law is operative only in the case of one of the four propellant compositions investigated, a pressure law obtaining for the remainder. We have already given in outline our reasons for not accepting their conclusions ||, and the question may be considered to be *sub judice* pending further experimental investigations, the results of which we hope to publish shortly.

Muraour and Aunis ¶, on the other hand, have brought forward fresh experimental evidence on which they reject a density law entirely. The object of the present paper is to examine the circumstances of their experiments and the validity of their conclusions.

1. Assuming propellant combustion during the explosion to take place by parallel layers, and defining the size D of the propellant to be such that D/2 is the greatest depth burnt away below any receding surface before the whole of the grain is consumed, then, if $\phi(f)$ be the fraction by weight of propellant burnt

* Communicated by the Authors.

† Crow and Grimshaw, Phil. Trans. A, ccxxx. 691 (1932).

‡ Hunt and Hinds, Proc. Roy. Soc. A, cxxxviii. p. 696 (1932).

§ Crow and Grimshaw, Phil. Trans. A, ccxxx. 682, p. 54 (1932).

|| Crow and Grimshaw, ' Nature,' cxxxi. p. 60 (1933).

¶ Muraour and Aunis, *Comptes Rendus*, cxcvi. pp. 404, 478, and 544 (1933).

off at any instant corresponding to a remaining thickness Df, for all normal shapes of grain

$$\phi(f)=(1-f)\,(1+\theta f), \quad . \quad . \quad . \quad . \quad . \quad (1)$$

where $|\theta|\not\gg 1$, end-effects being neglected. The rate of burning law following the vibrational energy hypothesis is

$$-\mathrm{D}\frac{df}{dt}=\mathrm{B}\lambda\Delta', \quad . \quad . \quad . \quad . \quad . \quad . \quad (2)$$

where t is the time measured from the start of burning, B and λ are constants depending on the nature of the propellant and gas composition, and Δ' is the gas density at the instant t.

We have

$$\mathrm{B}\lambda=\frac{5{\cdot}2648\times 10^{3}\mathrm{Z}\tilde{\Sigma}\sqrt{\mathrm{T}_0}}{\sigma\delta(\mathrm{T}_i-\mathrm{T}_p)}, \quad . \quad . \quad . \quad . \quad (3)$$

where Z is a weighting factor for the incident vibrational energy, T_0 is the uncooled temperature of explosion for the propellant, T is the touch-off temperature * of the propellant grain surface under the conditions of burning, T_p is the initial propellant temperature prior to ignition, σ is the specific heat of the solid propellant, δ is the propellant density, and $\tilde{\Sigma}$ is given by

$$\tilde{\Sigma}=\Sigma\Big[\frac{g}{\sqrt{\mathrm{M}}}\{[\tilde{\mathrm{C}}_v]_{t^\circ}t^\circ-[\tilde{\mathrm{C}}_v]_{t_i^\circ}t_i^\circ\}\Big], \quad . \quad . \quad . \quad (4)$$

where g and M symbolize respectively gm. mols./gm. and molecular weight of each individual constituent of the gas complex incident on the propellant surface, and $\tilde{\mathrm{C}}_v$ is the vibrational contribution to the mean molecular heat at constant volume of any constituent of the gas complex between 0° C. and t° C.

The weighting factor Z has been shown to be invariant for the four propellant compositions investigated in establishing equation (2), taking the value $1{\cdot}66\times 10^{-3}$ in the experimental conditions prevailing.

* This is not the ignition temperature as ordinarily understood in connexion with chemical stability tests, but corresponds to the low limit of the temperature of the surround giving rise to instantaneous inflammation of the propellant surface.

2. Whatever be the conditions governing an explosion in a closed vessel, the relationship between Δ' and f is

$$\Delta' = \frac{\Delta_i\left(1-\frac{\Delta}{\delta}\right)+\Delta\phi(f)}{1-\frac{\Delta}{\delta}\{1-\phi(f)\}}, \quad . \quad . \quad . \quad . \quad (5)$$

where Δ_i is the density of the igniting gases, and Δ is the density of loading (the ratio of the charge-weight to the volume of the enclosure), units being based on the C.G.S. system.

Eliminating Δ' between equations (2) and (5), and integrating,

$$D\int_{f_0}^{f_1} \frac{1}{B\lambda} \frac{1-\frac{\Delta}{\delta}\{1-\phi(f)\}}{\Delta_i\left(1-\frac{\Delta}{\delta}\right)+\Delta\phi(f)}\,df = -\int_{t_0}^{t_1} dt. \quad . \quad (6)$$

If conditions can be arranged to ensure that the algebraic form of $B\lambda$ for f is conserved during the explosion, a necessary consequence is that the total time of burning for a propellant of given composition and size is determined uniquely by the values of Δ_i and Δ, being independent of other circumstances of the explosion. A first test of the adequacy of the vibrational energy hypothesis is, therefore, that, provided conditions be not exaggerated, charges of the same propellant composition and size, fired at the same density of loading in enclosures of differing volumes and shapes, should give the same total explosion times. In practice a difficulty lies in the accurate assessment of the duration of explosion, but within the limits of measurement no systematic difference has been observed by us between times for corresponding conditions in the two enclosures employed in our experiments *.

3. Following this line of reasoning, Muraour and Aunis have carried out a series of experiments †, from which they deduce that total explosion times become prolonged as cooling conditions are intensified, and on this ground alone they reject the applicability of a density rate of burning law. Their experimental method was as follows :—

* Phil. Trans. A, ccxxx. 682, p. 55 (1932).

† *Loc. cit.* cxcvi. pp. 404 and 544 (1933).

The closed vessel used had a volume of 150 cm.^{3}, the ratio of the surface of the walls to the volume of the vessel being 1·41 cm.$^{-1}$. To obtain increased cooling effect a steel spiral could be inserted into the vessel, reducing the volume and giving a ratio of effective cooling surface to available volume of 5·15 cm.$^{-1}$. Two propellant compositions were employed, a solventless powder containing 9 per cent. of diethyldiphenylurea, and an unstabilized nitrocellulose powder of the Poudre B type. Pressures were measured by crushers, and to obtain an estimate of the start of the explosion proper the weight of the black-powder igniter was increased sufficiently to produce a small compression of the crusher on ignition.

In the case of the propellant containing diethyldiphenylurea, charges were fired with and without the steel spiral at loading densities varying from 0·0210 to 0·2029, and at similar densities of loading the authors obtained the following comparative figures :—

	Without spiral.			With spiral.		
Δ.	p max. (kg./cm.^{2}).	$\int p\,dt$.	10^3t (sec.).	p max. (kg./cm.^{2}).	$\int p\,dt$.	10^3t (sec.).
0·110	1120	21·9	37	866	19·3	42
0·065	554	18·8	64	367	16·9	79
0·038	275	16·0	104	162	13·8	120

From these results Muraour and Aunis infer that (1) total explosion times increase with increased gas cooling, and (2) a linear relationship exists between $\int p\,dt$ and t, whatever the cooling conditions.

For the nitrocellulose powder a somewhat different experimental arrangement was followed in that all firings were at low densities of loading to accentuate effects generally, and that a comparison was made on the basis of approximately equal maximum pressures with and without the spiral. Mean figures (means of four observations in each case) are tabulated below :—

Without spiral				With spiral.			
Δ.	p max. (kg./cm.^{2})	$\int p\,dt$.	10^3t (sec.).	Δ.	p max. (kg./cm.^{2}).	$\int p\,dt$.	10^3t. (sec.).
0·040	366	4·70	23·8	0·052	373	4·60	24·4
0·025	216	3·97	29·5	0·035	227	4·20	30·0
0·016	131	3·49	46·9	0·023	124	3·46	47·5

The authors deduce that (1) total explosion times for a given value of maximum pressure are unaffected by variations in Δ ranging from approximately 30 per cent. to 40 per cent., and (2) for a propellant of given size, shape, and composition $\int p\,dt$ is a linear function of t only, whatever may be the procedure adopted for varying t, whether by varying Δ, modifying cooling effects, increasing the weight of the igniter, or adding to the propellant charge a proportion of a quicker burning propellant, the composition or proportion added being immaterial. Evidence in support of this final conclusion is adduced

Fig. 1.

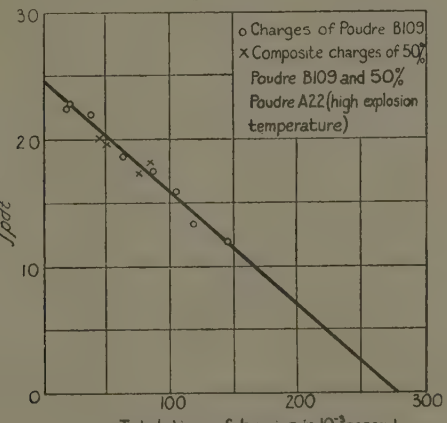

An experiment of Muraour and Aunis.

in a third paper, dealing with the behaviour of composite charges of two different propellant compositions, illustrated in fig. 1, which is reproduced direct from the paper by Muraour and Aunis in question *. It will be seen that, according to this graph, $\int p\,dt$ passes through a zero value for a total combustion time of approximately 0·28 second.

4. To conserve the invariance of the algebraic form of the Bλ term for f in equation (6) to any given value of Δ must correspond a definite value of Δ_i, otherwise the gas complex for any f will be varied. When the

* *Loc. cit.* cxcvi. p. 478 (1933).

cooling spiral is inserted into the vessel, the charge-weight of propellant must be reduced, in view of the reduced volume available for the gases, to maintain the value of Δ constant for comparison with observations with no spiral, and it follows that a proportionate reduction must also be made in the weight of the igniter. There is no indication that this precaution has been observed in the experiments under discussion, and, if it has not, the application of the criterion fails. Further, for any given value of Δ the fall in recorded maximum pressure due to the presence of the spiral indicates considerable cooling, and this affects the igniter gases before the ignition of the charge proper to at least as great an extent as it affects the propellant gases. The effective value of $\tilde{\Sigma}$ for the igniter gases differs, therefore, appreciably for the two cases of firing with and without the spiral, being much smaller in the former case. It follows that the time to ignition of the propellant grain surface differs appreciably in the two cases, and the ignition temperature of the propellant, which varies with the time and conditions of heating *, can no longer necessarily be taken to be equal to T_i, so that $B\lambda$ will take different values for the propellant for the two conditions of firing. Again, if, as Muraour and Aunis state, the igniter is sufficiently powerful to produce a measurable compression of the crusher on ignition, the time from ignition of the igniter to ignition of the main charge is included in their measured total time, which no longer corresponds to the actual duration of the propellant explosion as such. It may be noted that if cooling conditions are sufficiently accentuated the time to ignition of the propellant may be excessively prolonged, as, for example, in the case of a hang-fire.

An essential requirement in applying equation (6) is that firing conditions must be arranged to ensure that the propellant burns in accordance with the geometrical model assumed in equation (1). Such a requirement can be fulfilled only if every particle of the explosive is ignited simultaneously over its entire surface. It has long been recognized that the only satisfactory way of achieving this end is by means of gas ignition † ;

* Phil. Trans. A, ccxxx. 691, pp. 407–408 (1932).

† Petavel, Phil. Trans. A, ccv, 397, pp. 372–373 (1905) ; Crow and Grimshaw, Phil. Trans. A, ccxxx. 682, p. 41 (1932).

with the type of igniter used by Muraour and Aunis ignition of the propellant is selective, the portions nearest the igniter starting to burn first. Comparative experiments with the two forms of ignition show that the shape of the pressure-time curve varies in important particulars, the general tendency being for the recorded duration of the explosion to become drawn out when a gunpowder igniter is used. Considerations of this nature have led the majority of experimenters using crushers and powder igniters to adopt the Vieille criterion * in interpreting pressure-time curves, namely, concentrating on the region of the curve lying between one-third and two-thirds of maximum pressure, discarding observations on either side of this region, and restricting themselves to differential rather than integral methods for ascertaining apparent rates of burning.

The conclusion is reached, therefore, that the criterion of equal times of combustion for equal densities of loading is not applicable in the circumstances of the experiments as carried out by Muraour and Aunis.

5. We propose now to examine briefly the circumstances in which crushers can be used to measure the pressures of explosions. The functioning of copper crushers has been discussed by us in considerable detail elsewhere †, and in the present connexion it will be sufficient to recall only the relevant points. The assumption originally underlying the use of crushers was that a definite one-to-one correspondence exists between the crush on the copper and the pressure that has produced the deformation, the relationship being ascertained under static conditions of pressure application. The first indication that the resistance of the crusher cannot be expressed solely in terms of the compression was given by Charpy ‡, who showed that for a given maximum pressure the compression of the crusher can be varied between relatively wide limits by varying the rate of application of the load. Later, Charbonnier and Galy-Aché § found that the final resistance of a crusher compressed by an

* The objects of this are twofold, namely, to eliminate as far as possible the effects of selective ignition, and to minimize the errors attendant in the use of crushers.

† R. D. Report, no. 64, H.M.S.O. (1927); see also 'Mémorial de l'Artillerie Française,' vii. pp. 435–482 (1928).

‡ 'Mémorial de l'Artillerie de la Marine,' pp. 119–121 (1898).

§ 'Mémorial de l'Artillerie de la Marine,' pp. 391–567 (1900).

explosive pressure is always greater than that of a crusher brought to the same final height by slow pressing. An alternative calibration table was accordingly put forward by them for interpreting the results of observation under conditions of rapid application of the load. Vieille and Liouville * next took up the problem to determine the magnitude of the correction applicable under conditions of firing in closed vessels, and proposed a calibration table, similar to that used now in the French service, differing but slightly from the table proposed by Charbonnier and Caly-Aché. The accuracy of the calibration now accepted in France has been verified by us as regards closed-vessel firings, where the pressure fall from maximum is relatively slow, but we have shown that, as far as observations in ordnance are concerned, considerable modifications are necessary, the correction to be applied to the recorded maximum pressure varying with the calibre of the gun and the loading conditions †.

6. It is clear, therefore, that, provided a suitable calibration table be employed, crushers can be used in closed-vessel explosions to determine maximum pressures with fair confidence. It is quite another matter, however, to attempt to use them to indicate the development of pressure with time. In the first place the crusher does not start to compress at all until the pressure has reached an appreciable magnitude, of the order of 135 kg./cm.^{2} in the case of the British service crusher, which corresponds closely to that used in the French service for measuring high pressures. This critical pressure varies with the dimensions of the crusher used, but it is in all cases an appreciable fraction of the maximum pressure reached during the explosion. Secondly, the resistance of the crusher at any stage of the compression is not only dependent on the actual rate of compression at that stage, but is also dependent on the path by which that stage has been reached. This point has been brought out by our own investigations ‡ and by J. H. C. Thompson in a discussion of the theory of visco-elasticity §. Applying the principle of virtual work, and using the

* *Comptes Rendus*, cxlii. pp. 1057–1058; cxliii. pp. 1218–1221 (1906).

† R. D. Report, no. 64, pp. 42–45 (1927).

‡ R. D. Report, no. 64, pp. 33–36 (1927).

§ Phil. Trans. A, ccxxxi. p. 703 (1933).

first and second laws of thermodynamics, he has shown that the stress-strain relations, taking temperature changes into account, depend on the previous strain history through the presence of a term involving the dissipation function. Experiments show that a consequence of this mode of functioning is that the crusher resistance attains a maximum at some intermediate stage of the compression, when the pressure is rapidly applied, the crusher coming to rest under a falling pressure. It is this property of the crusher that accounts for the varying correction that needs to be applied tc recorded maximum pressures in ordnance, referred to above.

Fig. 2.

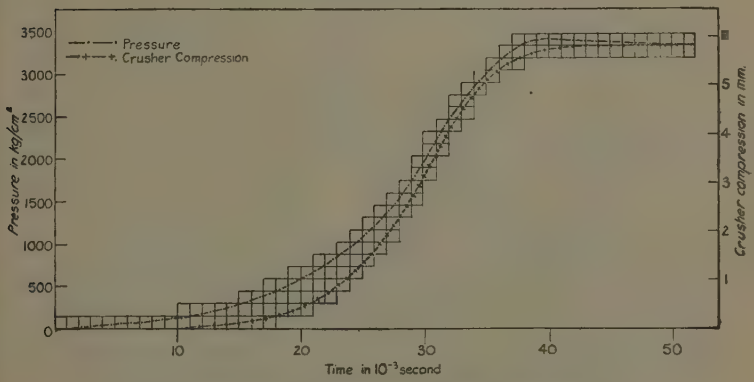

Time correlation of pressure and crusher compression.

7. The points under discussion are well illustrated in fig. 2, which gives a direct comparison between a pressure-time curve of an explosion in a closed vessel recorded by our standard spring manometer *, and the corresponding compression-time curve of a copper crusher. The density of loading employed was 0·25, the maximum pressure being 3360 kg./cm.². For the experiment a special crusher gauge was designed to screw into the vessel, the movement of the piston being recorded optically in the same way as the movement of the piston of the spring manometer, and to the same time-scale, the

* R. D. Report, no. 64. pp. 17–21 (1927).

conditions being strictly comparable. The difficulty encountered in interpreting the crusher curve is the relative placing of the two curves to a time basis, and this has been done on the assumption that the crusher starts to compress when the applied pressure has reached a magnitude of 135 kg./cm.^{2}, a figure which obtains under conditions of static pressing at varying speeds. In fig. 3 curve I. shows the pressure-compression relationship with the positioning adopted; curve II. shows the same relationship, assuming that the crusher and spring start to compress together; curve III. shows

Fig. 3.

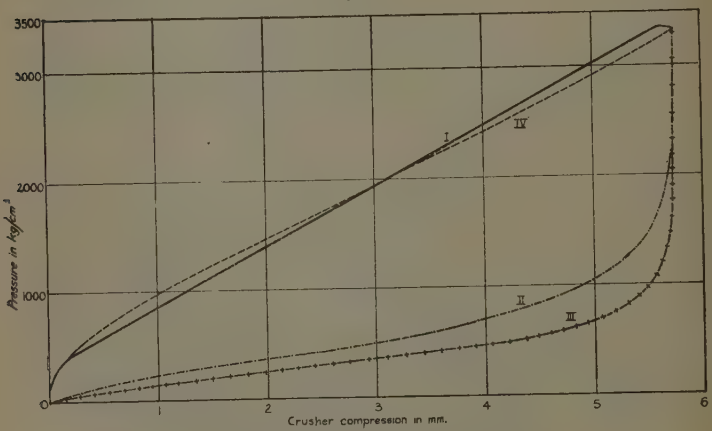

Pressure-compression relationships.

the effect of assuming the crusher and spring to finish compressing together; and curve IV. is the calibration table for closed-vessel firings. It is clear that curve I. most nearly approaches the calibration table; the effect of slightly varying the assumed critical pressure corresponding to the start of compression results in a worse fit. Further, to interpret crusher readings after the manner of Muraour and Aunis, curve IV. (or its French equivalent) must necessarily be used, and the positioning adopted therefore places the crusher indications in the most favourable light as regards acceptance of pressure values.

From fig. 2 it will be seen that the crusher is out of step with the spring throughout the explosion, and that it continues to compress for 0·013 second after maximum pressure has been reached. The total time of compression of the crusher, which would correspond to the time-interval measured by Muraour and Aunis, is 0·042 second, whereas the true time from the first movement of the crusher to the occurrence of maximum pressure is 0·029 second. While the experiment was carried out at a relatively high density of loading, by reason of employing a slow-burning propellant the time of explosion is of the same order of magnitude as encountered in the experiments of Muraour and Aunis, and the error in their estimate of total time will be comparable with that indicated here.

8. From the foregoing it is clear that if the use of crushers is to be extended to the measurement of the variation of pressure with time during an explosion, the interpretation of their indications should be restricted to the region covered by Vieille's criterion, and a differential method should be followed for determining the ballistic characteristics of a propellant. This has been generally recognized in the past by investigators using crushers, and they have for the most part been led to avoid methods of analyzing crusher records involving integration. The danger of such methods is that the main contribution to the total area of a pressure-time curve up to maximum pressure is in the region of maximum pressure; in analysing a crusher record the position of maximum pressure must be assumed to coincide with the end of motion of the crusher, so that the value of $\int p\,dt$ deduced from the crusher movement greatly exceeds the value of $\int p\,dt$ for the true pressure-time curve, and there is not necessarily any connexion between the two values. A rough correlation may possibly exist where firing conditions are not too diversified, but the range over which such a correlation may hold is certainly limited. It would seem that the relationship shown in fig. 1 may be interpreted, not as exhibiting the burning characteristics of the propellant, but rather as establishing some connexion between the impulse applied to the crusher under explosive conditions and the time taken

by the crusher to come to rest under the mechanical effect imposed.

It may be concluded, therefore, that the experiments carried out by Muraour and Aunis fail to disprove the validity of the temperature-density rate of burning law.

XIII. *Flame Temperatures in Carbon-Monoxide and Air Mixtures.* *By* Prof. W. T. David, *Sc.D.*, *and* J. Jordan, *M.Sc.**

IN a previous paper † we described experiments in which the temperatures of fine platinum-rhodium wires were recorded during the pre-pressure period in explosions of hydrogen and air and carbon-monoxide and air mixtures over a limited range of mixture strengths. We pointed out that as it was possible to control accurately the mixture strength in this way, it seemed a desirable method of correlating flame temperature (as determined by a platinum wire) with mixture strength.

The present paper contains an account of experiments of a similar type, but with improved apparatus, with carbon-monoxide and air mixtures covering a wide range of mixture strengths. Two series of experiments were made, the one at a density of one atmosphere, and the other at five atmospheres density. A few experiments were also made at eight atmospheres density.

Description of Apparatus and Method of Calibrating the Wires.

The experiments were conducted in a spherical explosion vessel 18 inches in diameter ‡, and the mixtures were fired electrically by means of a centrally placed spark gap formed by long electrodes passing vertically upwards through a screwed plug in the bottom of the vessel §. The platinum-rhodium thermometer wires were

* Communicated by the Authors.

† Phil. Mag. xii. p. 1043 (Nov. 1931).

‡ For the slow burning weak mixtures it was found more convenient to use a smaller vessel.

§ The weakest spark which would just ignite the mixture was used throughout.

0·0005 inch in diameter and about 2 inches long. They were fused at their ends to thick leads of the same material which passed into the vessel through a gas-tight holder, provision being made for altering the position of the wire relative to the spark by fitting the holder into a gas-tight gland. The holder also carried a pair of duplicate leads for compensating purposes. A description of the apparatus and recording systems for both pressure and temperature measurements was given in the previous paper *.

Each wire used was calibrated directly in an electric furnace against a standard thermocouple up to 1200° C. The calibration curve thus obtained was extrapolated to higher temperatures by recording the deflexion of the galvanometer when the wire was completely immersed in the flame of a bunsen burner, and, finally, the melting-point was obtained by fusing it in the explosion of a strong mixture. The wire during this process was mounted on its usual leads and was in every respect in the same condition as when placed in the explosion vessel. It was never allowed to remain in the furnace for more than about two seconds, a time insufficient to admit of any appreciable heating of the comparatively thick leads. During the whole of this time a photographic record of the galvanometer deflexion was taken and it was found to remain quite constant.

The temperature assumed for the bunsen flame was 1750° C., since it was found that a piece of platinum wire of the same diameter and approximately the same length as the platinum-rhodium wires just melted when placed in the flame above the inner cone. The temperature of fushion of platinum-rhodium (90 per cent. pt., 10 per cent. rho.) used was taken as 1850° C.

No difficulty was experienced in obtaining a steady temperature in the bunsen flame, provided the wire was completely immersed in the flame and that it was placed above the inner cone; indeed, it was found that slight variations in the amount of primary air supplied to the burner produced no appreciable alteration in the temperature of the wire †.

The direct method of calibration was adopted, firstly,

* *Ibid.* p. 1.

† This is in accord with the experiments of Loomis and Perrot (see p. 176).

because the temperature coefficient of the platinum-rhodium alloy used has not been accurately determined at high temperatures, and secondly, because it automatically compensates for conduction to the cold leads with an accuracy probably greater than could be obtained by correction for this effect if the temperature had been directly inferred from the resistance. That this would be so is to be expected in view of the similarity of the conditions of the wire in the furnace and in the flame of the explosions, and it is further proved by the results of experiments with wires of widely varying lengths. These show that the temperature recorded in a given mixture was independent of the length of the wire even when this was varied from about $\frac{1}{4}$ inch to 2 inches.

Fig. 1.

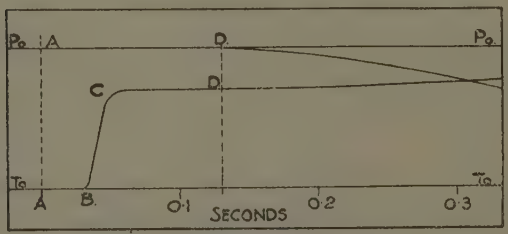

PRESSURE & TEMPERATURE RECORD FOR A 17% CO-AIR MIXTURE.

Results of Experiments.

A typical record for a mixture of 17 per cent. CO and air is shown in fig. 1. P_0P_0 is the line of zero pressure corresponding to the initial pressure in the vessel before ignition, and T_0T_0 is the line of zero temperature corresponding to the resistance of the platinum-rhodium wire at room temperature. The point A marks the passage of the spark. Shortly afterwards the flame passed over the wire (as shown at B), and its temperature increased rapidly to C. It then remained practically constant * until the pressure began to rise at D.

* While the temperature of the wire usually remained remarkably constant after its initial rise, as shown in fig. 1, many records were obtained in which the wire showed considerable cooling in the interval between the attainment of maximum temperature and the beginning

This point *D* marks the beginning of a further increase in the temperature of the wire due to adiabatic compression of the gas at the centre of the vessel produced as a result of the burning of the outer layers.

Experiments with the Mixtures at Atmospheric Density.

The experiments with the mixtures at atmospheric density are summarised in fig. 2. Curve *Tw* gives the maximum steady temperatures reached by the wires during the pre-pressure period for mixtures ranging from 14 per cent. CO on the "weak" side to 69 per cent. on the "over-rich" side. The curve *Ti* shows the ideal temperatures which the products should have attained when burned at constant pressure assuming complete combustion. These temperatures have been calculated on the basis of specific values given by Partington and Shilling * which range up to 2000° C. The dotted portion of this curve in the calculation of which dissociation has been neglected, is based upon extrapolated specific heat values. The dotted curve *Td* gives the ideal temperatures taking dissociation into account. *Ti'* and *Td'* are similar curves based upon the specific heat values furnished by the Planck-Einstein equation for the specific heats of diatomic and triatomic gases †. These values are considerably higher than those of Partington

---

of the pressure rise. When this occurred the maximum temperature (during the pre-pressure period) was found to be less than for an experiment in a similar mixture in which by a suitable rearrangement of the apparatus, cooling was prevented.

The effect was ultimately traced to the influence of currents of gas which had previously been cooled by contact with the spark electrodes, and in certain cases even by the wire leads themselves. A study of these currents has shown that very considerable errors may be introduced by them whenever they are moving in such a way relative to the wire as to strike a cold part of the internal apparatus before coming into contact with it. Moreover, the direction of these currents varies from mixture to mixture in an extremely complicated and (in weak and very "over-rich" mixtures) erratic manner, and it is this which has constituted the main difficulty in connexion with these experiments. To overcome this we have repeated each of our experiments under as widely varying conditions as possible, both as regards the position of the wire in the vessel and its position relative to the spark electrodes, and no result has been admitted to the series until it is clear that the wire was not influenced by cold currents and it could be repeated within very fine limits.

* 'The Specific Heats of Gases' (Benn, 1924).

† Nernst and Wohl, *Z. Tech. Phys.* (Nov. 1929).

and Shilling and give calculated temperatures correspondingly lower *.

The dotted curve marked *LP* shows the temperatures obtained by Loomis and Perrot † using the spectral line reversal method for carbon-monoxide and air mixtures burning under constant pressure conditions in the open flame. These temperatures were measured at a point just above the inner cone. Those marked $GA_{max.}$ and $GA_{min.}$ give the results obtained by Griffiths and Awbery‡, using a similar method, for their maximum and minimum rates of flow.

Comparing our results with the open flame experiments

Fig, 2.

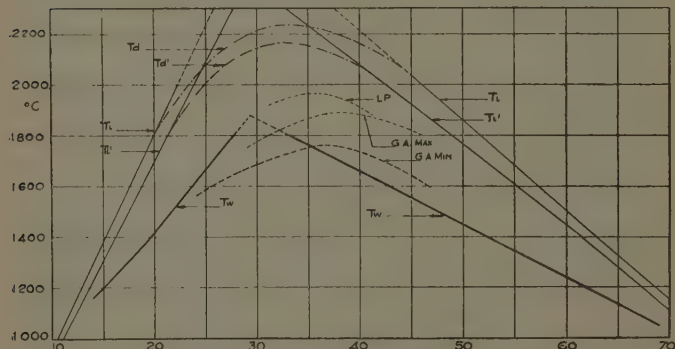

COMPARISON BETWEEN MEASURED AND CALCULATED TEMPERATURES FOR CO—AIR MIXTURES AT ATMOSPHERIC DENSITY.

it will be seen that the maximum temperatures are of the same order. There is, however, the important difference that whereas the open flame maximum tem-

* Recent experiments by Henry (Proc. Roy. Soc. A, cxxxiii. p. 992 (1931)) and Eücken and Mücke (*Z. Phys. Chem.* B. 18, p. 136 (1932)) have yielded values for the specific heats of CO, O_2, N_2, and CO_2 at temperatures between 0° C. and 800° C. very close to those calculated from the quantum theoretical equation, but no confirmation has yet been obtained for the theory at temperatures as high as those dealt with in the present paper. The results of experiments by other workers in this laboratory, however, would seem to suggest that the actual molecular heats of these gases cannot be greater than the Planck-Einstein values, and the curves Ti′ and Td′ would thus represent the lower limit for the ideal temperatures in these experiments.

† Ind. and Eng. Chem. p. 1007 (Oct. 1928).

‡ Proc. Roy. Soc. A, cxxiii. (1929).

peratures are attained for mixture strengths very much on the over-rich side, the maximum temperature in our experiments is reached in the mixture in which carbon-monoxide and oxygen are present in their combining proportions—or very nearly so. This would appear to be correct, for the temperatures are well below that at which dissociation of carbon-dioxide begins to be appreciable. A possible explanation would appear to be that infiltration of secondary air occurs in the open flames, though it must be admitted that it is difficult to see how such infiltration could take place at the point (just above the inner cone) at which Loomis and Perrot measured their temperatures, and it may be that a more fundamental explanation is necessary to account for the difference between the open flame spectral line results and our own results obtained by platinum thermometry.

Perhaps the most outstanding feature of our experiments is that the difference between the ideal and the wire temperature is very much greater for the strong mixtures than for the weak and very over-rich mixtures. Thus for a 28 per cent. mixture this difference is more than 600° C.* when the ideal is calculated upon the basis of extrapolated Partington and Shilling specific heat values, or 500° C. when the ideal is calculated upon the basis of the Planck-Einstein specific heats, while for a 14 per cent. mixture it is only 120° C. or 60° C., and for a 69° C. per cent. mixture only 140° C. or 100° C.

We have obtained qualitatively similar results for experiments (not yet completed) with other gases and also with carbon-monoxide and oxygen mixtures with other diluents than nitrogen. Hopkinson's results for coal-gas and air mixtures are also in accord, although when he made his experiments he did not have the advantage of reliable specific heat data, and he interpreted his experiments in another way. He used two mixtures, a weak mixture containing 8·7 per cent. coal gas and a medium one containing 10 per cent.

* These temperature differences are obtained by comparing the actual wire temperatures with the ideals calculated on the assumption that there is no dissociation. This seems a correct comparison, for the temperature of the actual flame is only 1850° C., at which temperature dissociation is generally assumed to be neglible. A comparison in which reference to dissociation is avoided may be made for the strong 45 per cent. mixture. Here the difference between the ideal and the wire is about 450° C. or 350° C.

In the weak mixture he found a wire temperature during the pre-pressure period of 1000° C., which is 130° C. below the ideal calculated on the basis of the specific heat values of Partington and Shilling, or 85° C. below that calculated upon the basis of the theoretical specific heats. In the medium mixture the wire temperature was 1225° C., which is 215° C. or 140° C. below the calculated ideal.

The experiments with open flames show precisely the same thing. Indeed, as will be seen from the curves in fig. 2, the open flame temperatures vary with the mixture strength to an even less extent than is the case in our experiments. It will be clear that these results are not to be explained in terms of ordinary thermal dissociation, since the measured temperatures are well below that at which this effect begins to be appreciable.

Two possible explanations will at once occur to the mind, viz.: (1) radiation loss from the wire, and (2) radiation loss from the products of combustion, both of which, of course, increase rapidly with temperature. These we will now briefly discuss, and it will be shown that they cannot account for our results to any appreciable extent.

The difference between the temperature of the gas and that of the wire due to radiation depends upon the rate at which heat is transferred from the gas to the wire and the emissivity of the wire at the temperature concerned. If the rate of heat reception by the wire is λ calories per second per degree difference in temperature between the wire and the gas and the heat radiated is E calories per second, it is easily seen that the radiation correction is given by the ratio E/λ. The value of λ at any given temperature can be obtained from the slope of the wire temperature record during the initial heating of the wire, and analysis in this way of a number of records gives 40° C. as an upper limit for this correction when the temperature of the wire is 1800° C., a correction which is negligibly small in comparison with the observed differences between the measured and the calculated temperatures *.

* In drawing up the curves of figs. 2 and 3 no allowance has been made for radiation. A correction of 40° C. to the maximum measured temperature at atmospheric density, would bring our result into better agreement with that of Loomis and Perrot.

The cooling of the burnt gases by radiation within the period of time occupied by our pre-pressure measurements has been proved to be small. Mr. R. M. Parkinson, working in this laboratory, measured the radiation from the gases during the pre-pressure burning and found that the radiation emitted by strong CO and air mixtures did not exceed more than from 1 to 2 per cent. of the heat of combustion of the gases inflamed during this period.

This, at first sight, seems completely at variance with the radiation measurements from open flames, which show radiation losses amounting to about 10 per cent. of the heat of combustion. Dr. H. Hartley, however, has recently shown that only about one-seventh of the total radiation from open flames is emitted by the visible flame (including the inter-conal gases *), thus providing an explanation of the apparent discrepancy between open flame measurements of radiation and measurements made during the pre-pressure period in explosions in closed vessels.

Experiments with Mixtures at Five Atmospheres Density.

Similar experiments to those already described were made with CO and air mixtures at a density of five atmospheres. The results are shown in fig. 3 ($Tw5$). For purposes of comparison the previous results at one atmosphere density are also shown ($Tw1$). A few experiments were also made at eight atmospheres density ($Tw8$). These could not be continued without danger to the explosion vessel and fittings. The ideal temperature curves Ti and Ti' have been taken from fig. 2.

It will be noticed that the temperatures recorded at the higher densities are considerably greater than those recorded at atmospheric density—the comparison, of course, being made for similar mixture strengths, but apart from this the general characteristics of the results are precisely the same.

Discussion.

In the discussion of the results previously reported, we suggested that the wire temperature differed from the temperature corresponding to the mean translational

* Communication No. 63 Inst. Gas Engineers, 1932, p. 22.

energy of the molecules of the products of combustion because of some kind of surface action between the hot wire and the freshly burnt gas. This was obviously true of the very weak hydrogen mixtures in which the temperature was very much above the ideal, and unless we suppose it to be true also of the weak CO-air mixtures we are forced to the conclusion that combustion is a more efficient process in weak mixtures than in strong ones, a conclusion which appears to be untenable on the basis of generally accepted chemical theory.

For the stronger mixtures both our own experiments

Fig. 3.

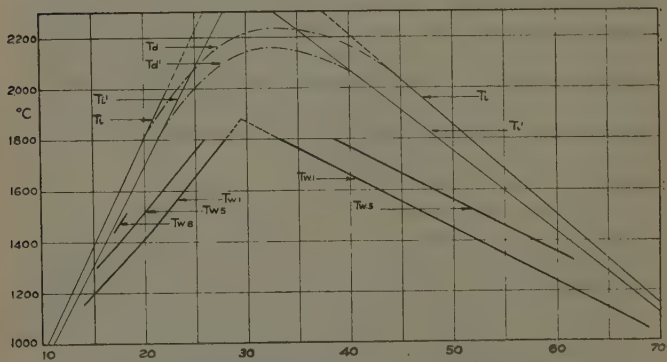

Comparison between measured and calculated temperatures for CO — Air Mixtures at different densities.

and those of other workers which we have quoted leave no doubt that the temperature of a flame as measured by the specific change which takes place in a thermometric substance (*e. g.*, resistance of a fine platinum wire, luminosity of excited sodium atoms, etc.) when introduced into the flame is less than that which is to be expected on the basis of the heat of combustion of the mixture and the specific heats of the products to an extent wholly unexplainable in terms of heat loss and dissociation. At first sight this might not appear obvious, and indeed other workers in comparing measured flame temperatures with those calculated on the assumption of chemical equilibrium, have suggested that there is reasonable

agreement and that the difference (about 200° C. in the case of CO-air mixtures and about 100° C. in the case of certain hydrocarbon gases) could be explained in terms of radiation from the gas. Their case is approximately represented by comparing the maximum temperature measured by Loomis and Perrot with the lower dissociation curve *Td'* in fig. 2; but in making this comparison it is to be noted that in order to raise the temperature of the gas from the measured to the calculated value, the heat added must be sufficient not only to raise the internal energy of the gas but also to bring about the necessary change in the equilibrium concentrations of the reacting gases. In the case of our 28 per cent. mixture at atmospheric density the energy required to do this amounts to about 22 per cent. of the heat of combustion when the calculation is made with the theoretical specific heats, and 29 per cent. when the Partington and Shilling values are used. Both of these figures are very greatly in excess of the measured radiation from open CO-air flames, and the discrepancy becomes still more pronounced when regard is had to the fact that by far the greater proportion of the heat radiated from such flames comes from the products of combustion outside the luminous region

Whether or not in these strong mixtures there exists thermal equilibrium in the ordinary sense between the wire and the gas is at present difficult to say, but that there is some kind of abnormality in the freshly burnt gas seems quite certain, and we reserve a fuller discussion until the results of experiments with other gases now in progress are available.

XIV. *The Surface Tension of Liquid Metals.*—Part V. *The Surface Tension of the Lead-Tin Alloys.* *By* L. L. Bircumshaw, *M.A., D.Sc.** (*From the National Physical Laboratory.*)

VERY little work has been published on the surface tension of alloys. With the exception of a few observations by Matuyama[1] the only measurements which have been recorded this century appear in the very interesting papers of Sauerwald and his collaborators[2].

* Communicated by Sir J. E. Petavel, K.B.E., D.Sc., F.R.S.

Results are given for a number of alloys of each of the systems bismuth–lead, copper–antimony, copper–tin, gold–copper, silver–copper, and some alloys of iron. From the results of his own experiments Sauerwald divided alloy systems into two groups—those which deviate only slightly from the mixture rule, like bismuth–lead and bismuth–tin, and, on the other hand, systems like copper–antimony and copper–tin which show considerable deviation.

It is somewhat surprising that a thorough study does not hitherto appear to have been made of the lead–tin system, and the present communication deals with the measurement of the surface tension of a number of these alloys right across the composition range and at temperatures from 200° C. to 800° C.

Experimental.

The method used was that previously described [3], and consisted in the measurement of the pressure required to detach a bubble from each of two tubes arranged concentrically and immersed to the same depth in the molten metal. The apparatus used is shown in fig. 1, and was similar to the one described in the first paper of this series, but was modified in respect of the following details. The alundum crucible L and clay cover M were replaced by a pot and cover of silica, and the Mabor cylinder which supported the crucible was replaced by a silica tube sealed at the top by a flat end. The plate G was water-jacketted, and the pitch joint previously used was replaced by a wax one. In all other respects the apparatus was virtually the same as the original. The hydrogen was prepared and dried as described formerly [4]. Owing to the great difficulty experienced in obtaining concordant results at the lower temperatures, due presumably to traces of oxygen or water vapour still present in the hydrogen, just before the gas entered the furnace it was passed over magnesium heated to a temperature just below its melting-point. The tubes used had the following dimensions :—

Mean external diameter of outer tube ..	1·010 cm.
Mean internal diameter of outer tube ..	0·817 ,,
Mean external diameter of inner tube ..	0·100 ,,

Fig. 1.

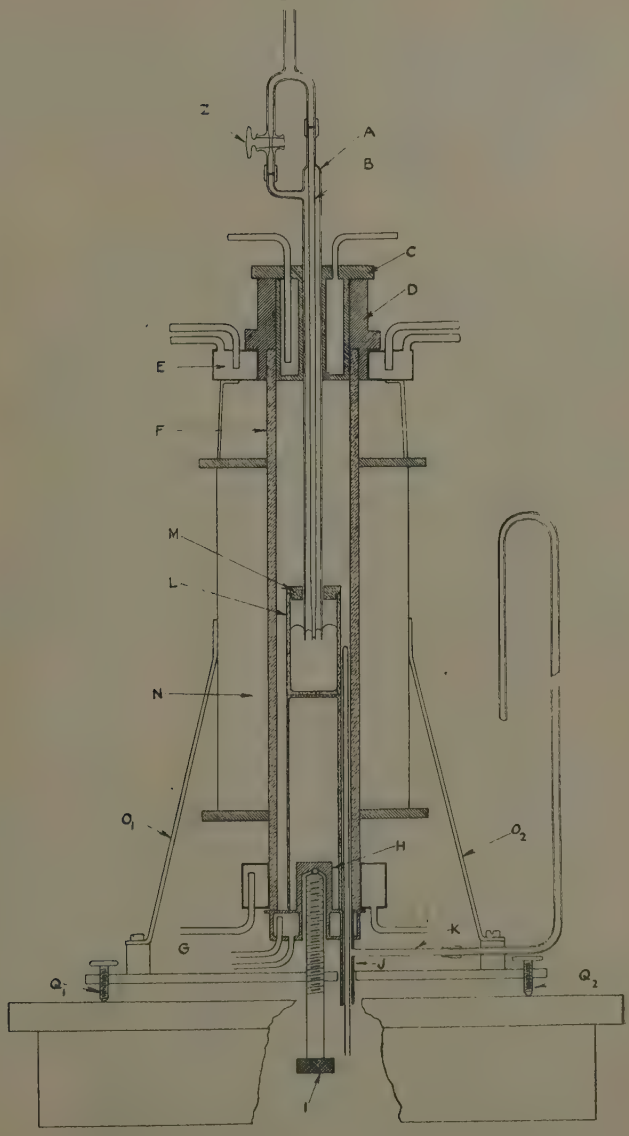

The diameter of the container was 3·2 cm.* and the zero of the manometer was 0·5 cm. The temperature of the room was always very close to 20° C. and the manometer readings were corrected to 4° C. The densities of the lead and tin and the alloys were taken from the data given by Day and Sosman[5] and Arpi[6]. The results were calculated from the formula [7]

$$a^2 = \frac{H}{1/X_1 - 1/X_2}.$$

The calculation of the correction to be applied for the alteration of the head of metal in the container when a bubble is blown from the outer tube was that given previously[8]. For lead and tin at 800° the approximate values of a^2 used for the beginning of the calculation in each case were the values obtained in the previous work, while for each successively lower temperature the previous value was taken. For the alloys two or three values at the lead end of the series were calculated from initial values of a^2 obtained on the assumption that it was additive as regards composition, and the curve so obtained extrapolated to the value for pure tin. The final values of a^2 for the other alloys fell very close to the curve. This was done for the whole series at 800°, and for a particular alloy at lower temperatures the same method was used as for the pure metals.

TABLE.

	Temp.	P wide.	P narrow.	Density.	a_1.	γ dynes/cm.
Mercury	20°	20·4	32·8	13·546	0·07274	483†
Lead	800°	15·35	26·8	10·132	0·08230	409
	600°	15·1	27·1	10·352	0·08389	426
	400°	14·9	27·2	10·580	0·08447	438
	350°	14·8	27·2	10·615	0·08470	441
Alloy A.	Atomic per cent. Sn 4·43.					
	800°	16·25	27·7	9·980	0·08392	411
	600°	15·95	28·0	10·193	0·08564	428
	400°	15·7	28·4	10·425	0·08749	447
	350°	15·6	28·4	10·480	0·08752	450

* In the case of mercury the container had a diameter of 2·85 cm.

† The value obtained in the previous work was 480.

TABLE (*cont.*).

	Temp.	P wide.	P narrow.	Density.	a^2.	γ dynes/cm.
Alloy B.	Atomic per cent. Sn 16·30.					
	800°	15·75	27·5	9·560	0·08849	415
	600°	15·4	27·65	9·786	0·08968	430
	400°	15·15	28·0	10·030	0·09104	448
	350°	15·05	27·95	10·088	0·09086	450
	320°	15·0	28·0	10·111	0·09131	453
Alloy C.	Atomic per cent. Sn 37·40.					
	800°	16·7	28·8	8·831	0·09727	421
	600°	16·35	29·1	9·048	0·09963	442
	400°	16·05	29·3	9·287	0·10031	457
	300°	16·1	29·45	9·396	0·09990	460
	280°	16·1	29·75	9·410	0·10169	469
Alloy D.	Atomic per cent. Sn 63·90.					
	800°	15·6	28·85	7·904	0·1154	447
	600°	15·3	28·9	28·9	0·1153	457
	400°	15·1	29·1	8·298	0·1154	470
	300°	14·95	29·15	8·395	0·1153	475
	250°	14·95	29·2	8·440	0·1153	477
Alloy E.	Atomic per cent. Sn 75·10.					
	800°	15·85	29·65	7·512	0·1250	461
	600°	15·6	29·75	7·677	0·1250	471
	400°	15·35	29·8	7·856	0·1245	480
	300°	15·25	30·0	7·940	0·1255	489
	200°	15·15	30·0	8·066	0·1244	492
Alloy F.	Atomic per cent. Sn 84·1.					
	800°	16·5	30·95	7·194	0·1354	478
	600°	16·3	31·2	7·343	0·1363	491
	400°	16·15	31·25	7·500	0·1351	497
	300°	16·05	31·45	7·582	0·1355	504
	250°	16·0	31·5	7·620	0·1361	509
Alloy G.	Atomic per cent. Sn 93·85.					
	800°	16·9	32·0	6·885	0·1464	494
	600°	16·7	32·3	6·976	0·1486	508
	400°	16·55	32·5	7·105	0·1489	519
	300°	16·5	32·7	7·181	0·1493	526
	250°	16·5	32·8	7·205	0·1496	529
Alloy H.	Atomic per cent. Sn 98·45.					
	800°	17·1	32·65	6·691	0·1541	506
	600°	16·9	32·9	6·800	0·1554	518
	400°	16·8	33·2	6·916	0·1563	530
	300°	16·75	33·4	6·982	0·1570	538
	250°	16·75	33·5	7·002	0·1573	540

TABLE (*cont.*).

	Temp.	P wide.	P narrow.	Density.	a^2.	γ dynes/cm.
Tin.....	800°	17·3	33·05	6·637	0·1566	510
	600°	17·2	33·45	6·738	0·1590	526
	400°	17·1	33·75	6·850	0·1598	537
	300°	17·05	33·95	6·920	0·1603	544
	250°	17·05	34·15	6·940	0·1618	550

The results are shown in the table. A comparison with the results for lead and tin previously obtained shows that the new curve for lead lies slightly below the old one. The agreement is quite good, however, the maximum deviation being about 2 per cent. The results for tin agree excellently, with the exception of those at 250° and 300°. In the latter case the difference from the previous value is about 4 per cent. The graphs from the pure metals are shown in fig. 2. The results for the alloys are shown graphically in fig. 3, and it will be seen

Fig. 2.

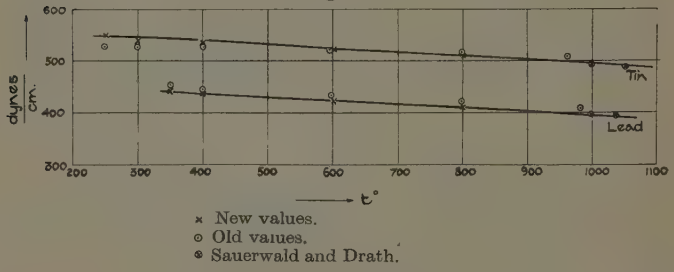

× New values.
⊙ Old values.
⊛ Sauerwald and Drath.

that the surface tension temperature coefficient in all cases is negative. They are plotted against composition (atomic) in fig. 4. It will be observed that although small quantities of lead lower the surface tension of tin considerably, small quantities of tin have a relatively slight effect on the surface tension of lead; also that with rise of temperature the lowering of the surface tension of tin by lead gradually decreases.

The relatively large lowering of the surface tension of the tin-rich alloys by the lead necessitates, in accordance

with Gibbs's equation, a positive adsorption of lead at the interface. In view of the fact that, up to the present, adsorption in a binary metallic system does not appear

Fig. 3.

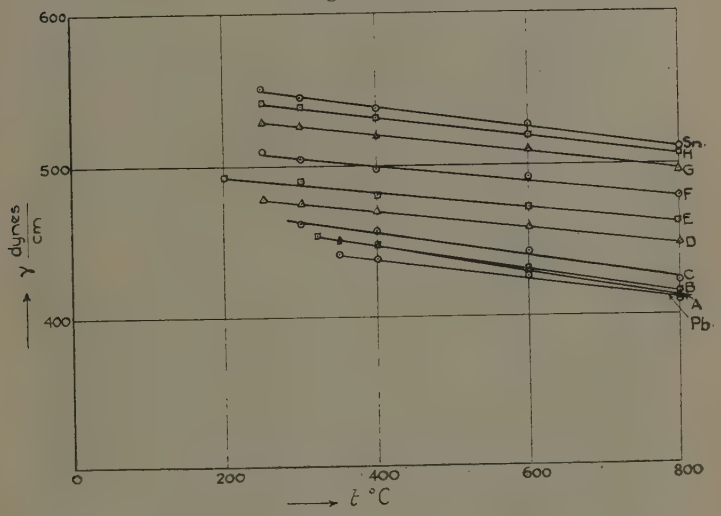

Fig. 4.

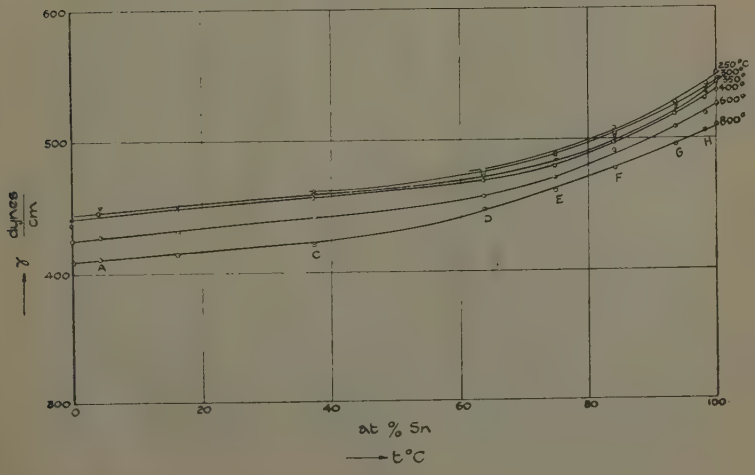

to have been studied, it is of considerable interest to consider the present results from this standpoint. Adsorption in concentrated solutions has been examined in recent years by Schofield and Rideal[9], Wynne-Jones[10], and Butler and Wightman[11]. Schofield and Rideal dealt with solutions of ethyl alcohol and pyridine in water, and by combining the data for surface tension and vapour pressure they were able to use the exact form of Gibbs's equation and calculated values of Γ, the excess surface concentration, for concentrations of solute up to 100 per cent. In the case of ethyl alcohol, plotting Γ against mol fraction of alcohol, a curve is obtained which rises first rapidly and then more slowly to a maximum value until a concentration of 0·3 mol fraction is reached, when the value of Γ falls to a value which remains practically constant from 0·7 to 1·0 mol fraction. The first portion of the curve they explained on the very probable hypothesis of the gradual building up of a unimolecular layer of alcohol, but for the second portion, which they rightly remark is not so readily interpreted, they offered two explanations: (1) a decrease in the degree of orientation of the alcohol molecules when the more polar water is replaced by the less polar alcohol; (2) the formation in strong alcohol solutions of a layer relatively rich in water below the surface layer of adsorbed alcohol.

Schofield and Rideal's views have been criticized by Wynne-Jones, who considers that the total amount of solute in the surface is the Γ as defined by Gibbs plus the amount normally present in the absence of adsorption. Using more recent results for the vapour pressures, Wynne-Jones obtains a curve for the total amount present in the surface which rises to a maximum at 30 per cent. alcohol and then remains constant to 100 per cent. alcohol.

Butler and Wightman apparently accept Wynne-Jones's argument in principle, but consider the magnitude of his correction a little excessive. They arrive finally at the conclusion that the observed adsorptions are inconsistent with the hypothesis that only a single layer of molecules at the surface differs in composition from the bulk of the solution, but point out that the differences between the requirements of this theory and the observed values are comparatively small.

In view of the absence of definite information on the activity of lead in molten lead–tin alloys it is necessary in dealing with the present results to use the approximate form of the Gibbs equation

$$\Gamma = -\frac{c}{RT}\frac{d\gamma}{dc},$$

Fig. 5.

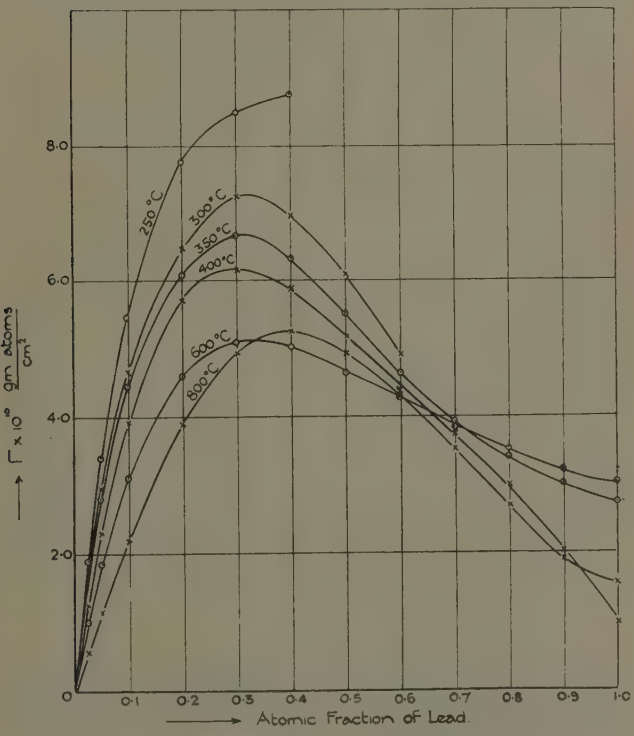

where Γ is the surface excess, γ the surface tension, and c the mass concentration. In addition it must be mentioned that in the case of alcohol-water the surface tension can be determined with a much greater accuracy than that of lead-tin, and the argument and results which follow must necessarily be regarded as approximate. Values of $d\gamma/dc$ were obtained from the smoothed surface-tension-

concentration curve from which Γ was calculated. The results are shown graphically in fig. 5. The most interesting feature to be observed is that the curves have the same shape as that given by a capillary active substance, *i. e.*, alcohol in water ; also, with the exception of 600° and 800°, for which the surface excesses are almost equal, the adsorption rises considerably with fall of temperature, and at all temperatures the position of the maximum

Fig. 6.

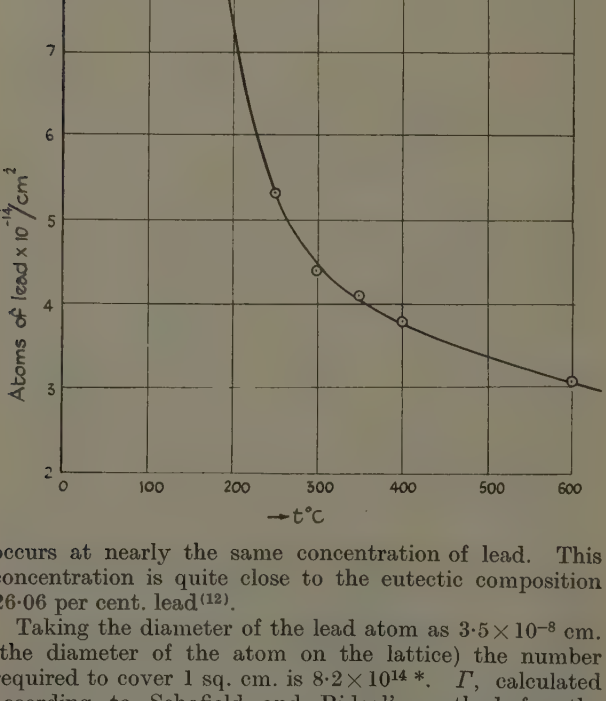

occurs at nearly the same concentration of lead. This concentration is quite close to the eutectic composition 26·06 per cent. lead[12].

Taking the diameter of the lead atom as $3{\cdot}5\times10^{-8}$ cm. (the diameter of the atom on the lattice) the number required to cover 1 sq. cm. is $8{\cdot}2\times10^{14}$ *. Γ, calculated according to Schofield and Rideal's method for the temperature 600°, is $3{\cdot}1\times10^{14}$, and the numbers for

* It has been assumed that the lead atoms form a square network in the adsorbed layer. If a triangular network is postulated a slightly larger value is obtained.

lower temperatures are plotted against temperature and shown in fig. 6. If we make the assumption that a unimolecular layer of lead atoms is formed on an alloy of the eutectic composition at its freezing-point (184°), then a smooth curve is easily drawn through all the points.

Summary.

The surface tension of a number of lead–tin alloys across the whole composition range from pure lead to pure tin has been determined at a number of temperatures from just above the freezing-point to 800° C.

The surface tension of all the alloys decreases with rise of temperature.

Small quantities of lead produce a marked fall in the surface tension of tin, but relatively large quantities of tin have very little effect (slight rise) on the surface tension of lead.

Assuming that the lead atom has the same dimensions as it has on the solid lattice, and using the method employed by Schofield and Rideal for determining the composition of the surface layer, it is shown that the latter, in the case of an alloy of eutectic composition, may consist of a unimolecular layer of lead atoms. It must be emphasized, however, that the deduction of this conclusion involves several assumptions.

I should like to thank Professor C. H. Desch, F.R.S., for his interest in these results, Mr. J. Trotter for assistance in the experimental work, and Mr. J. A. G. Smith for some help in the calculations involved.

References.

(1) Science Reports Tóhoku University, xvi. p. 553 (1927).
(2) *Zeit. f. Anorg. Chem.* cliv. p. 79 (1926); clxii. p. 301 (1927); clxxxi. p. 353 (1929).
(3) Phil. Mag. ii. p. 341 (1926).
(4) Journ. Chem. Soc. 1931, p. 2213.
(5) Amer. Journ. Science, xxxvii. p. 10 (1914).
(6) *Zeit. f. Metallkunde*, p. 142 (1914).
(7) Phil. Mag. ii. p. 341 (1926).
(8) Phil. Mag. xii. p. 596 (1931).
(9) Proc. Roy. Soc. cix. p. 57 (1925).
(10) Phil. Mag. xii. p. 907 (1931).
(11) Journ. Chem. Soc. 1932, p. 2089.
(12) Stockdale Journ. Inst. Met. xlix. p. 267 (1932).

The National Physical Laboratory, Teddington.
4th September, 1933.

XV. *Overtones and Fundamental Period of an Electric Oscillatory Circuit.* *By* ERIK HALLÉN, *Uppsala* *.

IN a previous paper †, "Allgemeine Theorie des elektrischen Schwingungskreises," the author has deduced theoretically that a circuit consisting of a capacity C_{es} (e.s.u.) and a coil inductance with one layer of turns has an infinite number of free periods determined by the roots P of the equation

$$\frac{C_{es}}{R} = \frac{\pi}{2} \cdot \frac{\Phi_1(P)+(\log 16a-2)\Phi_2(P)}{\Phi_3(P)+(\log 16a-2)\Phi_4(P)},$$

where

R = radius of coil in cm.,

a = ratio of diameter to length of coil,

P = proportional to frequency $P = \frac{\pi l}{\lambda}$,

l = length of wire in coil,

λ = wave-length in air.

Φ_1, Φ_2, Φ_3, and Φ_4 are certain functions expressible in Bessel and trigonometrical functions, sine integrals and cosine integrals. The equation above holds for the fundamental and odd overtones, a similar equation containing another capacity governing the even overtones. The equations are of importance, firstly, for the fundamental period when $\frac{C_{es}}{R}$ is not large, in which case the Thomson formula is not valid, and, secondly, for all the overtones not accounted for by the elementary theory.

In order to check these theoretical results I have carried out some measurements at the Physical Institution in Uppsala, a description of which is given here.

For the circuit investigated two different coils were used, to be referred to as nos. 1 and 2. These were both made of 0·25 mm. double silk-covered copper-wire closely wound in one layer. Their sizes were respectively as follows :—length of wire 164·7 m., 396·9 m. ; diameter of coil 23·54 cm., 35·09 cm. ; length of coil 7·02 cm.,

* Communicated by Prof. E. V. Appleton, F.R.S.

† E. Hallén, *Arkiv f. Mat. Astron. o. Fysik*, Stockholm, Band xxiv. A, no. 5 (1933).

11·11 cm.; number of turns 223, 360; ratio a, defined above, 3·353, 3·158. Coil 1 was wound on a hollow cylinder of 0·4 cm. micanite projecting about 1 mm. beyond the coil at each end. Coil 2, with only a paper support, was shellaced and supported by a wooden cross. A set of six brass plate condensers, made and ground at the Institution, was used. The plates of nos. 1–5 were 0·96 cm. thick, those of no. 6 1·39 cm. The diameters of the plates of nos. 1 and 2 were 5·65 cm., of nos. 3, 4, and 5 11·28 cm., and of no. 6 15·94 cm. Air gaps of various sizes (0·1 to 0·3 cm.) were made by means of small ground amber beads. The capacity was calculated by the Kirchhoff * formula. A small correction to this formula must be done for the amber beads. By varying the number of beads this correction, amounting to $\frac{1}{2}$ to 2 cm., could be experimentally determined. The coil was connected to the condensers by means of the ends of its own wire, brought out perpendicular to its axis, so that their mutual distance d was equal to the length of the coil. The capacity of these wire connexions, calculated as $\frac{l}{4 \log \frac{d}{r}}$, where r is the radius of the wire and l the distance between the surface of the coil and the edge of the condenser (60–80 cm.) is included in the capacity C_{es}.

The measurements were made with a heterodyne wave-meter from L. M. Ericsson, Stockholm, the calibration of which was checked by comparing its frequencies and their harmonics with those of the Stockholm (Spånga) and Uppsala broadcasting stations on 435·4 m. and 453 m. respectively, and a circuit mainly consisting of a small receiving coil, crystal detector, and d.c. galvanometer. With the wave-meter and receiving circuit in the position of zero coupling the circuit under investigation was loosely coupled to both and the points of resonance sought. Although the sender-receiver system had a sensitivity, which varied with frequency, the sharpness of the resonance curves made a direct reading of the resonance point easy. Fig. 1 shows a resonance curve for the third oscillation; that for the fundamental

* *Cf.* Geiger and Scheel, *Handbuch der Physik*, Bd. xii. p. 485 (Berlin, 1927).

frequency is still sharper. On moving the receiving coil along the surface of the measuring coil parallel to its axis the nodes and antinodes, were easily seen, and thus the order of the oscillations determined.

The direct result when the circuit contained coil no. 1 was that the fundamental frequency for the greatest capacity agreed almost exactly with the theoretical value; but as the capacity decreased it gradually fell below, so that when the capacity was only that of the ends of the wire it differed by 10 per cent. from the calculated value. The frequency of the first odd overtone was about 30 per cent. below the calculated value. As these

Fig 1.

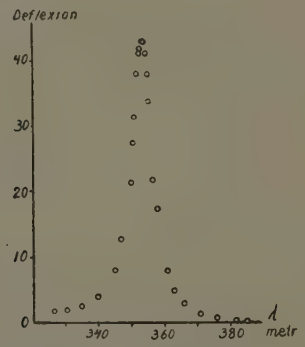

disagreements might be attributed to the supporting micanite cylinder allowing more lines of electric force to pass between the charged parts of the coil, and thus increasing the wave-length, the following test was made. A new micanite cylinder, exactly similar to that previously used, was cut along a generator and placed around the coil. The frequencies now decreased. Assuming that a double micanite envelope would increase the wave-length twice as much as a single one, the wave-length without any micanite support at all could be extrapolated for the fundamental oscillation; for the overtones the difference is too great to expect linearity. The points given as experimental determinations in fig. 5 of my previous paper were obtained in this manner. They agree with the calculated curve to within 2 per cent., the

difference reaching this value only for the smallest capacity.

In order to obviate the effect of the supporting cylinder coil no. 2 was made, having only a sheet of paper and a layer of shellac as support. Fig. 2 shows the experimental values of the odd frequencies without correction, the theoretical curves for coil 2, and the experimental values of the first odd overtone of coil 1. (The ratio a being a little different for the two coils, the theoretical curve should not exactly coincide with that of coil no. 2, but the difference is too small to be seen in the figure.) Even for coil no. 2 a disagreement with the calculated values still remains, due, no doubt, to the remaining extra capacity from the insulating and supporting materials. A single sheet of paper similar to that used in the coil, placed round this, also gave a perceptible decrease in the frequencies. The form of

Coil No. 2.

C'_{es}.	P.	C'_{es}.	P.
0	2·28	0.....	4·93
Wires 79 cm.	2·21	Wires 79 cm.	4·86
Condenser no. 1	2·20	Condenser no. 1 ...	4·87
,, 5	2·18	,, 5....	4·85
,, 6	2·17	,, 6....	4·84

the curves, however, agrees well with the theoretical curves. Thus, if the theoretical frequency of the third oscillation is reduced in the ratio 1 : 0·916, and of the fifth in the ratio 1 : 0·87, all the measured points fall within $\frac{1}{2}$ per cent. of the theoretical ones.

The two first even overtones were also measured. They do not depend upon the capacity C_{es} but upon the capacity C'_{es} of the condenser plates when charged with electricity of the same sign. This capacity for the condenser plates can easily be calculated, but the connecting wires must also be taken into account, and it is difficult to determine their contribution. As is proved by cutting them off, they are important, and it has not at present been possible to correlate the measured points with the curves. They are given in the above table. In all cases when the condensers 1, 5, or 6 were used

Fig. 2.

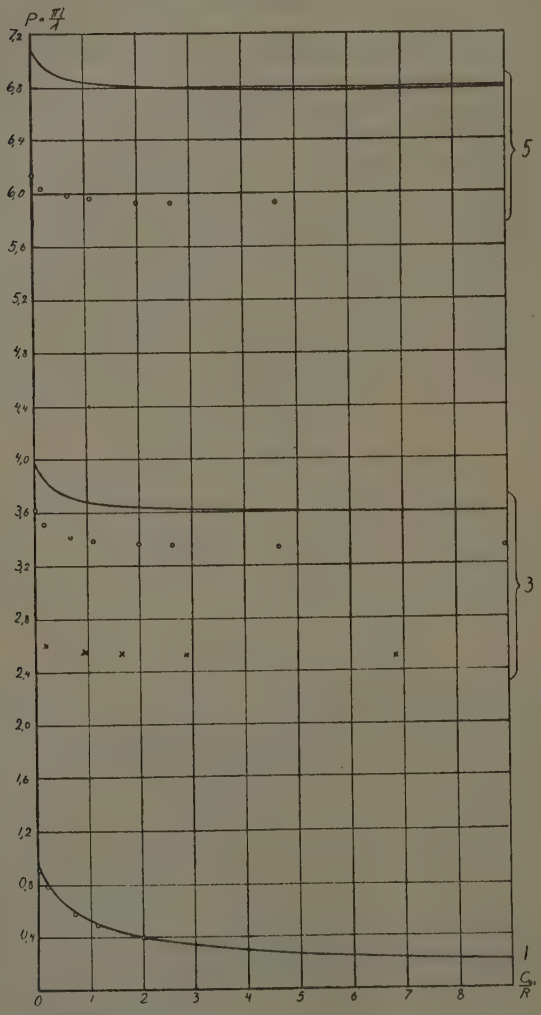

———, theoretical curve.

Measurements: ×, coil on 4 mm. micanite cylinder (coil 1); o, shellaced coil on paper support (coil 2).

the centres of the condenser plates were at a distance of 74 cm. from the nearest part of the coil.

In conclusion, it is my pleasant duty to express my thanks to the Director of the Institution, Prof. M. Siegbahn, for granting me accommodation and the use of apparatus, and the construction at the Institution of the precision condensers.

XVI. *Note on the Paper "On Models of the Electric Field and of the Photon" (Phil. Mag., Oct.* 1933). *By* Sir J. J. Thomson, *O.M., F.R.S.**

THE model described in my paper "Models of the Electric Field and of the Photon" (Phil. Mag. xvi. p. 809) would serve to illustrate the production of positive and negative electrons by γ rays impinging on matter as well as the case considered in the paper when they were supposed to be produced by the impact of corpuscular rays

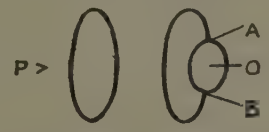

of great energy. An electric charge in the model is represented by a tube of force, *i. e.*, a vortex filament with one end on a cavity in the medium. It thus requires two things—a vortex filament and a cavity. The photon is represented by a closed vortex filament; if this ring were severed it would provide a vortex filament if there were a cavity in the medium on which its end could rest. In the nucleus of a heavy atom the density of the energy is very great; in the model the medium which is the seat of the energy is regarded as having the properties of a fluid, but in a fluid where the density of the energy at a point exceeds a certain limit proportional to the pressure at some distance from the point cavitation takes place and a hole is produced at the point. Thus in the photon we have the material for supplying a vortex filament, while in the nucleus we have the cavity; if we could combine these an electric charge would result.

* Communicated by the Author.

Suppose P is the photon of a γ ray moving from left to right towards a cavity O, when it strikes the cavity it must be interrupted, since it cannot exist where there is no medium, suppose A and B are the ends of the filament. Since a filament ending on a cavity represents a charge of electricity there is a charge of electricity of one sign at A and an equal charge of the opposite sign at B. The filament is in a state of tension, so that A will be pulled one way and B the other; if there is sufficient energy in the photon to separate A and B by much more than atomic distances a free position and a free negative charge will be created, and as each will receive the same energy they will have the same mass.

If we could produce electric fields whose intensity was greater than a critical value we could dispense with both the photon and the nucleus, for if R is the electric force at a point the density of the energy is $R^2/8\pi$; if this were of the order of that to be found in the nucleus cavitation would occur, while the vortex filaments would be provided by the tubes of force in the electric field. These could not pass through the cavity, and, as in the case just considered, would have ends A and B on its boundary. If the energy in the electric field were great enough to pull A and B apart a positive and a negative electron would be produced, or, possibly, if the energy were great enough a positive and a negative proton. On this view, therefore, matter might be produced from the ether by very intense electric fields.

OBITUARY NOTICE.

Professor Joly.

The death of Professor John Joly has removed from us a distinguished geologist and physicist as well as one of the editors of the Philosophical Magazine. Like other Fellows of Trinity College, Dublin, he was well known in subjects differing from that of the Chair he primarily occupied, viz., that of Geology and Mineralogy: and Joly is almost better known as a physicist than as a geologist.

An early invention of his was a steam-calorimeter, in which the substance whose heat-capacity was to be measured was hung on the end of a balance in a saturated atmosphere,

and the amount of steam condensing upon it was weighed. He also devised an instrument for determining the temperature of the melting-point of minerals by observing the temperature of a strip of platinum on which they began to run. And he applied the three-colour theory of vision to colour photography, where the photograph was both taken and viewed through a plate finely ruled with lines of three carefully selected colours. Viewed at a little distance, these lines merged into one another and gave a composite effect, whereof the yellow patches looked at through a magnifier were seen to be composed of nothing but red and green lines. This plan was afterwards superseded by the starch-grain method, and seems better adapted for demonstrating the fact of three-colour vision than for practical colour- photography.

But the work in which he made his chief reputation was the physics of the crust of the earth and of the rocks composing it. In particular he applied the subject of radioactivity to geology: and in his Halley Lecture at Oxford in 1924, under the title of "Radioactivity and the Surface History of the Earth," he gave a detailed and remarkable contribution to our knowledge of mountain-building, which he subsequently published as a volume called 'The Surface-History of the Earth.' In this he stressed the great importance of radioactivity to geological history, and showed how the tide-generating forces, especially in past times, would give rise to long-period Revolutions, for which he worked out the thermodynamics; treating the continents as floating in a magma of molten basalt, and periodically rising and falling as the heat accumulates and periodically escapes. He shows that the condition of steady heat-flow to the surface could not account for the periodical events which are at the basis of geological history. And he argues that

> "the source of the periodicity lies in the facts that thermal discharge can only take place by convective movements and the co-operation of tidal effects; and that the rate of loss arising in this way so enormously outstrips that of the extremely slow rate of supply [by radioactivity] that reversion to solidity becomes inevitable: an essential condition being the growth of solidity from beneath upwards."

The age of the rocks was determined by Lord Rayleigh; but some of the evidence was displayed microscopically by specks of radioactive substance embedded in them, which gave rise to the pleochroic haloes which Joly studied in particular. These haloes were due to the particles shot off from the radioactive substance embedded in the rocks, the range to which they extended in the dense material being characteristic of the nature of their source; a thorium halo, for instance, extending to a certain distance, and a radium halo to another; the appearance being microscopic specks in the structure of the rocks, which were the subject of a Huxley Lecture given to the University of Birmingham.

In biology Professor Joly applied his knowledge, in conjunction with Professor H. H. Dixon, to explain the ascent of sap in trees. In medicine he perfected what is known as the "Dublin method" of extracting radium; and with Dr. Stevenson he devised a method for the deep-seated application of radium in hollow platinum needles, which at the present time is the universal method adopted for radium treatment.

He was elected a Fellow of the Royal Society in 1892, and received a Royal Medal in 1910; he also received the Murchison Medal of the Geological Society; and the Boyle Medal of the Royal Dublin Society, of which last in 1929 he was elected President. Cambridge awarded him the Sc.D.; and many other honours fell to his share.

He was a remarkably modest man, always ready to acknowledge the work of others; and he died unmarried.

OLIVER J. LODGE.

December 21, 1933.

[*The Editors do not hold themselves responsible for the views expressed by their correspondents.*]

Fig 1.

Fig. 2.

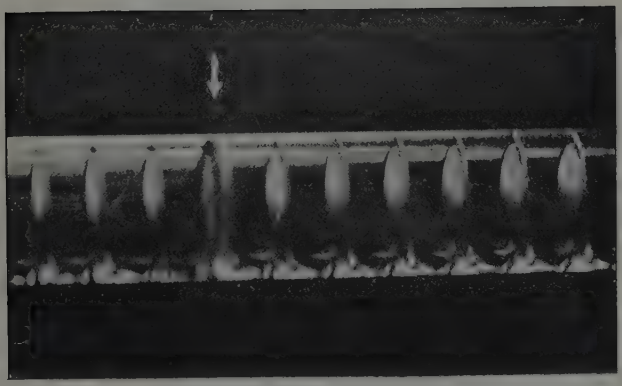

Fig. 3.

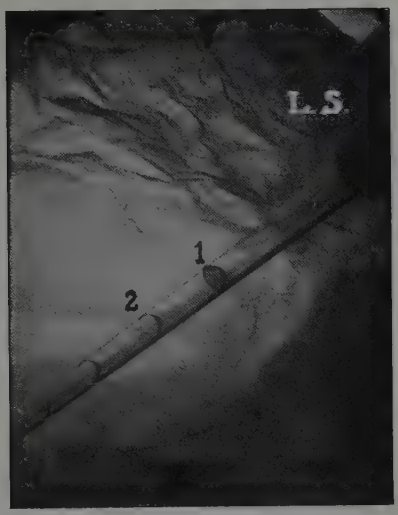

Fig. 4.

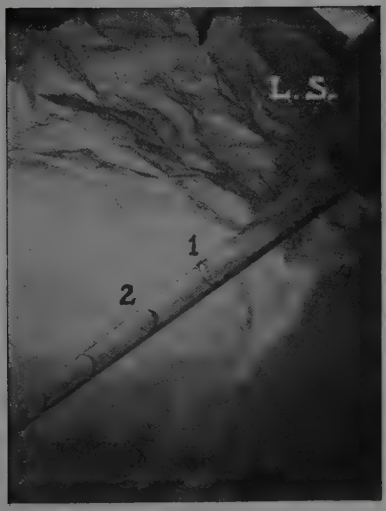

Fig. 5.

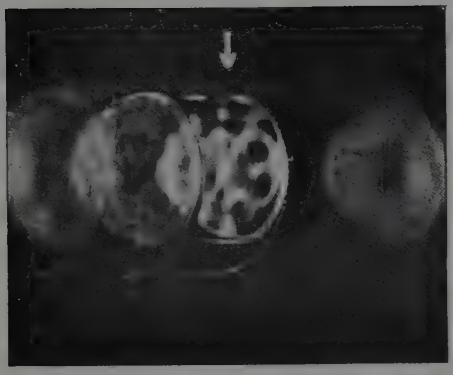

Fig. 6.

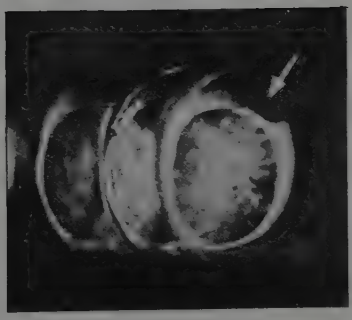

Fig. 7.

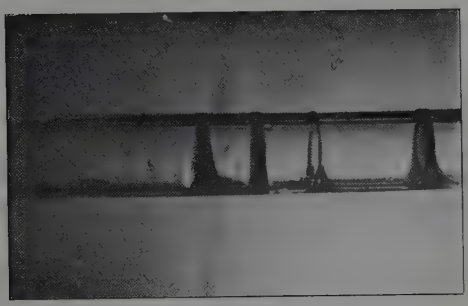

Fig. 8.

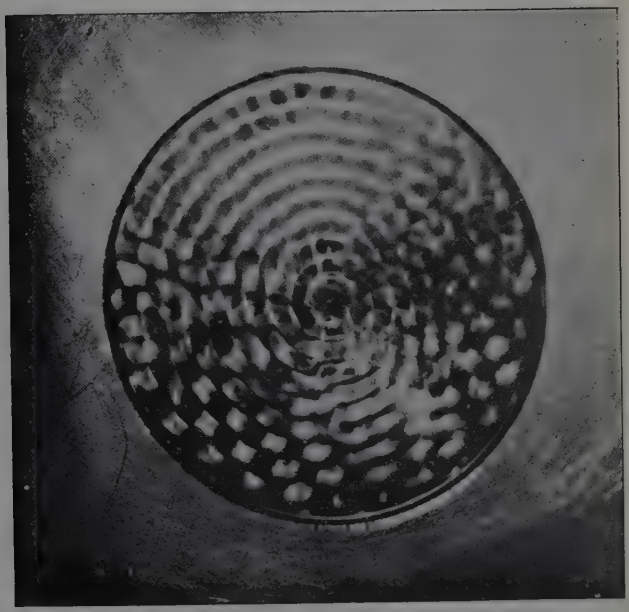

Fig. 9.

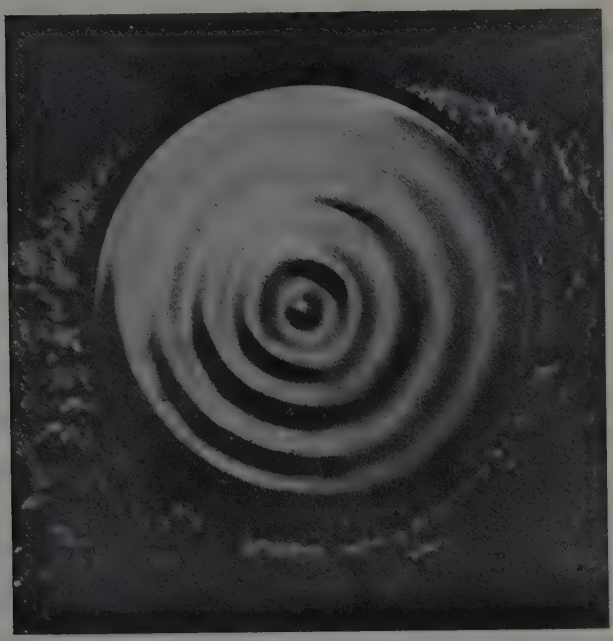

Fig. 10.

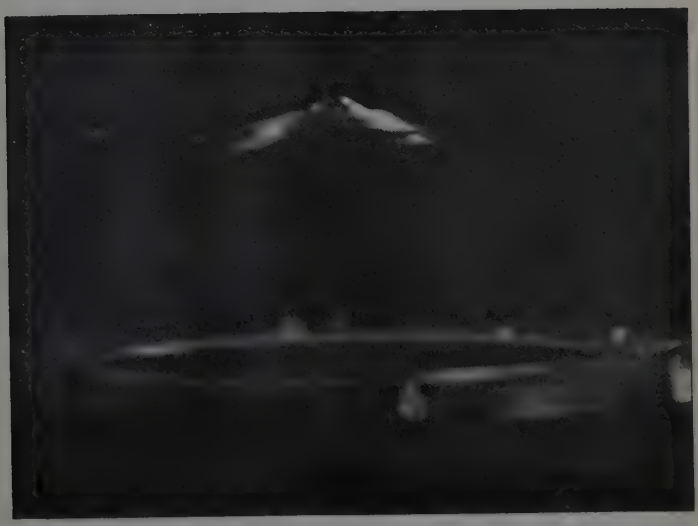

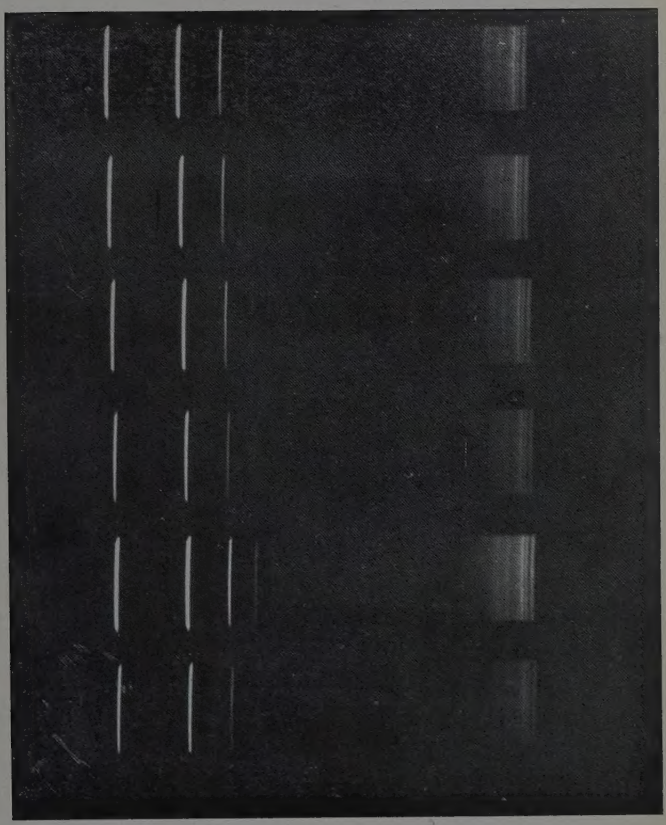

Balmer Series. Showing absence of background and variation of intensity with change of current through discharge-tube.

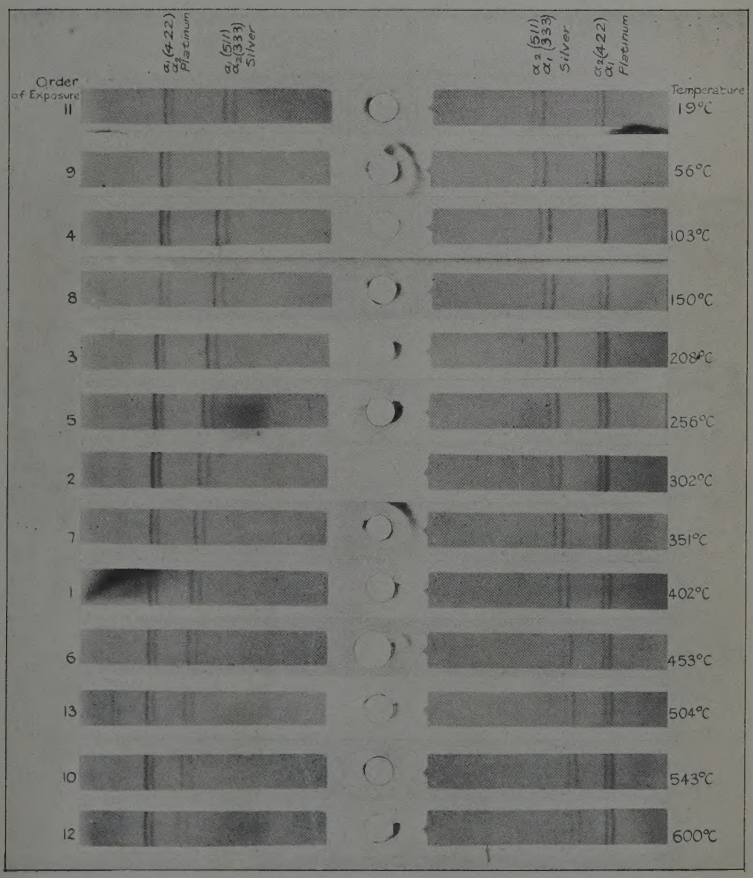

X-ray spectral lines of silver and platinum illustrating the thermal expansion of the crystal lattices.